INFORMATION TO USERS

The most advanced technology has been used to photograph and reproduce this manuscript from the microfilm master. UMI films the text directly from the original or copy submitted. Thus, some thesis and dissertation copies are in typewriter face, while others may be from any type of computer printer.

The quality of this reproduction is dependent upon the quality of the copy submitted. Broken or indistinct print, colored or poor quality illustrations and photographs, print bleedthrough, substandard margins, and improper alignment can adversely affect reproduction.

In the unlikely event that the author did not send UMI a complete manuscript and there are missing pages, these will be noted. Also, if unauthorized copyright material had to be removed, a note will indicate the deletion.

Oversize materials (e.g., maps, drawings, charts) are reproduced by sectioning the original, beginning at the upper left-hand corner and continuing from left to right in equal sections with small overlaps. Each original is also photographed in one exposure and is included in reduced form at the back of the book.

Photographs included in the original manuscript have been reproduced xerographically in this copy. Higher quality 6" x 9" black and white photographic prints are available for any photographs or illustrations appearing in this copy for an additional charge. Contact UMI directly to order.

U·M·I

University Microfilms International
A Bell & Howell Information Company
300 North Zeeb Road, Ann Arbor, MI 48106-1346 USA
313 761-4700 800 521-0600

Order Number 9020752

Surface-enhanced Raman spectroscopy of bipyridines and phenylpyridines

Diamandopoulos, Panayiotes S., Ph.D.

City University of New York, 1990

U·M·I
300 N. Zeeb Rd.
Ann Arbor, MI 48106

SURFACE ENHANCED RAMAN SPECTROSCOPY OF BIPYRIDINES AND PHENYLPYRIDINES

by

PANAYIOTES S. DIAMANDOPOULOS

A dissertation submitted to the Graduate Faculty in Chemistry in partial fulfillment of the requirements for the degree of Doctor of Philosophy, The City University of New York.

1990

This manuscript has been read and accepted for the Graduate Faculty in Chemistry in satisfaction of the dissertation requirement for the degree of Doctor of Philosophy.

12-11-89
Date

Thomas C. Stein
Chair of Examining Committee

12/12/89
Date

B. M. Loeb
Executive Officer

L. Mary Dian
A. David Baker
Supervisory Committee

The City University of New York

Abstract

SURFACE ENHANCED RAMAN SPECTROSCOPY OF BIPYRIDINES AND PHENYLPYRIDINES

by

Panayiotes S. Diamandopoulos

Advisor: Professor Thomas C. Strekas

Surface enhanced Raman spectroscopy (SERS) using metal colloids has provided a new and much improved approach to the study of condensed phase metal interfaces. The enhancement of the Raman scattered intensity of the analyte upon adsorption on the surface can be up to 10^7, while scattering from the solvent remains weak or non-observable. Isomeric bipyridines and phenylpyridines that were investigated in this study, were chosen because of their characteristic structural and symmetrical properties. They all possess one sigma electron donor nitrogen on each of their pyridine rings, as well as an extensive π type electron donor system through their aromatic rings. These two electron donor sites can compete for interaction with the metal surface during adsorption, thus resulting in different enhancements for the molecules. The metal surface, a silver colloidal suspension, was prepared by the reduction of a silver nitrate solution by sodium citrate. The SERS spectra of these compounds were recorded in the 700-1700 and 2900-3200 cm^{-1}

regions of the spectrum. The adsorption mode of these compounds on the silver surface was also investigated. According to surface selection rules, when a molecule adsorbs onto the metal surface one of its molecular axes would become the z axis (or normal) with respect to the metal surface. From the molecules studied it was found that the greatest enhancement is observed for those that adsorb on the surface in a perpendicular fashion (along the surface normal). For this type of adsorption the observed SERS enhancement is due to the molecular vibrations that derive their intensity from the $\alpha_{z\,z}$ component of the molecular polarizability.

To my parents Stavros and Asimina

ACKNOWLEDGEMENTS

I would like to express my warmest thanks to my thesis advisor Professor Thomas Strekas for his continuous support and advice throughout my studies. His patience, suggestions, and understanding have made this work possible.

I would like to thank the members of my advisory committee Profs. David Baker and Max Diem for their helpful comments and advice on my work. Also, Professor David Locke for his numerous and helpful suggestions on my many academic and professional questions. Special thanks to Mr. Robert Morgan for making the Organic part of my work much easier to deal with.

To my wife Helga, and my parents in law Manfred and Vera Franke, I thank them for their continuous help and encouragement throughout my graduate studies.

Finally I would like to express my gratitude to my parents Stavros and Asimina for everything that they have done for me. Their everlasting love and support has been the driving force behind this work.

TABLE OF CONTENTS

LIST OF TABLES

LIST OF FIGURES

GENERAL INTRODUCTION

The interaction of adsorbed molecules with a surface plays an important role in a wide variety of chemical processes such as: catalysis, adhesion, lubrication, and a great number of electrochemical reactions. The stability of the adsorbate-surface interface is largely determined by the strength of the interaction between them. Adsorption-desorption kinetics also play an important role in determining reaction rates at interfaces. If one has a clear understanding of these molecule-surface interactions, a considerable number of chemical applications like: catalysis, chromatographic separations, coatings, biosensors, etc. can be further understood and made more efficient.

For most of the chemical processes mentioned, the interfaces of interest are between two condensed phases: liquid-liquid, liquid-solid, or solid-solid. An ideal technique to study these interfaces would be an "in situ" one, that does not require elaborate experimental conditions, or modification of the original sample. The technique should also be able to provide some information about the amount, orientation, and strength of adsorption of the adsorbate, with the surface. Techniques utilizing vibrational spectroscopy are particularly suited for studying these types of interaction. Vibrational Raman or infrared (IR) spectra of species adsorbed on a

surface can provide valuable information on the processes occuring at these interfaces. For aqueous solution-solid type interfaces, Raman spectroscopy is superior to the IR technique, due to the inherent problems associated with IR spectra of aqueous solutions, (even though they can be dealt with by using Fourier transform IR technique). A Raman spectrum of a solution-solid interface can provide information in several ways. It can characterize the type of adsorbate from its "fingerprint" Raman signals. It can also provide information about the relative strength and orientation of the adsorbate on the surface, depending on the intensities of certain bands of the spectrum, and the differences between the Raman spectrum of the adsorbate on the surface and that in solution or in pure solid or liquid phase.

RAMAN SPECTROSCOPY

Raman spectroscopy is a type of molecular vibrational spectroscopy, which utilizes the principle that when monochromatic light is scattered by molecules, a small fraction of the scattered light is observed to have a different frequency from that of the irradiating light. This is known as the Raman effect(98). Raman spectroscopy has been an important technique for the eludication of molecular structure

for locating various functional groups or chemical bonds in molecules, and for the quantitative analysis of complex mixtures.

A unique feature of Raman scattering is that each molecule has a characteristic polarizability (α) , which is defined as the ratio of the dipole moment of the molecule (P) over the electric field strength (E) of a monochromatic light with frequency (v) that irradiates the molecule :

$$\alpha = P / E \qquad \text{where } E = E_0 \cos 2\pi v t$$

E_0 = amplitude of light wave

t= time

In order for a molecular vibration to be Raman active the polarizability of the molecule (α) must change during the vibration. This change is strictly a quantum effect. Most collisions of the incident light particles (photons) with the sample molecules are elastic (Rayleigh scattering). The electric field scattered by the polarized molecule oscillates at the same frequency as the passing electromagnetic wave, without any change in its polarizability. However, a small portion of the excited molecules (10^{-6} or less) may undergo a change in polarizability during one of the normal vibrational modes. Usually the incident radiation v_0 interacts with a molecule in its lowest vibrational state. If upon interaction

with the incident radiation, the excited molecule returns not to the original vibrational state, but to an excited vibrational level v_v of the ground electronic state, the scattered radiation is of lower frequency (v_0-v_v) than the incident radiation. This frequency difference is equal to a natural vibrational frequency of the molecule's ground electronic state. Several such shifted lines (called the Stokes lines), corresponding to different vibrations of the molecule constitute its Raman spectrum (Fig. 1).

The most frequently used source of monochromatic radiation is a continuous wave, a pulsed solid state, or a dye laser beam.

SURFACE ENHANCED RAMAN SPECTROSCOPY (SERS)

Conventional Raman spectroscopy is suitable for the study of aqueous solutions or solution-solid interfaces. Due to the weakness of the Raman scattering process, the technique has little or no success in studying solutions with small concentrations of analyte (except for resonance Raman), or probing thin layers or submonolayers on surfaces. Since its discovery in 1974 (1), the surface enhanced Raman effect has generated considerable interest in the spectroscopic community. Surface enhanced Raman spectroscopy (SERS) has

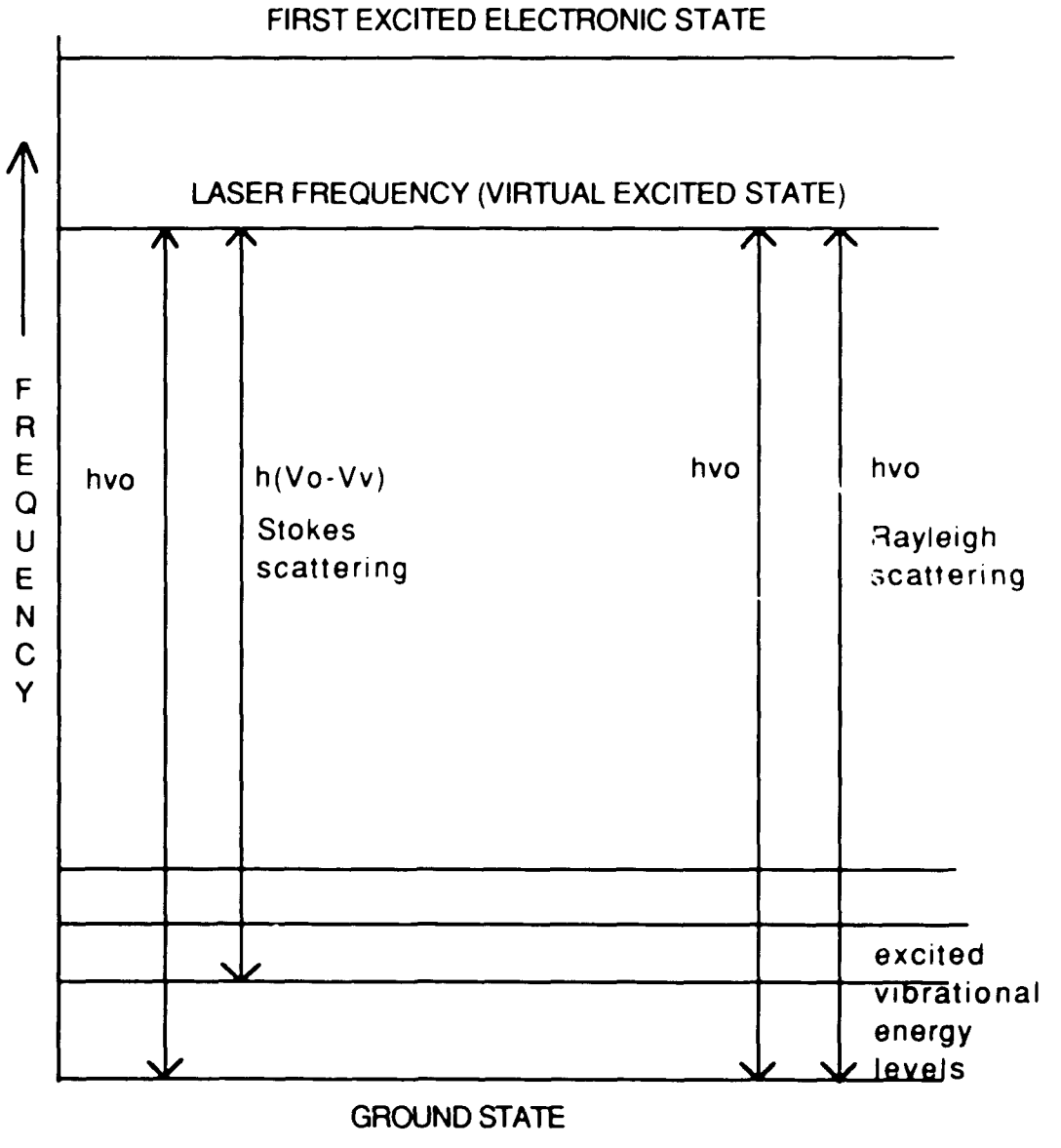

Figure 1: Energy interchange involved in Raman and Rayleigh scattering.

provided a new and much improved approach to the study of condensed phase metal interfaces. The enhancement of the Raman scattered intensity of the analyte upon adsorption on the enhancing surface, (usually a noble metal colloid of Ag, Au, Cu, or a noble metal electrode), can be up to 10^7 fold , while scattering from the solvent remains weak or non-observable. With current SERS techniques it is possible to study molecules in small concentrations adsorbed from solution onto the metal surface, and also observe and monitor the adsorbate surface interactions. Due to the selectivity and sensitivity of the technique, combined with the ease of sample preparation, handling, and small volume requirements of analyte, SERS can be used for a variety of applications with easily obtainable and reproducible results. Current detection limits of adsorbates on various metal surfaces are in the nanogram range (82). This detection limit of the SERS technique can be further expanded to even lower values if the adsorbates exhibit resonance enhancement in addition to surface enhancement of their Raman spectra.

THEORY OF SERS ON METAL COLLOIDS

Since the first observations of surface enhanced Raman scattering by molecules adsorbed on metal surfaces, it has been recognized that the intensity of Raman scattering is strongly dependent on the state of division of the metal surface. The early experiments and much of the later work has been carried out on silver electrodes randomly roughened by an electrochemical, reduction-oxidation cycle in aqueous electrolyte. Such ideally roughened surfaces give particularly large SERS signals, and they are ideal for investigating the adsorbate's chemistry on the silver electrode (1-20). However, they are less favorable for studying details of adsorption or of the enhanced Raman scattering, since it is difficult to measure some of their optical properties, and in particular their absorption spectra, and to account for these properties in terms of the surface roughness in a precise way. For this reason much attention has been directed to more regular finely divided metal surfaces, like colloidal suspensions or island films, which also exhibit SER scattering (23).

It has long been known (21) that stable dispersions of silver or gold particles of about 10-100 nm in diameter can be prepared by reduction of dilute solutions of simple silver or gold salts. These sols have one or more absorption (scattering)

maxima in the visible range, the wavelength of which depends on the particle size and shape (22). Depending on the preparation method, the absorption maximum(s) can change due to aggregation or particle growth. It is therefore important for optical studies that the particles are uniform in size and shape and that there is control of their aggregation. The usual source of silver or gold for the preparation of these colloids are salts containing Ag^{+1} or $(AuCl_4)^-$ ions. Various reducing agents have been used, including citrate, oxalate, hydroxylamine, borohydride, and ethylenediaminetetraacetate ions (21-24). A study done by Turkevich et al. (21) using transmission electron microscopy showed that citrate ions are particularly favorable as a reducing agent for giving particles of good sphericity and uniform particle size. Colloids prepared in our laboratory using citrate ions have proven to be stable for several months. SER spectra obtained with metal colloids show equivalent properties to those of electrodes (23,25-29).

Metal particles in aqueous colloidal suspensions usually bear a negative charge due to adsorbed anions, and provided the charge is sufficiently great, the colloids are stable to aggregation because of the electrostatic repulsion between the particles. Aggregation can be induced, however, (23) by the addition of neutral adsorbate molecules such as pyridine or bipyridine, which displace the adsorbed ions, thus reducing the

charge on the particles to the point where random collisions occur as a result of diffusional motion. On contact, the particles are then held together by short range attractive forces. At high concentrations of adsorbate this can result in relatively fast aggregation and precipitation. At low concentrations of neutral adsorbates however, there is a slow formation of initially small aggregates, which remain dispersed, and thus prevent fast precipitation of the colloid. Electron microscopic examination of silver colloids slowly aggregated with low concentrations of pyridine, show that in some cases they consist of strings of particles, rather than of globular clusters (30). The formation of these strings (often referred to as: pearl strings) rather than globular clusters has a large effect on the optical properties of the sols. It was observed that as the number of particles in a string was increased under controlled conditions from two to infinity, the absorption maximum of the colloid was shifted as much as 300 nm to higher wavelengths (30).

Surface enhanced Raman scattering by colloidal particles was first reported by Creighton, Blatchford and Albrecht, who made measurements on pyridine adsorbed on aqueous silver and gold colloids (23). The silver colloids were prepared by borohydride (BH_4^-) reduction of silver nitrate solution. It was found that the aggregated silver sols exhibited strong SER

scattering of incident light in the green-yellow region, and that the SER spectra were characteristic of adsorbed pyridine. The relative intensity of the SERS bands of the colloids was up to 5 times higher than the corresponding bands of 0.1 M aqueous pyridine solution, and it was thus clear that there was a significant Raman intensity enhancement. This result was in agreement with an earlier suggestion by Moskovits (31), that colloidal metal spheres covered with adsorbate, and isolated in a dielectric medium, might display Raman signals similar to SERS at roughened electrode surfaces.

Kerker and co-workers were the first to develop a theoretical description of the enhancement of Raman scattering by molecules adsorbed at the surface of isolated metal spheres (32-34). In this description the SERS effect owes its high intensity to an enhancement of the electromagnetic fields at the metal surface, due to the resonant response of the particle surface plasmons to the incident light, and a further resonant response to the outgoing Raman scattered light.

SURFACE ENHANCING MECHANISM FOR THE SMALL SPHERE MODEL

According to Kerker and al. (32-34), if one considers a small size colloidal particle (its radius being smaller than the excitation wavelength), and a molecule located at a distance (r') from the metal surface, then the electric field at the exciting frequency (ω_0) and at location (r') may be considered equivalent to the field of an electric dipole at the center of the metal sphere with radius (a) with dipole moment (ρ_0) :

$$\rho_0 = g_0.a^3.E_i(r',\omega_0)$$

where (r') is a vector pointing from the center of the sphere to a field point, (a) is the radius of the sphere, E_i is the incident field, and g_0 a parameter that is equal to :

$$g_0 = (m_0^2 - 1) / (m_0^2 + 2)$$

where m_0 is the refractive index of the metal sphere relative to that of the medium. The molecule that is located at (r') can be described by an electric dipole with dipole moment :

$$\rho_I = \alpha.E_\rho.(r',\omega_0)$$

where (α) is the polarizability of the molecule, and $E\rho$ is the incident field plus the field due to the dipole ρ_0. This field

depends on (a/r'^3) in the near zone of the sphere. At the observer coordinate (r), (r is a vector originating at the center of the metal sphere, and r>>r') , it can be shown that the scattered field $E_{SC}(r,\omega)$, (where (ω) is the shifted frequency) is the field of an electric dipole also located at the center of the particle with dipole moment also depending on (a/r'^3). The Raman radiation $E_R(r,\omega)$ at the observer coordinate (r) is given by :

$$E_R = E_\rho + E_{SC}$$

giving rise to an enhancement factor (G) for a monolayer on the metal surface of:

$$G = [\, 1+2g_0 + 2g + 4g.g_0 \,]^2$$

$$\text{where } g = (m^2 - 1) / (\, m^2 + 2)$$

and m = refractive index at shifted wavelength

m_0= refractive index at exciting wavelength

For the limiting case of metal particles being smaller than the excitation wavelength (so-called Rayleigh limit), the enhancement does not depend on the size of the metal sphere . However, for bigger size metal spheres, the radius of the sphere is important in the enhancement effect. Kerker et. al have shown that, in general, surface enhancement decreases with increasing sphere radius for a given excitation wavelength.

In general the magnitude of the enhancement depends on the wavelength dependent refractive index of the substrate, the size and shape of the metal particles, and the incident wavelength. The enhancement decreases by a factor of $(1 / r'^3)$ as the molecule moves away from the metal surface.

SURFACE SELECTION RULES FOR SERS

Moskovits et al. have done extensive work in order to determine the rules that govern the enhancement of an adsorbate on the metal surface (35-41). His work suggests that for Raman surface enhancement there exist three classes of vibrational modes with distinct spectral behavior.1) Those excited only by the normal component of the electric field at the metal surface, and resulting in an induced dipole moment with a strong component only in a direction perpendicular to the surface. 2) Those excited only by the tangential component of the field, and resulting in an induced dipole moment with a strong component tangential to the surface. And 3) the mixed cases (for example, a normal field exciting a dipole with a strong component parallel to the surface). If we call the direction along the surface normal the *z* direction, then modes of the first type are those which belong to the same irreducible representation to which α_{zz} belongs. Here (α) is

the Raman polarizability of the adsorbate. Modes of the second type belong to the same irreducible representations to which α_{xx} , α_{yy} , α_{xy} belong. Modes of the third type belong to the representations which span α_{xz} , and α_{yz}. In all the cases the subscripts refer to surface fixed coordinates. Moskovits has shown that for molecules adsorbed on metals, the most intense Raman signals will be obtained from vibrations which belong to the same irreducible representations to which α_{zz} belongs (where *z* is along the surface normal). Vibrations that are derived from α_{xz} , and α_{yz} were shown to be the next most intense, while those which transform as α_{xx} , α_{yy} , and α_{xy} are the least intense. If one assumes for simplicity that one of the principal molecule fixed symmetry axes of the adsorbate coincides with the surface normal, then the above implies that a molecule with C_{2v} symmetry will adsorb with its $C_2(z)$ axis along the surface normal. For example 2,2'-bipyridine adsorbed on silver particles (fig.2), will have A_1 vibrations enhanced the most since α_{zz} , α_{xx} , and α_{yy} contribute to the Raman intensity of A_1 modes, provided that the derived polarizability component α_{zz} is large. Of the three components α_{xx} , α_{yy} , and α_{zz} , the two whose subscripts define the plane in which the

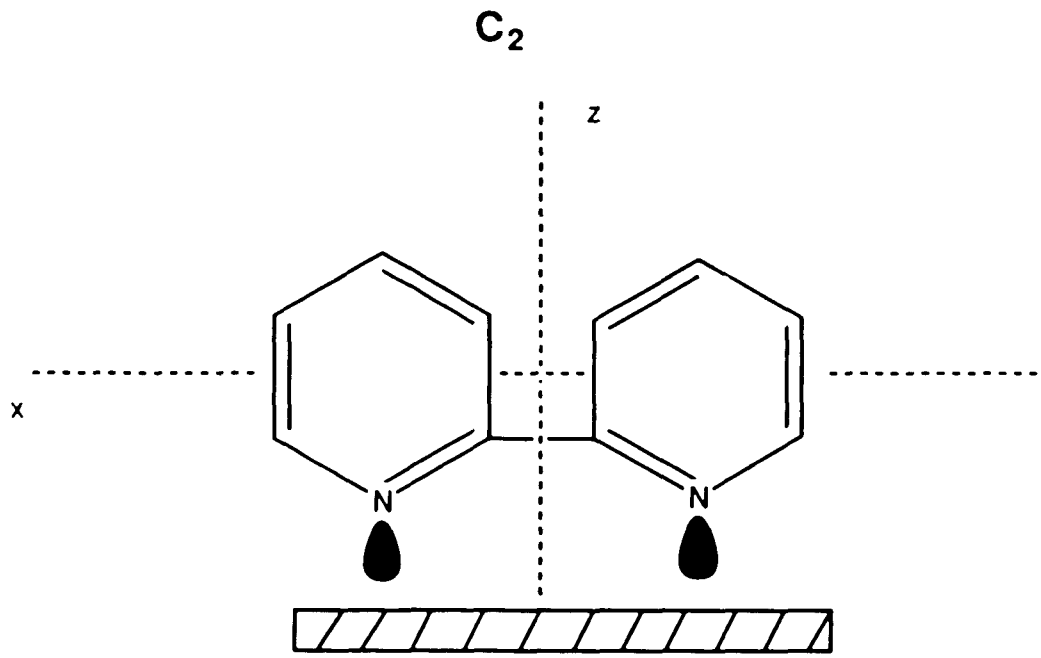

A_1 a_{xx} , a_{yy} , a_{zz}

B_1 a_{xz}

B_2 a_{yz}

Figure 2 : Vibrations of 2,2'-bipyridine when it is adsorbed with its C_2 axis along the surface normal

vibrational motion is contained are usually the largest. However, exceptions can occur especially in molecules that contain extensive π bonding . Hence, those A_1 vibrations, whose motions are directed normal to the surface, will be the most intensely enhanced. The next most intense bands will be those which belong to the same representations as α_{xz} , and α_{yz} . In a C_{2v} molecule these are the B_1 and B_2 vibrations.

The C-H stretch bands (about 3000 cm-1) in the SER spectra of planar aromatic compounds adsorbed on metal surfaces can play an important role in determining the adsorbed geometry of the molecule. In the case of a planar molecule like benzene the C-H stretching vibrations contribute significantly only to the α_{xy} , α_{xx} , and α_{yy} Raman polarizability components when the molecule is lying flat on the surface, thus resulting in a very weak enhancement of these vibrations. On the other hand if the molecule can stand up on the surface, the C-H stretching vibrations would obtain their intensities from α_{zz} , α_{xz} , and α_{yz} components , resulting in a higher SERS intensity for those bands (37)(Fig.3). Thus the observation of strong or weak C-H stretching bands in the SER spectrum of a planar aromatic molecule would constitute a straightforward criterion for determining the surface geometry of the molecule adsorbed on the metal (colloidal) surface.

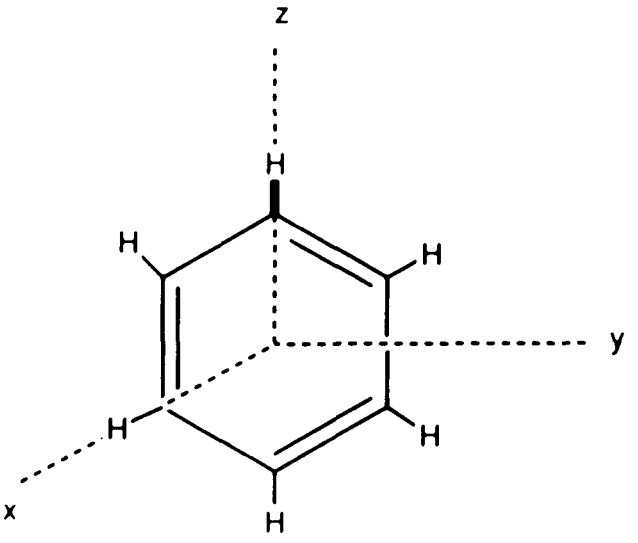

a_{zz} , a_{xz} , a_{yz}

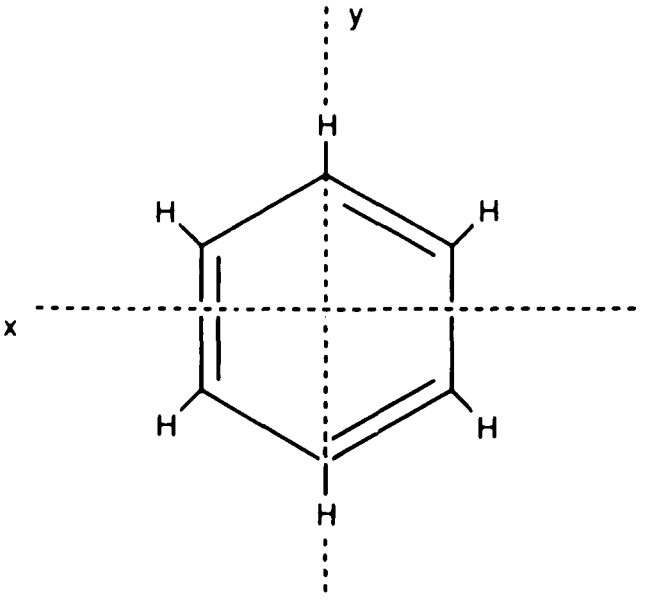

a_{xy} , a_{xx} , a_{yy}

Figure 3 : The CH stretch vibration of benzene when the benzene ring is normal (top), and parallel (bottom) on the silver surface

If a planar aromatic molecule is adsorbed on the metal surface lying parallel to it, then the following terms are used to describe that adsorption : 1) molecule lies flat on the surface , 2) molecule adsorbs through π bond interaction, referring to the π electron cloud of aromatic molecules (i.e. benzene), 3) the molecule adsorbs side-on to the surface. If the molecule is adsorbed standing perpendicular to the surface then the terms 1) normal to the surface, 2) σ bond interaction, referring to the interaction of the free electrons of certain functional groups with the silver surface (i.e. nitrogen lone pair in pyridine), and 3) face-on adsorption are used to describe it.

The above surface selection rules do not imply that the tangential (parallel) to the surface vibrational modes of a certain molecule must be weak. They only predict that in many cases a given vibrational mode will be more intense in the SER spectrum if the molecule is oriented in such a way so that the motion is normal to the enhancing surface rather than parallel to it. The work of other investigators in the field has produced similar results and theoretical explanations (42-47).

APPLICATIONS OF SERS WITH METAL COLLOIDS

The large enhancement effect (up to 10^7 fold) observed in SERS, and the spectroscopic information that can be obtained from it has led to an increased use of the technique in a variety of applications. Studies using colloidal suspensions as the enhancing medium have covered a wide spectrum of applications since its original discovery in 1974, and they are continuously expanding. Among the many classes of compounds that have been studied using colloidal SERS are different types of dyes such as : fluorescein(48-49), azo(50), rhodamine(51), avidin(52), and other types(53-55). A variety of carboxylic acids have been studied in order to both obtain their SERS spectra , and also study their interaction with the metal surface. These include naphthoic(40), phthalic, maleic, fumaric(36), and amino and nitro benzoic acids(6,36).

Other organic compounds that have been studied using colloidal SERS are : polymers(56-59), ketones(60), as well as a variety of homo and heterocyclic organic compounds(61-63).

Inorganic polyatomic ions have also been investigated. These include : chromate, molybdate, tungstate(64), cyanide, sulfate(65) etc.

The study of biological and biochemical molecules using colloidal SERS is another area where a significant amount of

work has been carried out. Some of the compounds studied are: Amino acids(66), peptides(67), heme and membrane proteins(68,69), nucleic acid components (70-71), chromosomes(72), DNA(73), enzymes(74), hemoglobin(75), porphyrins(76-78), and other biomolecules(79-80).

Various compounds of environmental importance have also been identified using colloidal SERS. Among them are organophosphorous pesticides(81), carcinogenic substances (pyrenes,nitropyrenes)(82), organic ground water contaminants (83), priority air pollutants(84), and trace analytes (85,86).

The growing use of SERS with metal colloidal suspensions has established it over the years as a valuable technique for identifying a diverse class of compounds, and also for studying the interaction of various adsorbates with the enhancing surface.

BIPYRIDINES AND PHENYLPYRIDINES

Isomeric bipyridines and phenylpyridines were the principal type of molecule investigated in this study. The isomeric bipyridines that were used, were chosen because of their characteristic structural and symmetrical properties. They all possess one sigma electron donor nitrogen atom on each of their pyridine rings, as well as an extensive π type electron

donor system, through their aromatic rings. These two electron donor sites can compete for interaction with the metal surface during adsorption, resulting in different enhancements for the molecules.

The pH range of the silver colloid used in this study (8.0-9.0 pH units), as well as the dissociation constants of the bipyridines and the phenylpyridines(87), indicate that in a moderately basic solution, like that of the silver colloid, both imino nitrogens are deprotonated, and can possibly interact with the metal surface. The relative position of the nitrogen atom on the pyridine rings was expected to play an important role in determining the mode of interaction. 2,2'-bipyridine is the only one of the bipyridines that has the potential of utilizing both of its imino nitrogens to adsorb in a chelating fashion on the silver surface. The remaining bipyridines do not have that chelating ability due to the asymmetric or distant position of their nitrogens on the pyridine rings, and their varying geometries might give rise to different surface enhancements.

The isomeric phenylpyridines were used in this study in order to investigate the importance of sigma type adsorption through the pyridine nitrogen versus steric effects on the metal surface. From the phenylpyridines studied the 4 and 3 phenylpyridines were expected to be able to interact with the

metal surface through the lone pair of the pyridine nitrogen without severe steric restraints. The third isomer, 2-phenyl pyridine, was not expected to be able to adsorb in a similar fashion due to the steric hinderance imposed on the pyridine nitrogen by the benzene ring at the 2 position to it.

The structural formulas of the isomeric bipyridines and phenylpyridines are shown on figures 4 and 5

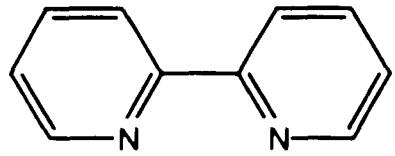

2,2'-bipyridine

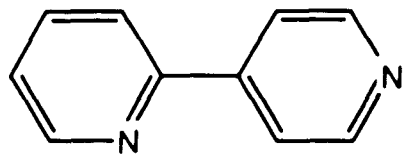

2,4'-bipyridine

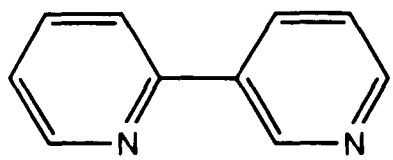

2,3'-bipyridine

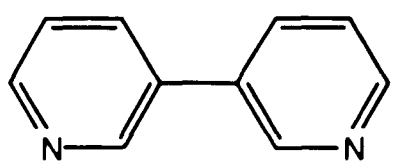

3,3'-bipyridine

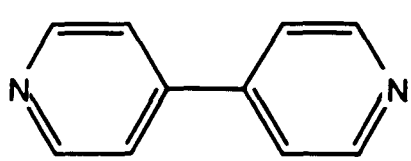

4,4'-bipyridine

Fifure 4 : Structural formulas of isomeric bipyridines

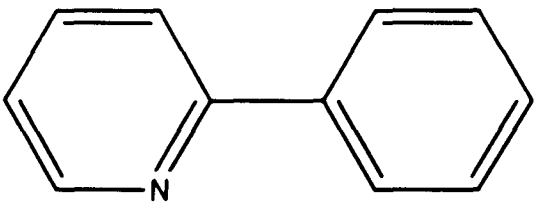

2-phenyl-pyridine

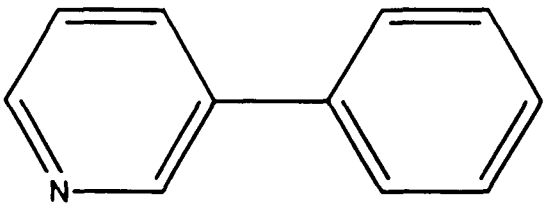

3-phenyl-pyridine

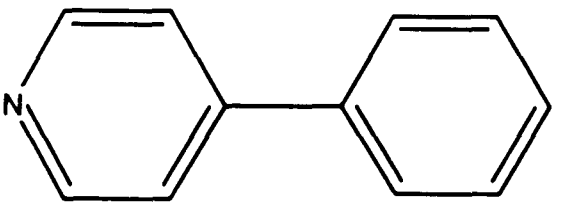

4-phenyl-pyridine

Figure 5 : Stuctural formulas of isomeric phenyl pyridines

EXPERIMENTAL

1. MATERIALS

All of the bipyridines and phenylpyridines as well as 1,10 phenanthroline, were purchased from Aldrich Chemical Co.. All the solids were further purified by recrystalization from diethylether. All liquid materials (2,3'-bipyridine, 2 and 3 phenylpyridine) were purified by vacuum distillation. 4,4'-dimethyl-2,2'-bipyridine was purchased from G. Frederick Smith Chemical Co.. The 2,2'-dipyridil silver(+1) complex was prepared in the laboratory, according to the method described by Halpern et al. (99). N-methyl-4,4'-bipyridinium was synthesized by Mr. Robert Morgan of Queens College Chemistry Dept. All solvents used were of spectral quality, and glass distilled water was used to prepare stock solutions of the molecules that were studied. All stock solutions were prepared by dissolving solid material in water to a final concentration of about 10^{-2} M. Ethanol-water mixtures (40/60) were used for preparing stock solutions of the phenyl pyridines because of their low water solubilities. The exact final concentration of all stock solutions was determined spectrophotometrically.

2. PREPARATION OF SILVER COLLOID

The silver sols were prepared according to the Lee-Meisel method (88). A 90 mg sample of silver nitrate was dissolved in 500 ml of glass distilled water and brought to boiling in a covered 1000ml beaker, while being purged with nitrogen gas at low regulator pressure (10-15 psi). A 10 ml aliquot of a 1.0% sodium citrate solution was added dropwise to the boiling silver nitrate solution under vigorous stirring by a magnetic stirrer (total addition time 1.5-2.0 minutes). The solution was kept boiling for about 1 hour under constant nitrogen purging with the beaker covered with a watch glass to prevent excessive evaporation of the sol. The stirring was also being monitored and adjusted according to volume changes due to evaporation. The final volume of the sol was about 200 ml, thus giving a nominal silver concentration of about 2.3×10^{-3} M. Absorption spectra of the sols consistently showed a broad peak centered at 420-440 nm (fig 6). Transmission electron microscopy (TEM) that was performed on similar type sols by Hildebrant and Stockberger (51) has shown that the average silver spheroid diameter was 35 nm. The sols were found to have a long shelf life without any special storing conditions. The sols gave reproducible SERS spectra for a period of more than 6 months.

Figure 6 : Visible absorption spectrum of fresh citrate type colloid used in this study.

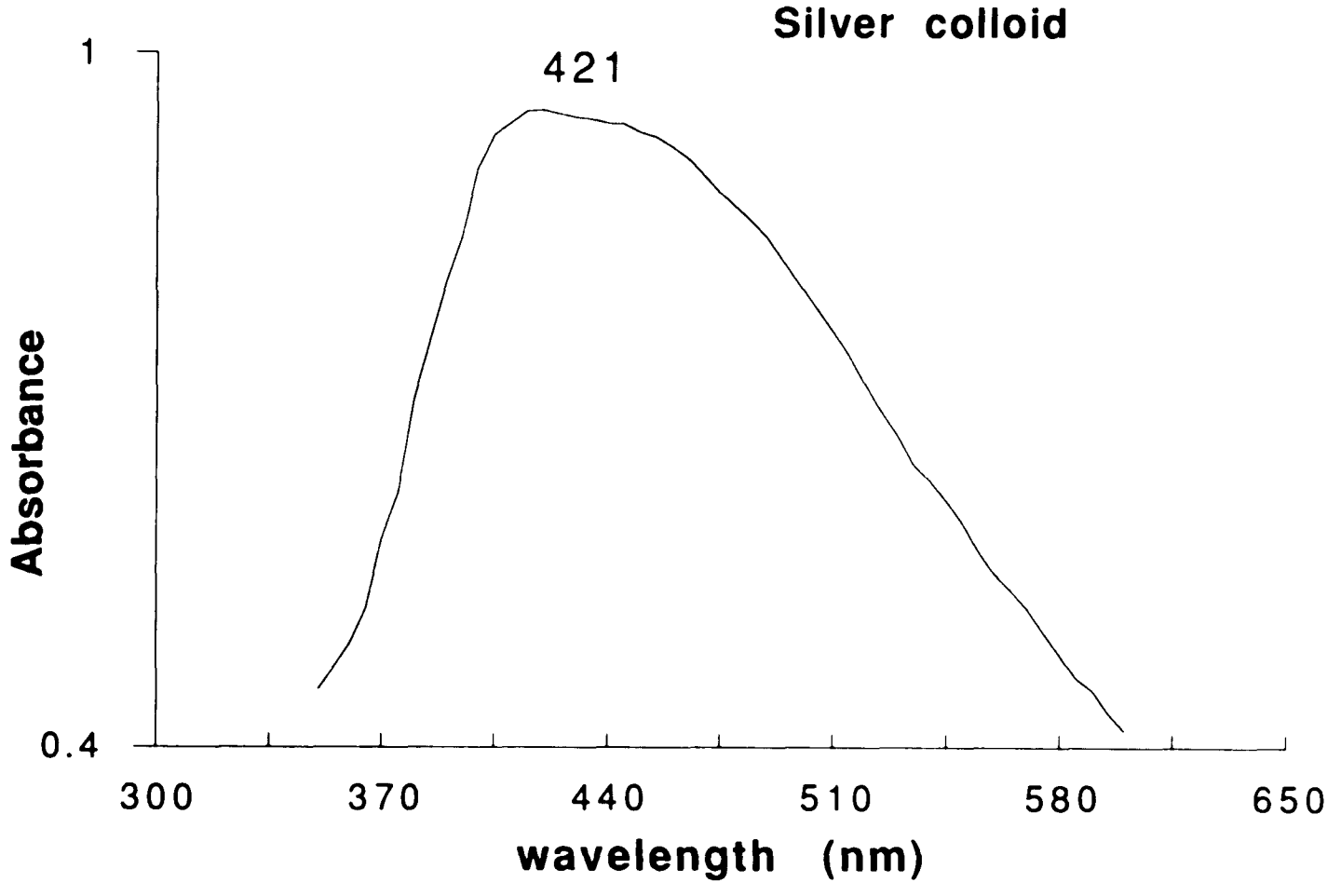
Silver colloid
421
1
0.4
Absorbance
300
370
440
510
580
650
wavelength (nm)

2. INSTRUMENTATION

ABSORPTION SPECTRA

All absorption spectra were recorded on a Perkin Elmer 320 double grating, double beam scanning spectrophotometer. All UV absorption spectra of the molecules were recorded between 400-200 nm using standard type quartz cells. Figures 7 and 8 show the UV absorption spectra of the molecules studied.

RAMAN SPECTRA

The main components of the Raman spectrometer used to record all Raman and surface enhanced Raman spectra are:

1. Laser source consisting of a Spectra Physics 265 exciter and a Spectra Physics 164-08 Argon ion continuous wave laser tube.
2. SPEX 14018 1.0 meter double monochromator with holographically ruled gratings. A 514.5 nm rejection filter was mounted before the entrance slit to the monochromator, to prevent unwanted laser radiation from entering it.
3. Princeton Instruments IRY-700G self scanning photodiode (SPD) array detector with 1024 photodiodes and 700 channels. This was mounted on the first half of the monochromator in order to obtain maximum spectral coverage.

Figure 7 : Ultraviolet absorption spectra of stock solutions (~ 2.0×10^{-2} M) of compounds studied.

Top left, 2,2-bipyridine, Top right, 2,3'-bipyridine, Middle left, 2,4'-bipyridine, Middle right, 3,3'-bipyridine, Bottom , 4,4'-bipyridine.

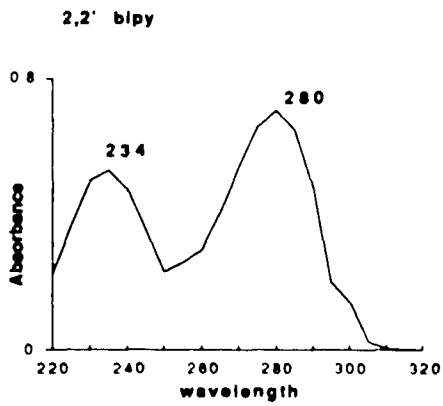
2,2' bipy
0.8
0
Absorbance
234
280
220
240
260
280
300
320
wavelength

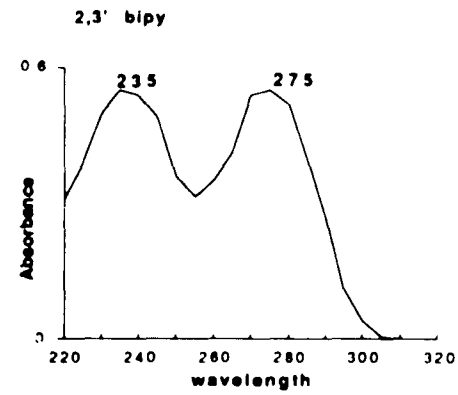
2,3' bipy
0.6
0
Absorbance
235
275
220
240
260
280
300
320
wavelength

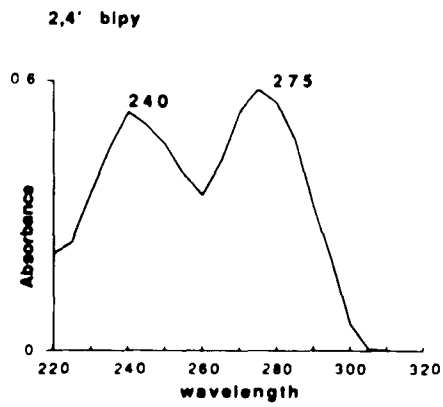
2,4' bipy
0.6
0
Absorbance
240
275
220
240
260
280
300
320
wavelength

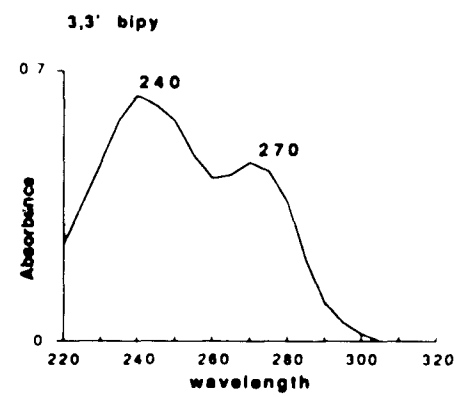
3,3' bipy
0.7
0
Absorbance
240
270
220
240
260
280
300
320
wavelength

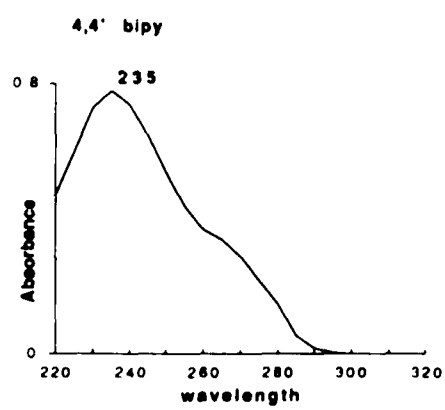
4,4' bipy
0.8
0
Absorbance
235
220
240
260
280
300
320
wavelength

Figure 8 : Ultraviolet absorption spectra of stock solutions (~ 2.0×10^{-2} M) of compounds studied.

Top left, 4,4'-dimethyl-2,2'-bipyridine,

Top right, $Ag(2,2\text{-bipy})_2(+1)$,

Middle left, 2-phenylpyridine,

Middle right, 3-phenylpyridine,

Bottom, 4-phenylpyridine.

4,4' dimethyl 2,2' bipy

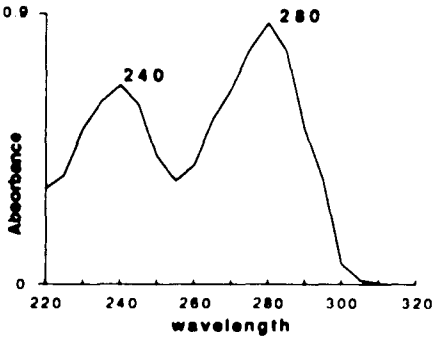

Ag(2,2' bipy)2 (+1)

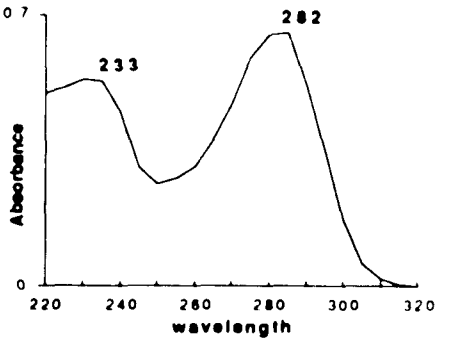

2 phenylpyridine

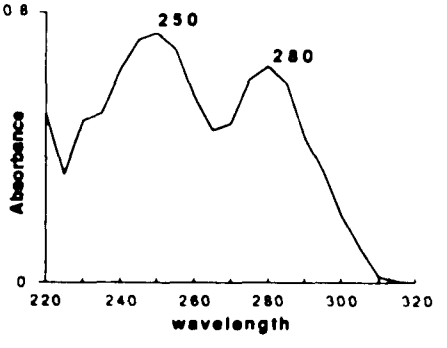

3 phenylpyridine

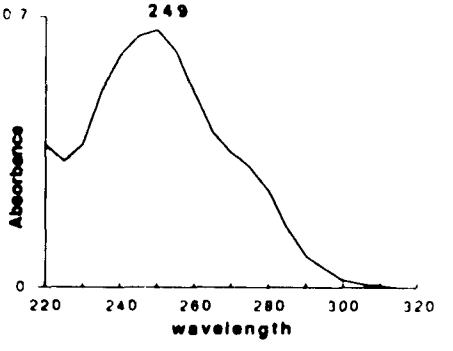

4 phenylpyridine

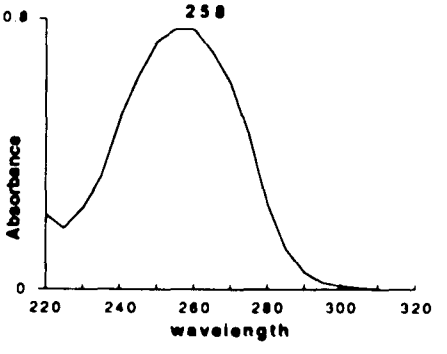

4. Princeton Instruments ST-100 detector controller. Used to provide power, thermostating and timing signals to the detector head.

5. PC Limited 286 personal computer equipped with a 20 Megabyte hard disk and interfaced to the detector controller. Spectra were collected and processed by using OSMA (Optical Spectrometric Multichannel Analyzer) operating system and software package. Spectra were plotted on an IBM 7371 color plotter.

Figure 9 is a diagram of the Raman spectrometer described above.

SAMPLE PREPAPATION

Samples were prepared by mixing 5 volumes of colloid (500 μl) with 1 volume (100 μl) of stock solution of the compound to be studied. The total volume prepared was always less than 1 ml. The final sol concentrations of the molecules studied fall in the range: $6.8X10^{-4}$ to $3.1x10^{-3}$ M. Dilution studies were conducted to check for qualitative changes in the SERS spectra of the molecules studied, but none were found.

All the mixtures of colloid and substrate molecule became unstable and led to the precipitation of large aggregates with deterioration of their SERS signal after a variable period of

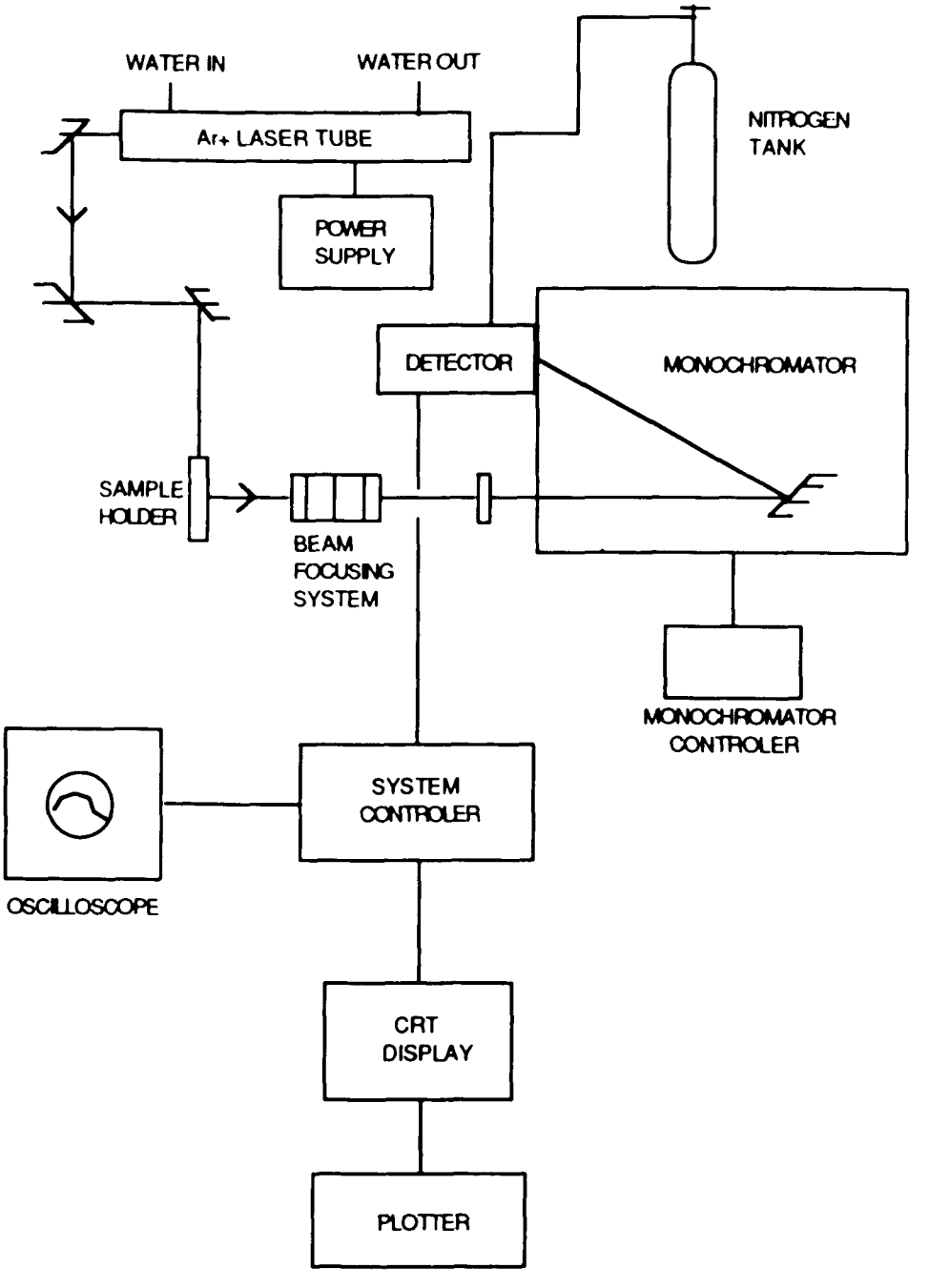

Figure 9 : Schematic of a laser Raman spectrometer with a diode array detector.

time. This time was on the order of about 10 minutes for the 4,4'-bipyridine and N-Methyl-4,4'-bipyridinium. For the remainder of the molecules investigated, the colloid substrate mixture was stable for at least one hour, as can be seen from the ability to record SERS spectra. Optimal SERS spectra corresponding to maximum surface enhancement of the molecule, were recorded after an initial time lag which ranged from several minutes to about one hour.

All Raman and SERS spectra were run in 100 μl 1mm i.d. glass capillary cells using transverse excitation and 90^{o} scattering.

RESULTS

The Raman spectra of the isomeric bipyridines in the 700-1700 cm^{-1} region are shown on the top of the following figures: 4,4'-bipyridine (fig.11), 2,4'-bipyridine (fig. 13), 3,3'-bipyridine (fig.15), 2,3'-bipyridine (fig. 16), and 2,2' bipyridine (fig.18). The SERS spectra in the same spectral region of these molecules are presented in the bottom of the same figures. The Raman and SERS spectra of the isomeric phenylpyridines in the 700-1700 cm^{-1} region are shown in the top (Raman) and bottom (SERS) of figures: 12 for 4-phenyl pyridine, 17 for 3-phenylpyridine and 24 for 2-phenylpyridine.

Figure 14 shows the SERS spectrum of N-methyl-4,4'-bipyridinium (700-1700 cm^{-1}). The Raman spectrum of 2,2'-bipyridine dissolved in 1M Hcl (monoprotonated) is shown in figure 19 (top). The SERS spectrum of the same compound is shown in the bottom of the the same figure (700-1700 cm^{-1}). In figure 20 the Raman spectrum of 2,2'-bipyridine dissolved in chloroform (bottom) is presented. The Raman and SERS spectra of Ag $(2,2'bpy)_2(+1)$ are shown on the top and bottom of figure 21 (700-1700 cm^{-1}). The Raman and SERS of the remaining compounds studied are shown in the top and bottom of figures: 22 for 1,10-phenathroline, 23 for 4,4'-dimethyl-2,2'- bipyridine, 25 for 2,2'-dipyridylketone, 27 for pyridine, and 28 for 2,2'-dipyridylamine (all in the 700-1700 cm^{-1} range). The SERS spectra for the C-H stretching region (2900-3200 cm^{-1}) for all the molecules studied are shown in figures 32 through 37.

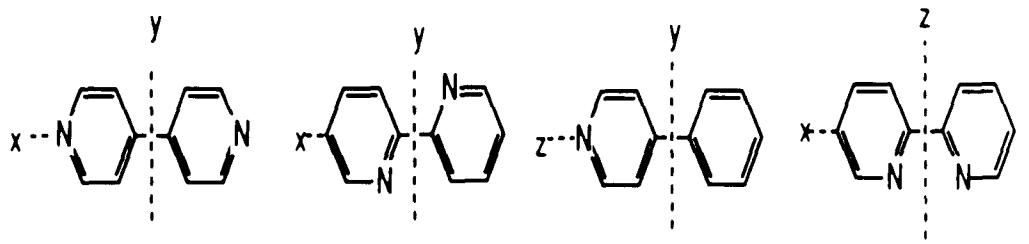

D_{2h}	C_{2h}	C_{2v}	C_{2v}
A_g x^2, y^2, z^2	A_g x^2, y^2, z^2	A_1 x^2, y^2, z^2	A_1 x^2, y^2, z^2
B_{1g} xy	A_g xy	B_2 yz	B_1 xz
B_{2u}	B_u	B_2 yz	A_1 x^2, y^2, z^2
B_{3u}	B_u	A_1 x^2, y^2, z^2	B_1 xz

Figure 10: Symmetry species of in plane modes for representative molecules, including molecular polarizability components and molecular axis designations.

Figure 11 : Top, Raman spectrum of solid 4,4'-bipyridine. Excitation wavelength 457.9 nm, laser power 100mW, entrance slit 500 microns, 30 exposures, 1.33 sec/exp. Bottom, SERS spectrum of 4,4'-bipyridine (1.0×10^{-3} M) dissolved in water adsorbred on silver sol. Excitation wavelength 514.5 nm, laser power 150 mW, entrance slit 400 microns, 30 exposures, 5.33 sec./exp.

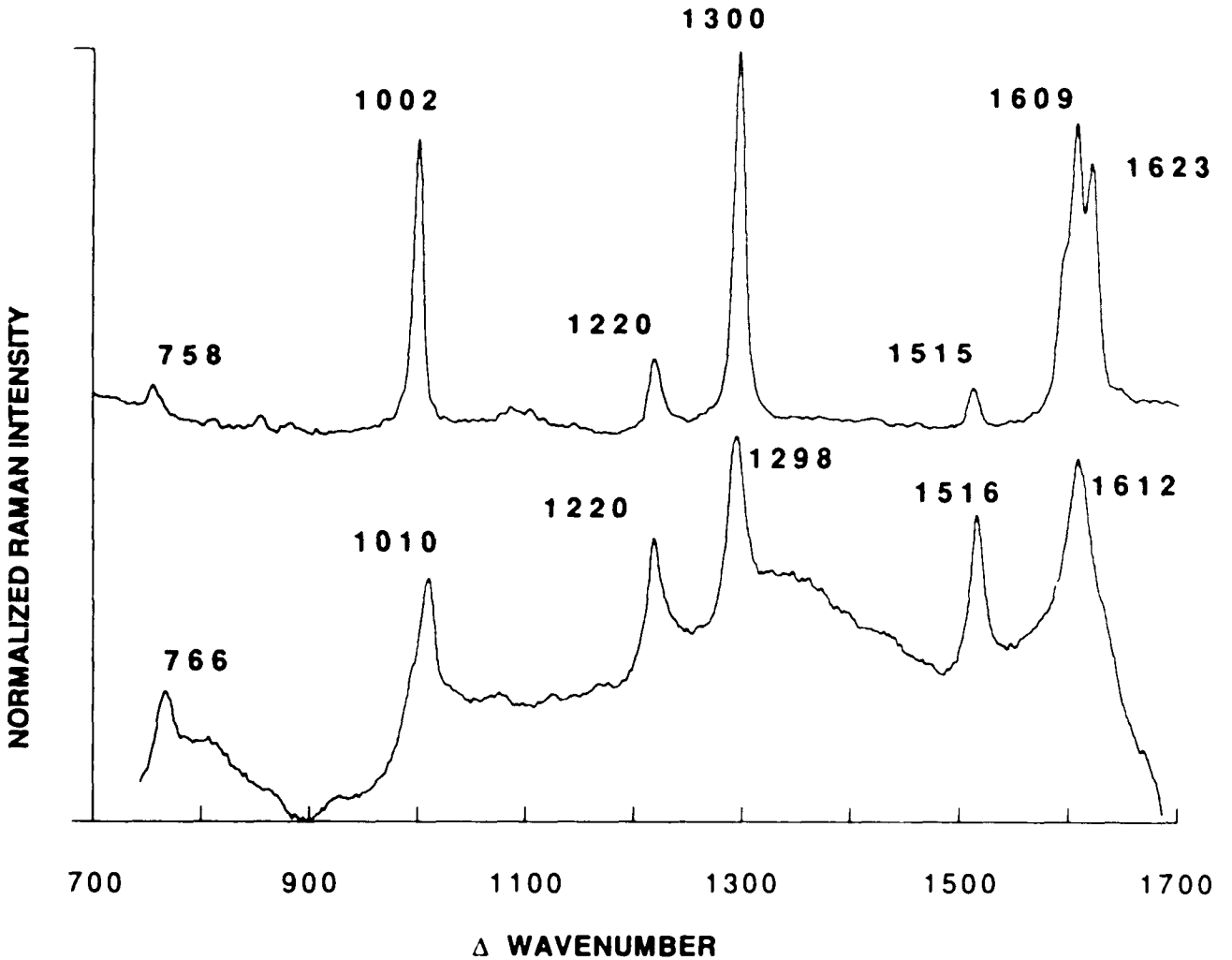
1300
1002
1609
1623
758
1220
1515
1298
1516
1612
1220
1010
766
NORMALIZED RAMAN INTENSITY
700
900
1100
1300
1500
1700
Δ WAVENUMBER

Figure 12 : Top, Raman spectrum of solid 4-phenylpyridine. Excitation wavelength 457.9 nm, laser power 100 mW, entrance slit 500 microns, 30 exposures, 1.33 sec./exp. Bottom, SERS spectrum of 4-phenylpyridine dissolved in 40% ethanol (1.0×10^{-3} M) adsorbed on sol surface. Excitation wavelength 514.5 nm laser power 100 mW, entrance slit 400 microns, 30 exposures,1.33 sec./exp.

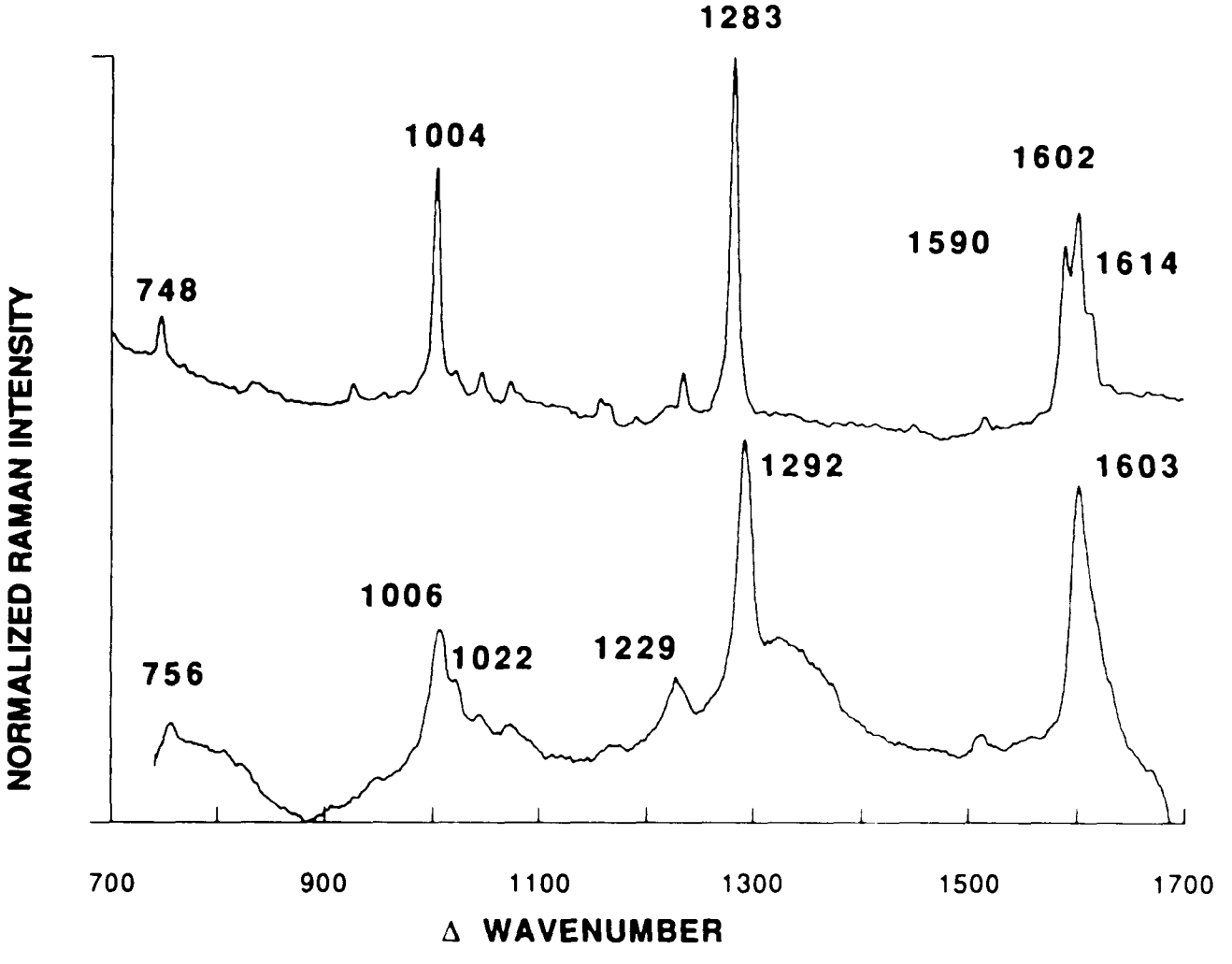
1283
1004
1602
1590
1614
748
1292
1603
1006
1022
1229
756
NORMALIZED RAMAN INTENSITY
700
900
1100
1300
1500
1700
Δ WAVENUMBER

Figure 13 : Top. Raman spectrum of solid 2,4'-bipyridine. Excitation wavelength 457.9 nm, laser power 100 mW, entrance slit 500 microns, 50 exposures, 6.67 sec./exp. Bottom. SERS spectrum of 2,4'-bipyridine dissolved in water, (1.0×10^{-3} M) adsorbed on silver sol. Excitation wavelength 514.5 nm, laser power 100 mW, 30 exposures, 1.33 sec./exp.

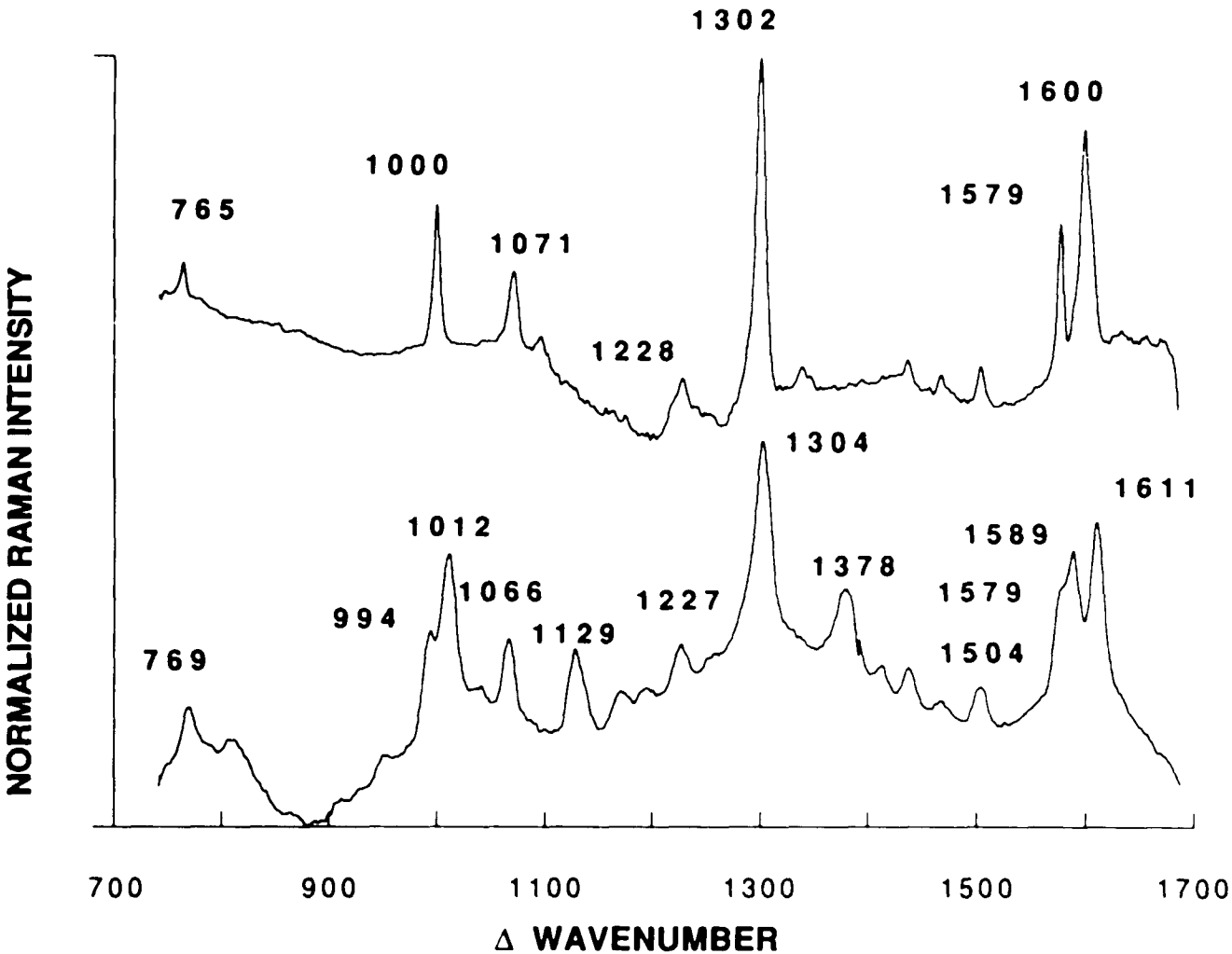
1302
1600
1000
765
1579
1071
1228
1304
1611
1012
1589
1378
1066
1579
994
1227
1129
1504
769
NORMALIZED RAMAN INTENSITY
700
900
1100
1300
1500
1700
Δ WAVENUMBER

Figure 14 : SERS spectrum of N-methyl-4,4'-bipyridinium dissolved in water (1.0×10^{-3} M), adsorbed on silver sol. Sample is unstable and decomposes fast upon mixing with sol. Excitation wavelength 514.5 nm, laser power 100 mW, entrance slit 500 microns, 30 exposures, 2.67 sec./exp.

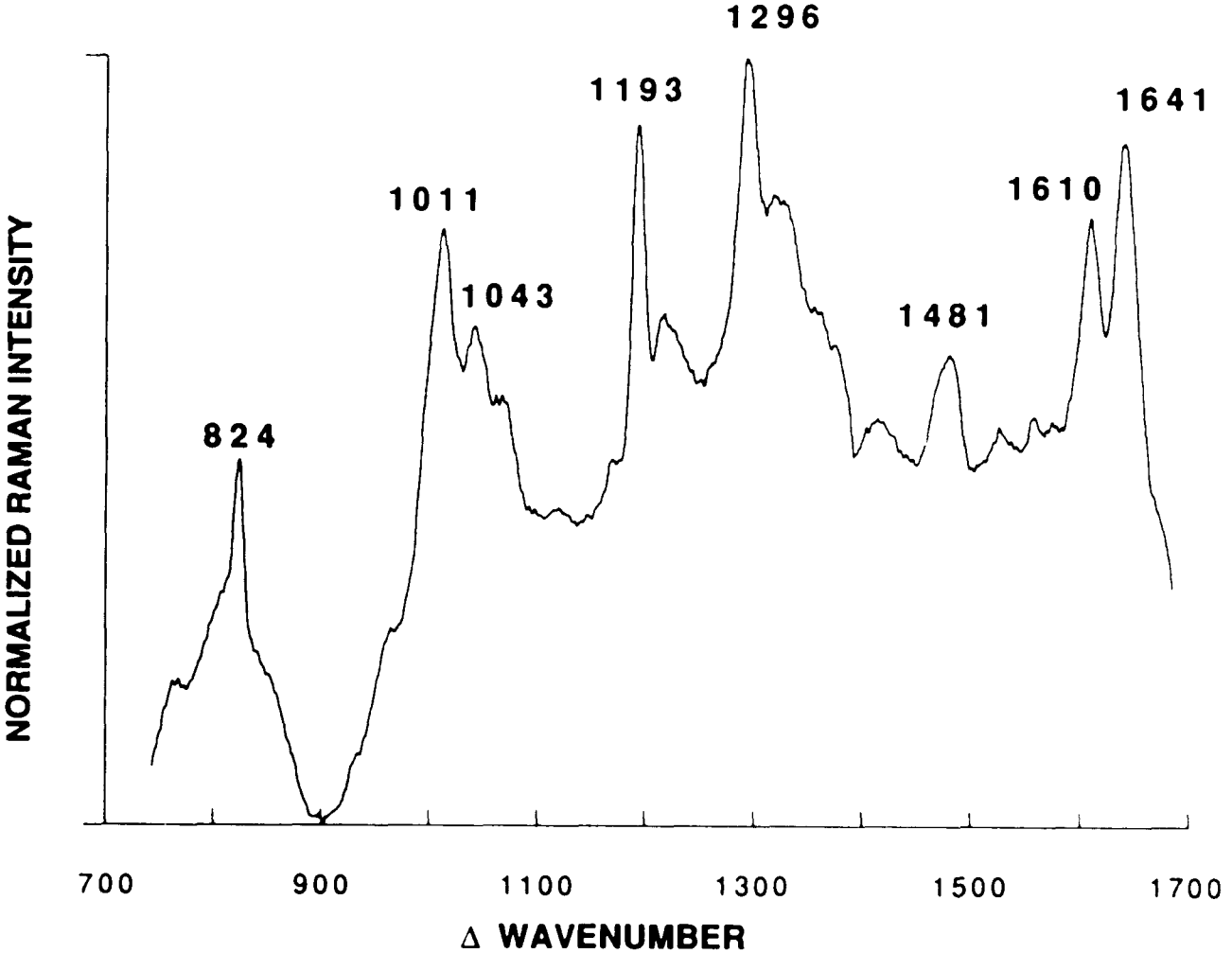
1296
1193
1641
1011
1610
1043
1481
824
NORMALIZED RAMAN INTENSITY
700
900
1100
1300
1500
1700
Δ WAVENUMBER

Figure 15 : Top. Raman spectrum of solid 3,3'-bipyridine. Excitation wavelength 457.9 nm, laser power 100 mW, entance slit 500 microns, 20 exposures, 1.67 sec./exp. Bottom. SERS spectrum of 3,3'-bipyridine dissolved in water (1.0×10^{-3} M), adsorbed on silver sol. Excitation wavelength 514.5 nm, laser power 100 mW, entrance slit 400 microns, 30 exposures, 1.33 sec./exp.

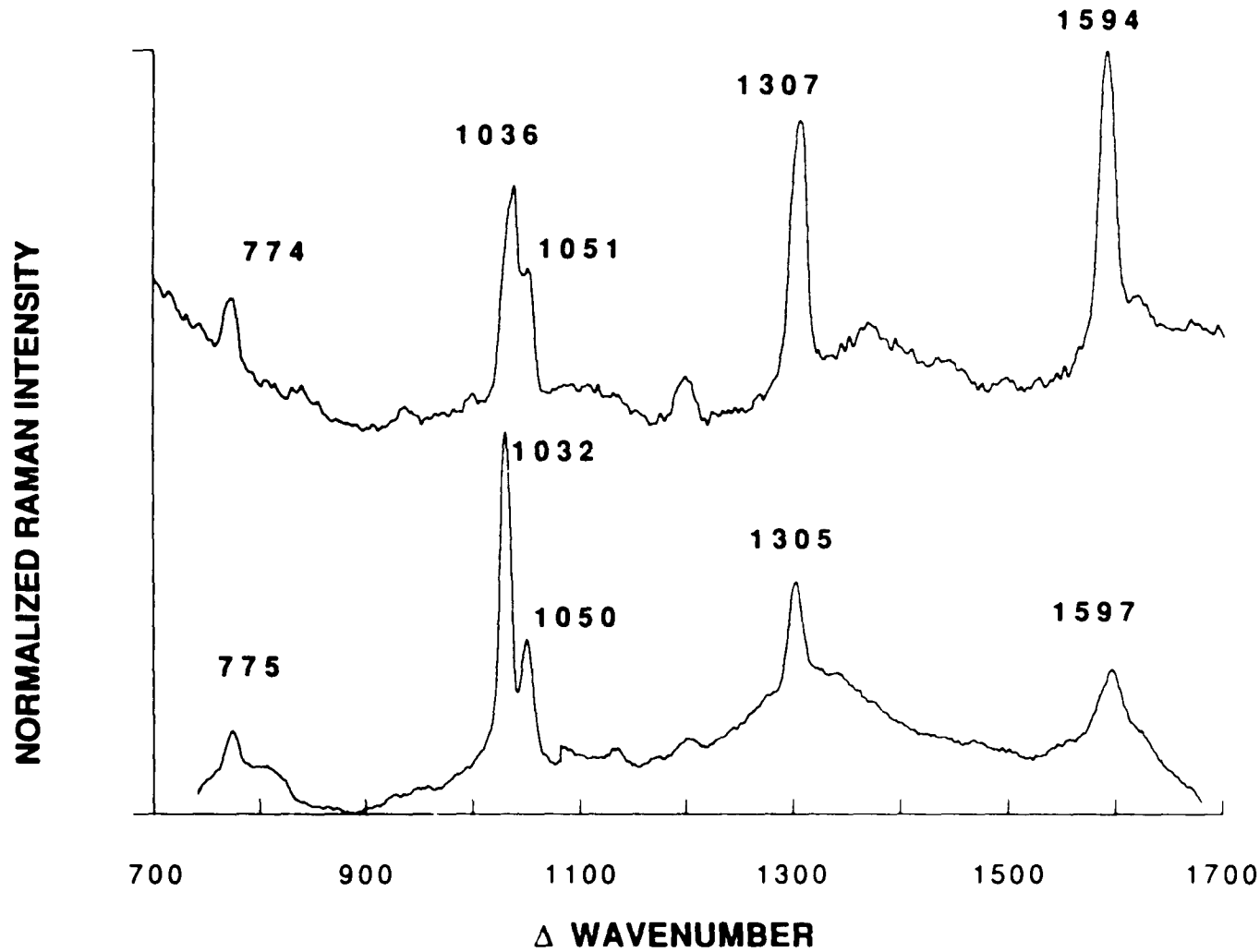
1594
1307
1036
774
1051
1032
1305
1050
1597
775
NORMALIZED RAMAN INTENSITY
700
900
1100
1300
1500
1700
Δ WAVENUMBER

Figure 16 : Top. Raman spectrum of liquid 2,3'-bipyridine. Excitation wavelength 514.5 nm, laser power 100 mW, entrance slit 400 microns, 30 exposures, 1.67 sec./exp. Bottom. SERS spectrum of 2,3'-bipyridine dissolved in water (1.0×10^{-3} M), adsorbed on silver sol. Excitation wavelength 514.5 nm laser power 100 mW, entance slit 400 microns, 30 exposures, 4.0 sec./exp.

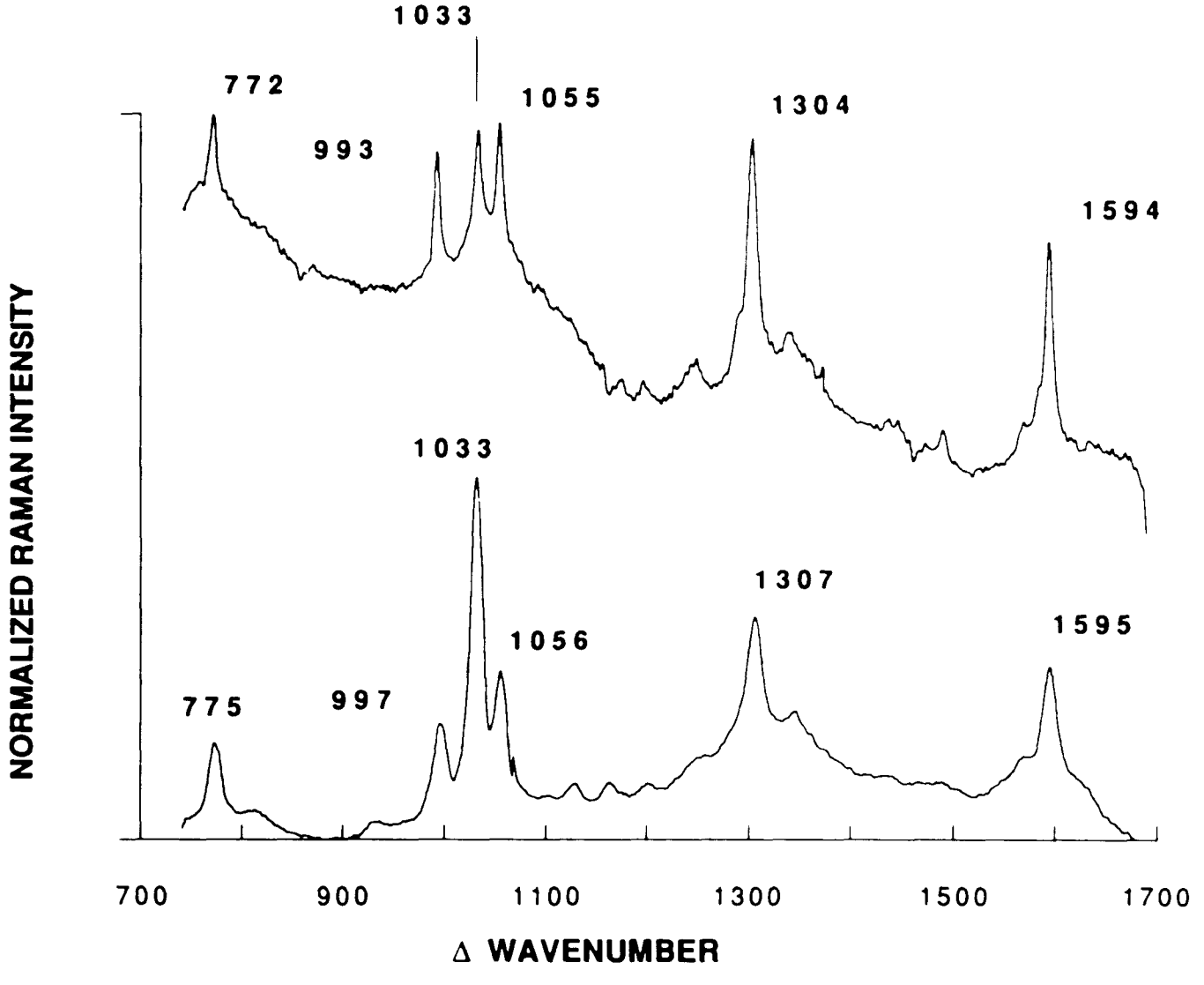
1033
772
1055
1304
993
1594
1033
1307
1056
1595
775
997
NORMALIZED RAMAN INTENSITY
700
900
1100
1300
1500
1700
Δ WAVENUMBER

Figure 17 : Top. Raman spectrum of liquid 3-phenylpyridine. Excitation wavelength 514.5 nm, laser power 100 mW, entrance slit 500 microns, 30 exposures, 1.33 sec./exp. Bottom. SERS spectrum of 3-phenylpyridine dissolved in 40% ethanol (1.0×10^{-3} M), adsorbed on silver sol. Excitation wavelength 514.5 nm, laser power 100 mW, entance slit 400 microns, 30 exposures, 1.67 sec./exp.

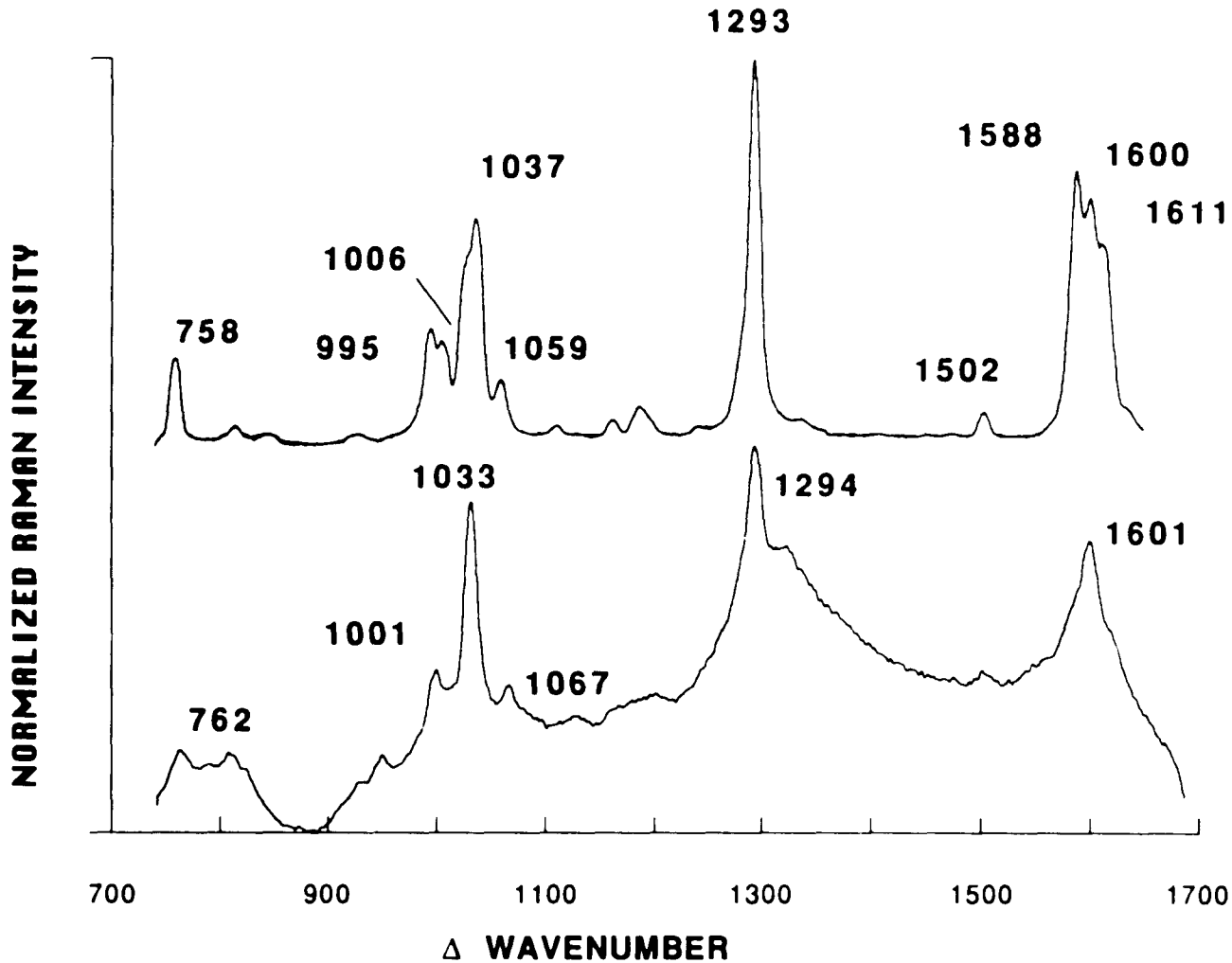
1293
1588
1600
1611
1037
1006
758
995
1059
1502
1033
1294
1601
1001
1067
762
NORMALIZED RAMAN INTENSITY
700
900
1100
1300
1500
1700
Δ WAVENUMBER

Figure 18 : Top. Raman spectrum of solid 2,2'-bipyridine. Excitation wavelength 457.9 nm, laser power 150 mW, entrance slit 400 microns, 30 exposures, 3.3 sec./exp. Bottom. SERS spectrum of 2,2'-bipyridine dissolved in water (1.0×10^{-3} M), adsorbed on silver sol. Excitation wavelength 514.5 nm, laser power 100 mW, entrance slit 500 microns, 30 exposures, 1.33 sec./exp.

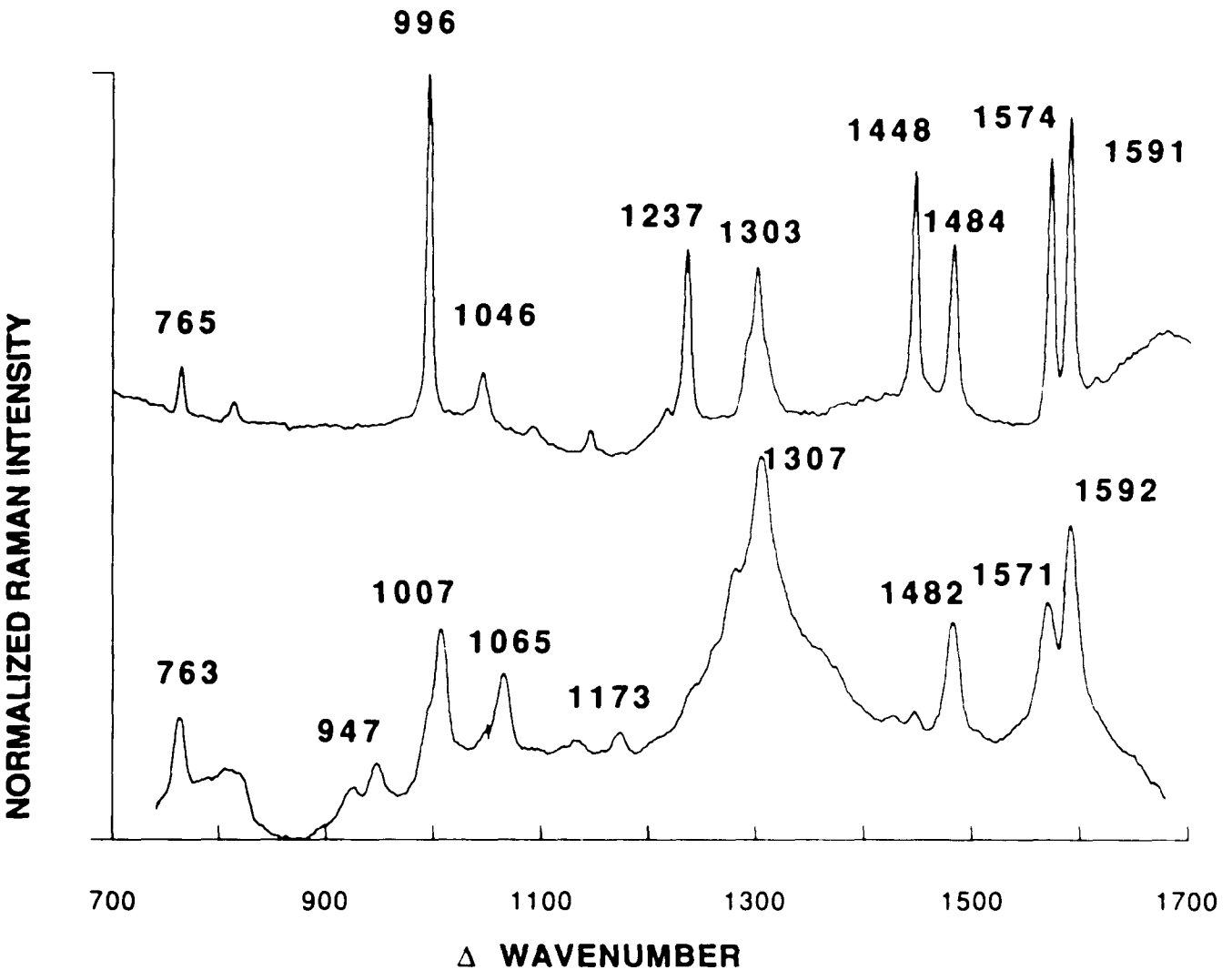
996
1448
1574
1591
1237
1303
1484
765
1046
1307
1592
1007
1482
1571
1065
763
1173
947
NORMALIZED RAMAN INTENSITY
700
900
1100
1300
1500
1700
Δ WAVENUMBER

Figure 19 : Top. Raman spectrum of 2,2'-bipyridine dissolved in 1.0 M HCl (monoprotonated). Excitation wavelength 514.5 nm, laser power 150 mW, entrance slit 500 microns, 40 exposures, 1.67 sec./exp.

Bottom. SERS spectrum of 2,2'-bipyridine dissolved in water (1.0×10^{-3} M) , adsorbed on silver sol. Excitation wavelength 514.5 nm, laser power 100 mW, entrance slit 500 microns, 30 exposures, 1.33 sec./exp.

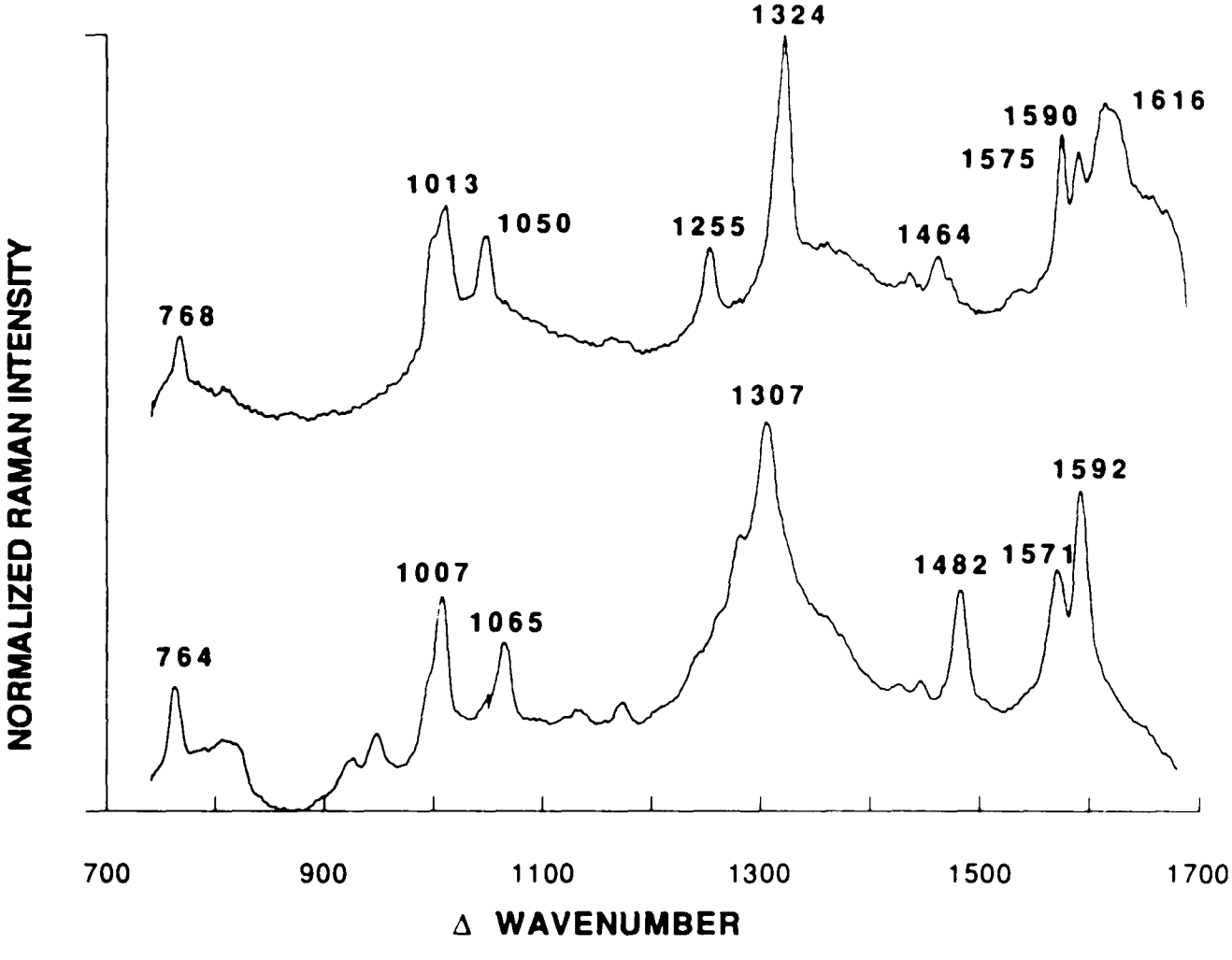
1324
1616
1590
1575
1013
1050
1255
1464
768
1307
1592
1482
1571
1007
1065
764
NORMALIZED RAMAN INTENSITY
700
900
1100
1300
1500
1700
Δ WAVENUMBER

Figure 20 : Top. Raman spectrum of solid 2,2'-bipyridine. Excitation wavelength 457.9 nm, laser power 120 mW, entrance slit 400 microns, 30 exposures, 3.3 sec./exp. Bottom. Raman spectrum of 2,2'-bipyridine dissolved in chloroform (2.0 M). Excitation wavelength 514.5 nm, laser power 100 mW, entrance slit 500 microns, 30 exposures, 1.33 sec./exp.

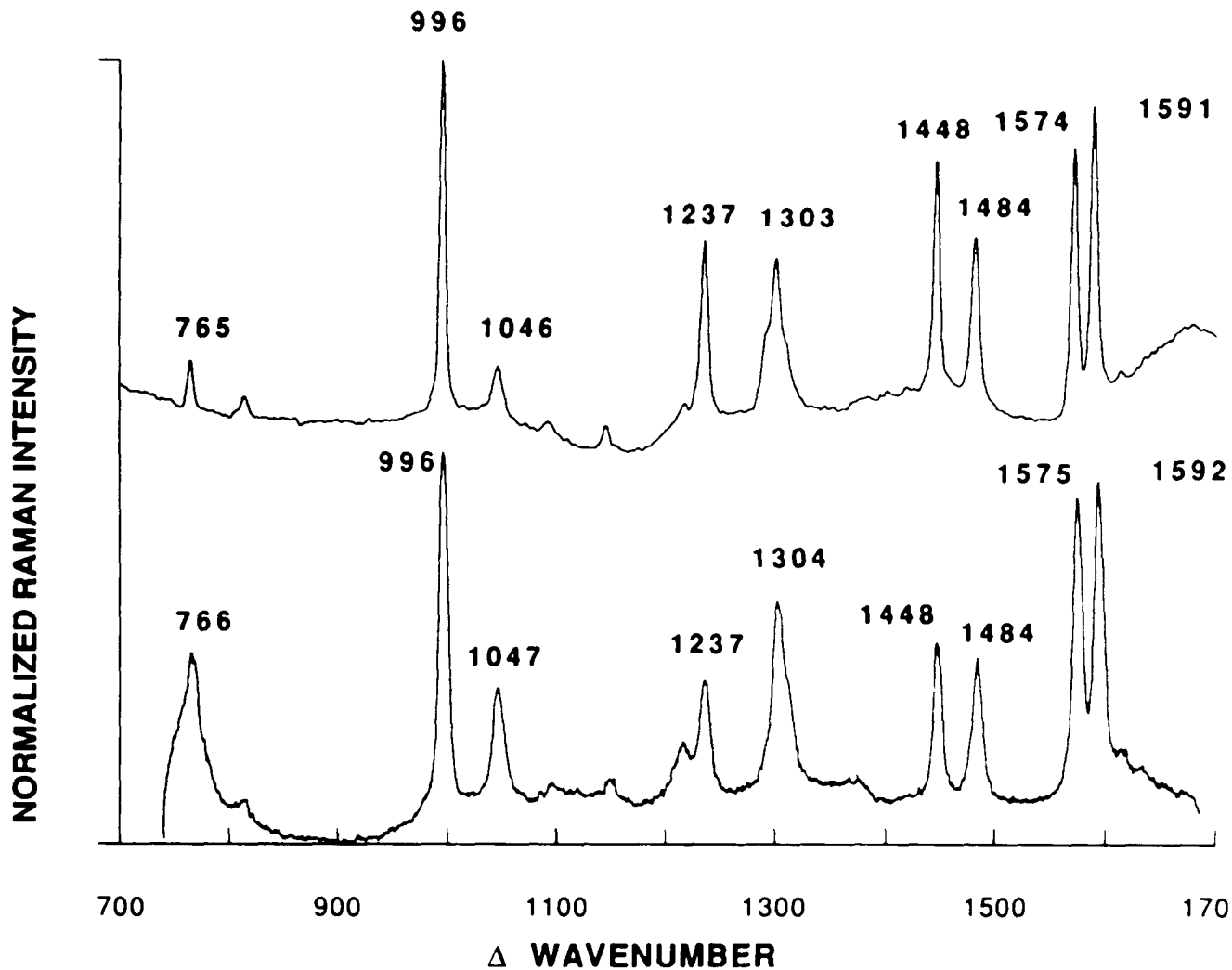
996
1448
1574
1591
1237
1303
1484
765
1046
996
1575
1592
1304
766
1448
1484
1047
1237
NORMALIZED RAMAN INTENSITY
700
900
1100
1300
1500
1700
Δ WAVENUMBER

Figure 21 : Top. Raman spectrum of solid $Ag(2,2'\text{-bpy})_2(+1)$. Excitation wavelength 514.5 nm, laser power 100 mW, entrance slit 600 microns, 30 exposures, 4.0 sec./exp. Bottom. SERS spectrum of $Ag(2,2'\text{-bpy})_2(+1)$ dissolved in water (1.0×10^{-3} M), adsorbed on silver sol. Sample unstable upon mixing with sol. Excitation wavelength 514.5 nm, laser power 100 mW entrance slit 500 microns, 30 exposures, 1.33 sec./exp.

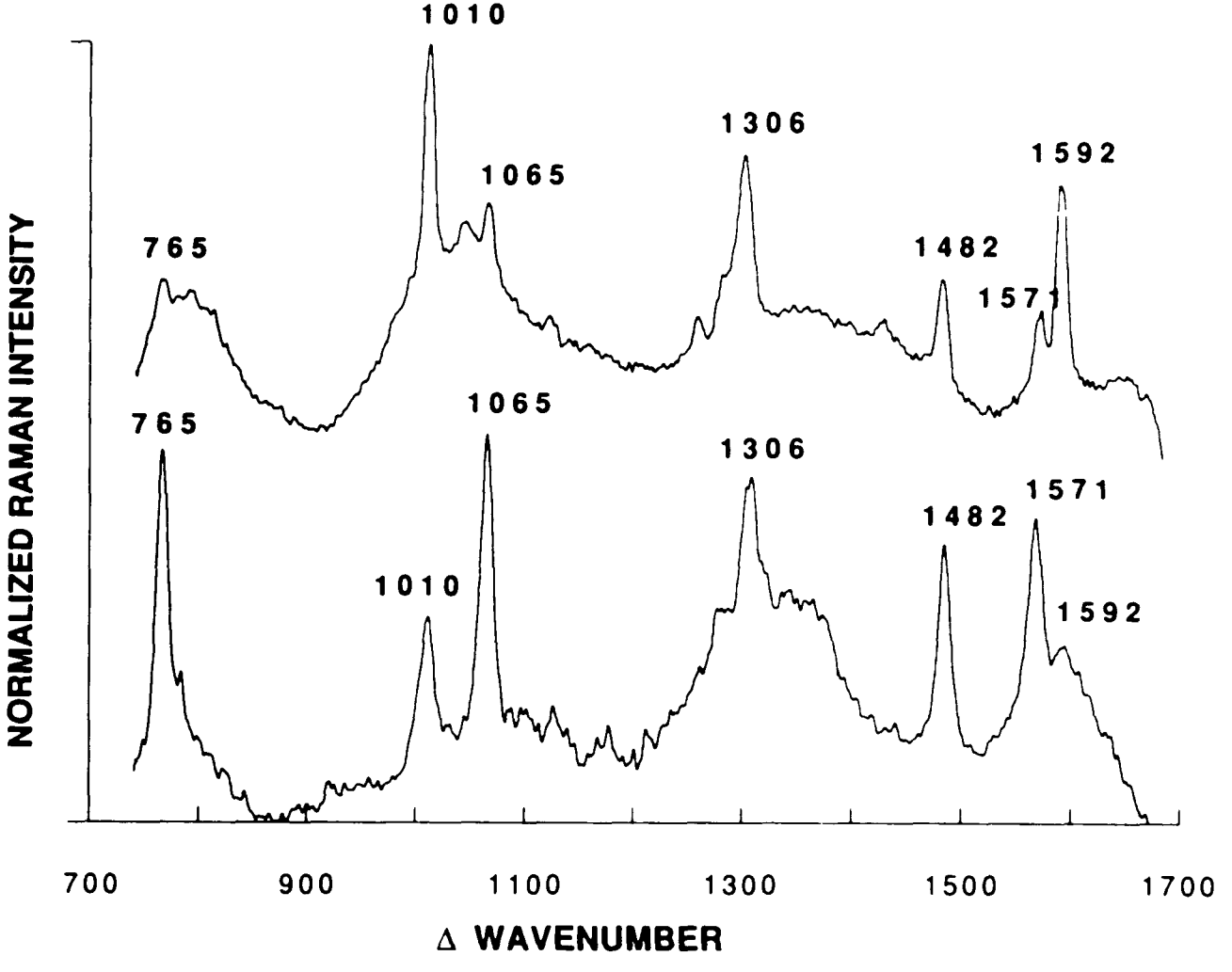
1010
1306
1065
1592
765
1482
1571
765
1065
1306
1571
1482
1010
1592
NORMALIZED RAMAN INTENSITY
700
900
1100
1300
1500
1700
Δ WAVENUMBER

Figure 22 : Top. Raman spectrum of solid 1,10-phenanthroline. Excitation wavelength 514.5 nm, laser power 50 mW, entrance slit 200 microns, 30 exposures, 1.33 sec./exp. Bottom. SERS spectrum of 1,10-phenantrhroline dissolved in water (1.0×10^{-3} M), adsorbed on silver sol. Excitation wavelength 514.5 nm, laser power 100 mW, entrance slit 500 microns, 30 exposures, 4.0 sec./exp.

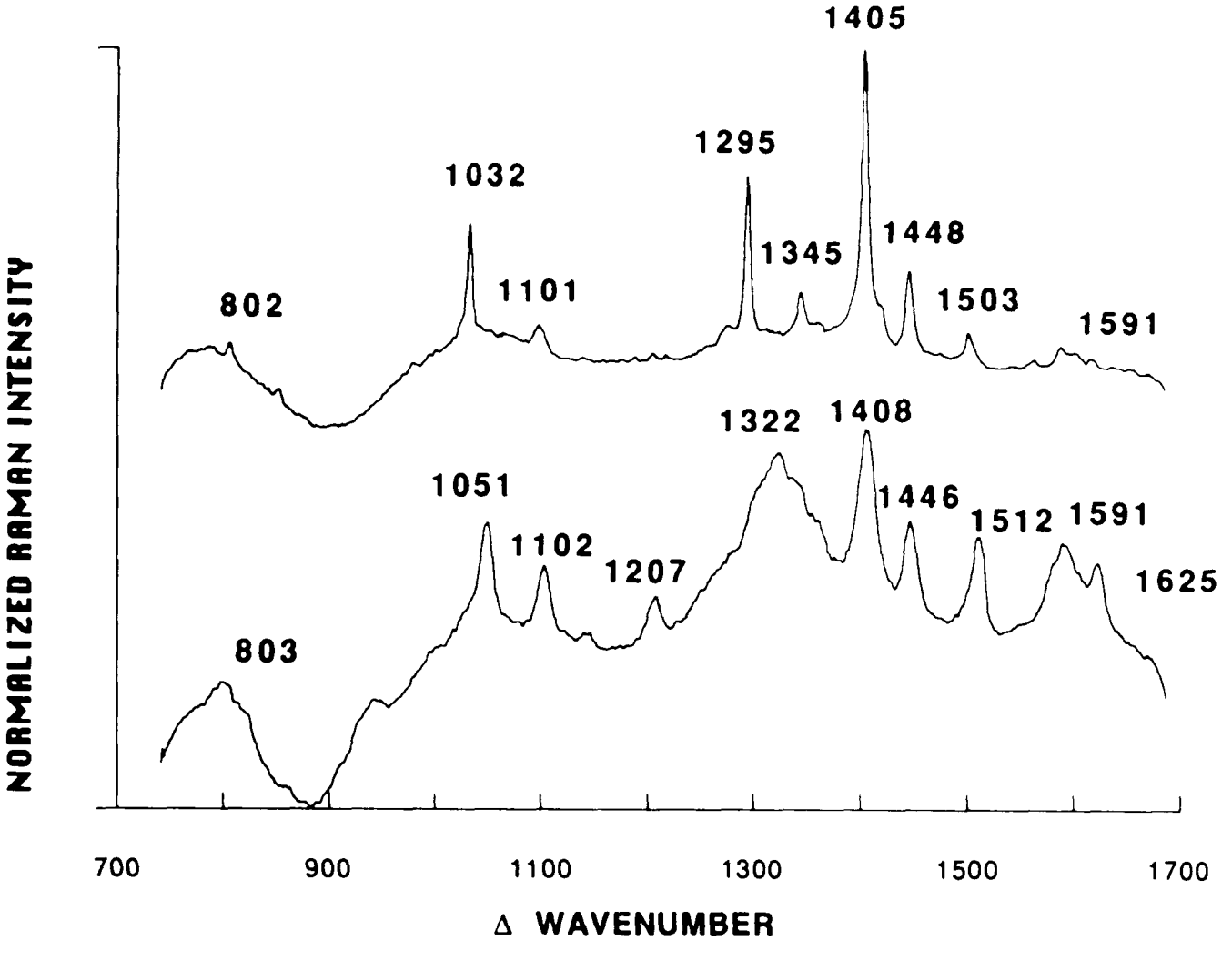
1405
1295
1032
1345
1448
802
1101
1503
1591
1322
1408
1051
1446
1512
1591
1102
1207
1625
803
NORMALIZED RAMAN INTENSITY
700
900
1100
1300
1500
1700
Δ WAVENUMBER

Figure 23 : Top. Raman spectrum of solid 4,4'-dimethyl-2,2' bipyridine. Excitation wavelength 457.9 nm, laser power 100 mW, entrance slit 400 microns, 30 exposures, 1.33 sec./exp.

Bottom. SERS spectrum of 4,4'-dimethyl-2,2'-bipyridine dissolved in water (1.0×10^{-3} M), adsorbed on silver sol. Excitation wavelength 514.5 nm, laser power 100 mW, entrance slit 600 microns, 30 exposures, 1.33 sec./exp.

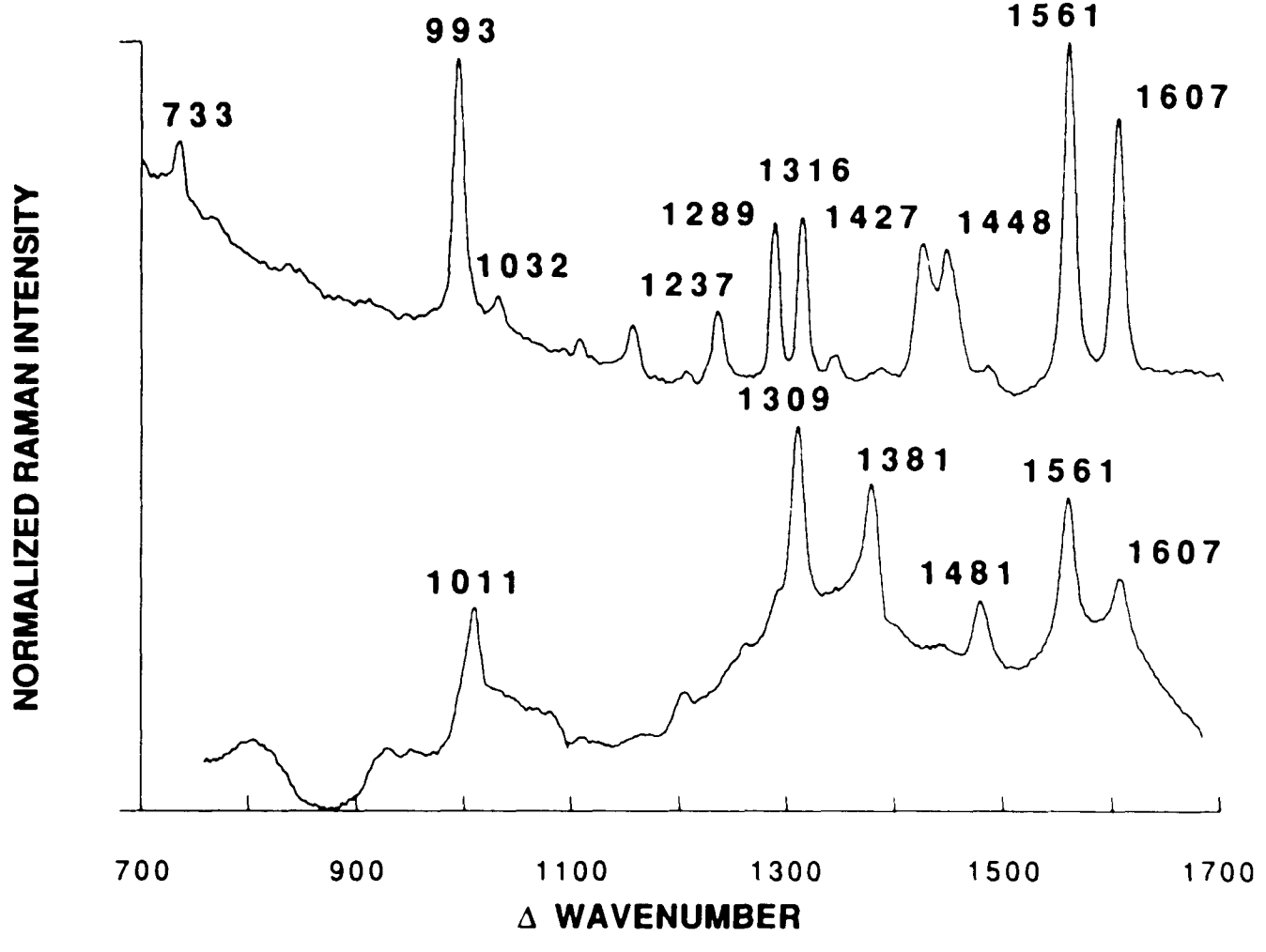
993
1561
733
1607
1316
1289
1427
1448
1032
1237
1309
1381
1561
1607
1011
1481
NORMALIZED RAMAN INTENSITY
700
900
1100
1300
1500
1700
Δ WAVENUMBER

Figure 24 : Top. Raman spectrum of liquid 2-phenylpyridine. Excitation wavelength 514.5 nm, laser power 100 mW, entrance slit 500 microns, 30 exposures, 1.33 sec./exp.
Bottom. SERS spectrum of 2-phenylpyridine dissolved in 40% ethanol (1.0×10^{-3} M), adsorbed on silver sol. Excitation wavelength 514.5nmlaser power 100 mW, entrance slit 400 microns, 30 exposures, 2.66 sec./exp.

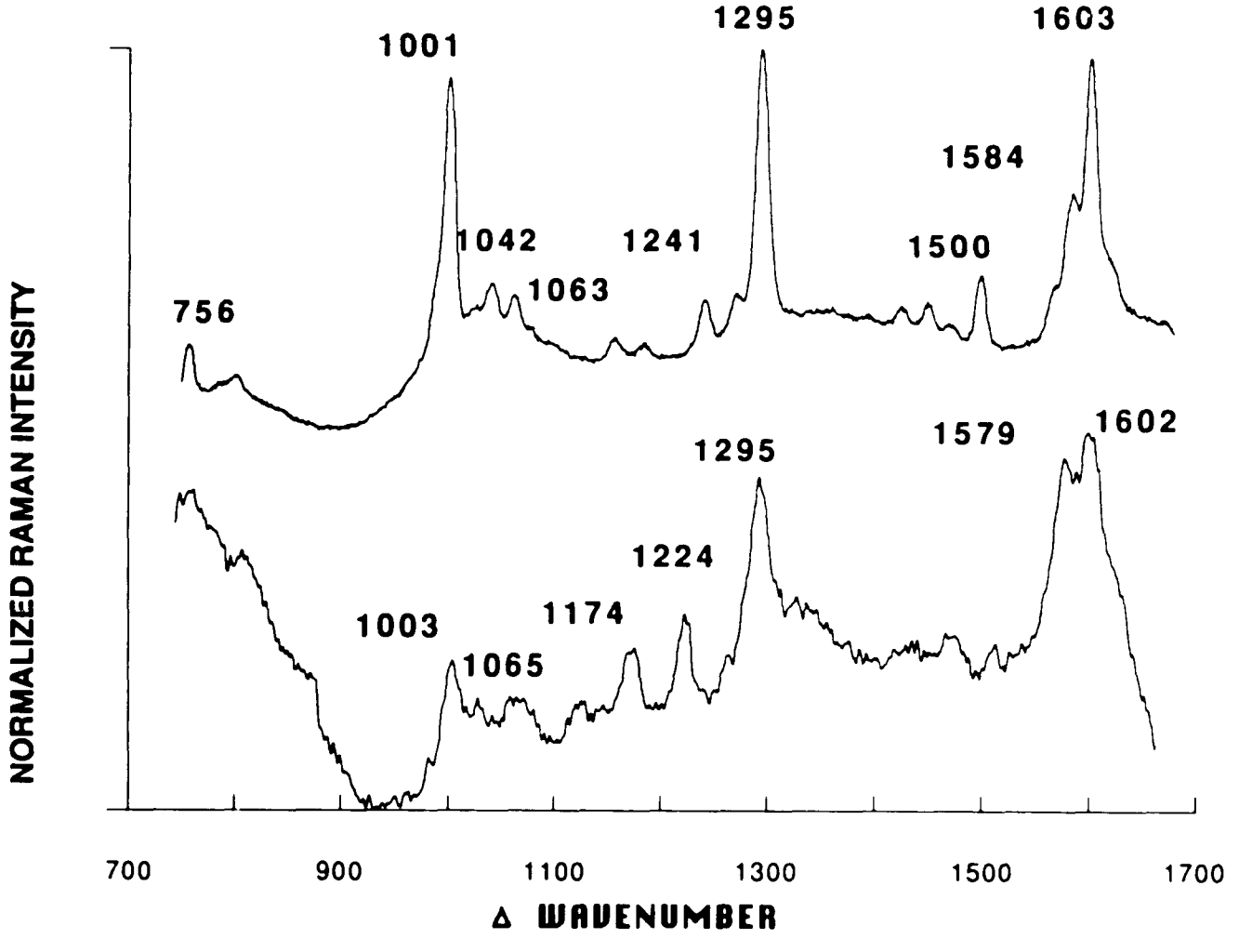
1001
1295
1603
1584
1042
1241
1500
1063
756
1579
1602
1295
1224
1003
1174
1065
NORMALIZED RAMAN INTENSITY
700
900
1100
1300
1500
1700
Δ WAVENUMBER

Figure 25 : Top. Raman spectrum of solid 2,2'-dipyridylketone. Excitation wavelength 457.9 nm, laser power 100 mW, entrance slit 300 microns, 30 exposures, 3.3 sec./exp.
Bottom. SERS spectrum of 2,2'-dipyridylketone dissolved in water (1.0×10^{-3}M), adsorbed on silver sol. Excitation wavelength 514.5 nm, laser power 80 mW, entrance slit 500 microns, 30 exposures, 1.33 sec./exp.

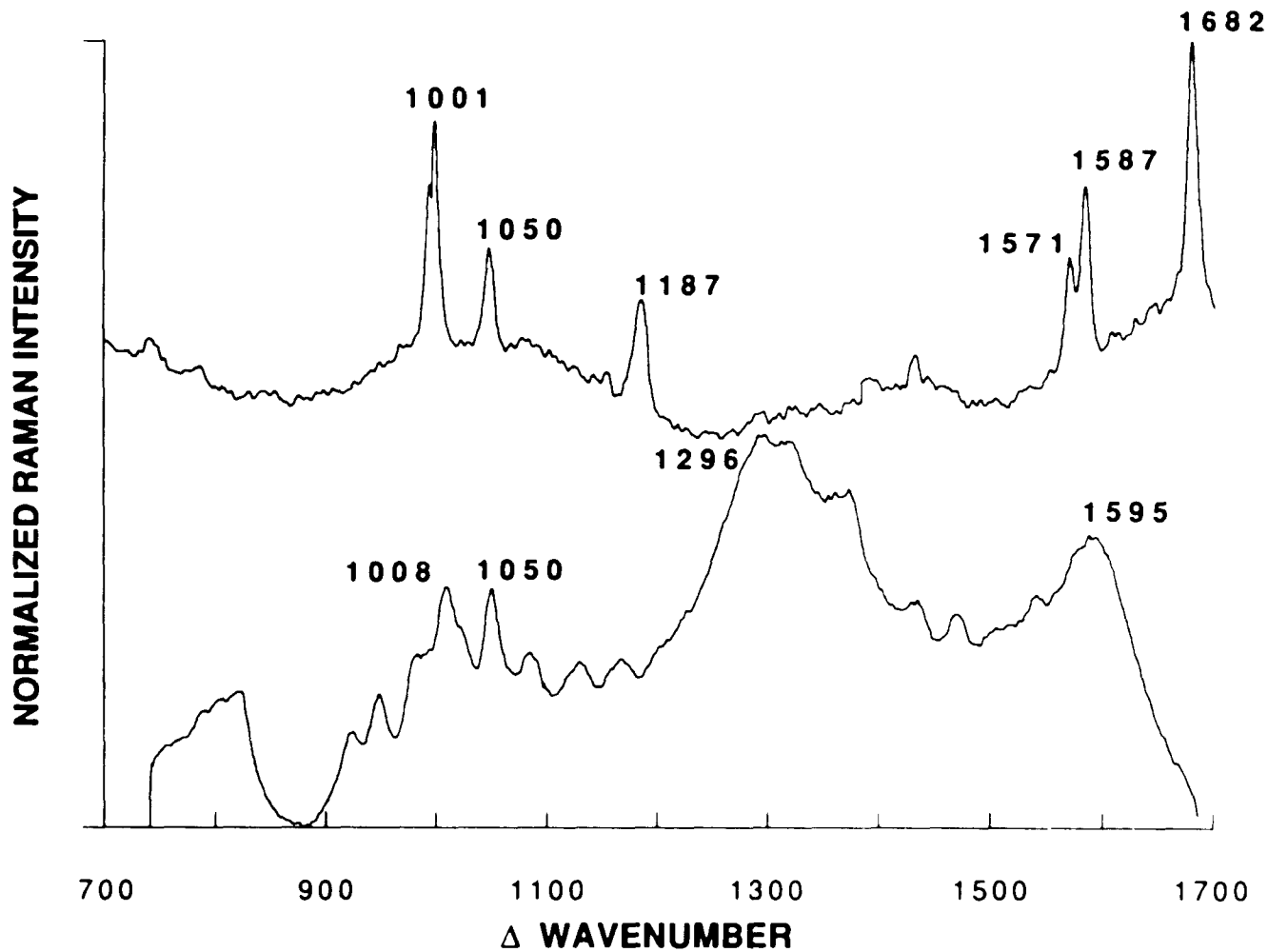
1682
1001
1587
1050
1571
1187
1296
1595
1008
1050
NORMALIZED RAMAN INTENSITY
700
900
1100
1300
1500
1700
Δ WAVENUMBER

Figure 26 : Top. SERS spectrum of 2,2-dipyridylketone dissolved in water (1.10×10^{-3} M), adsorbed on silver sol. Excitation wavelength 514.5 nm, laser power 80 mW, entrance slit 500 microns, 30 exposures, 1.33 sec./exp. Bottom. SERS spectrum of pyridine dissolved in water (1.0×10^{-3} M), adsorbed on silver sol. Excitation wavelength 514.5 nm, laser power 100 mW, entrance slit 500 microns, 30 exposures, 1.33 sec./exp.

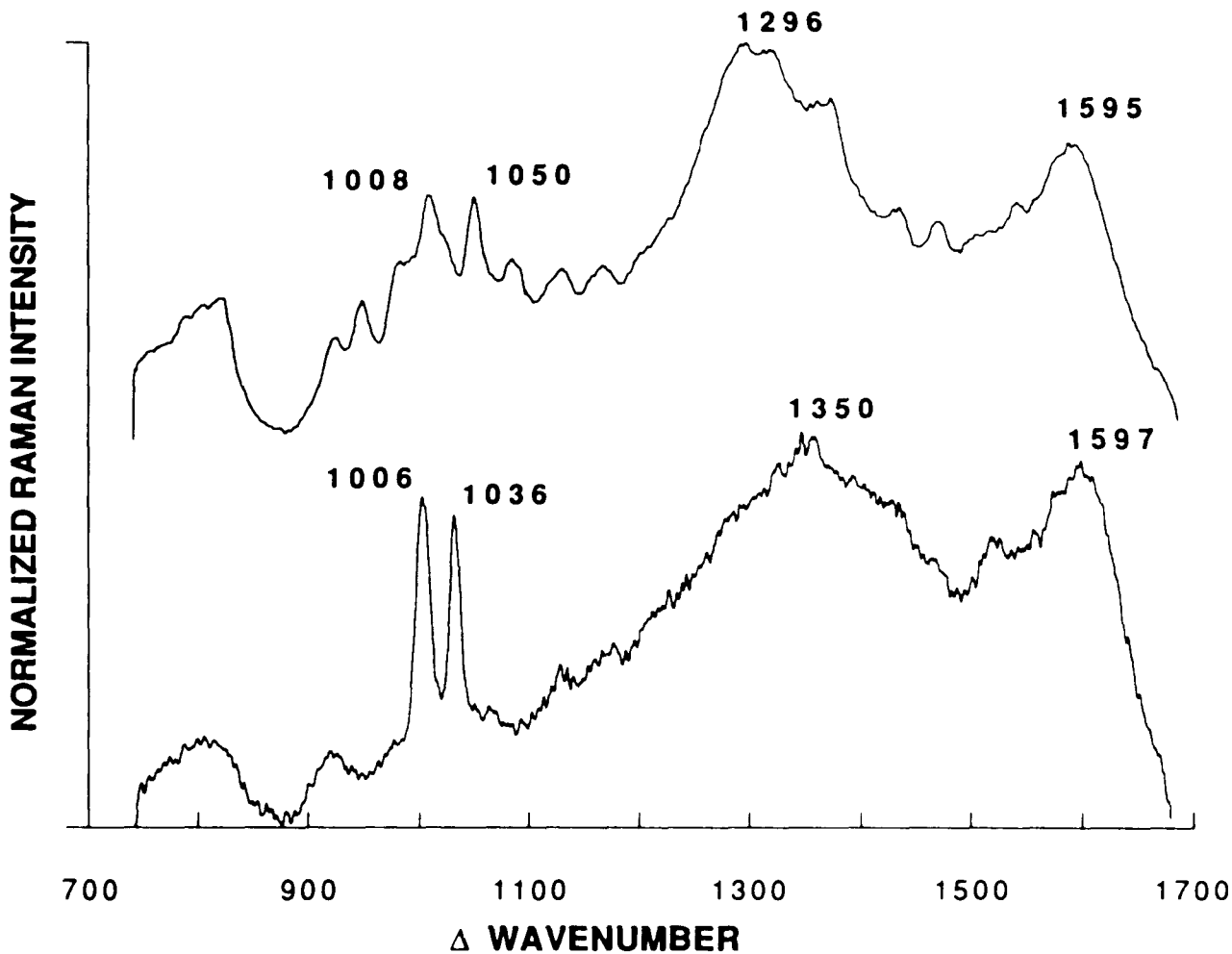
1296
1595
1008
1050
1350
1597
1006
1036
NORMALIZED RAMAN INTENSITY
700
900
1100
1300
1500
1700
Δ WAVENUMBER

Figure 27 : Top. Raman spectrum of liquid pyridine. Excitation wavelength 514.5 nm, laser power 100 mW, entrance slit 500 microns, 30 exposures, 1.33 sec./exp.
Bottom. SERS spectrum of pyridine dissolved in water (1.0×10^{-3} M), adsorbed on silver sol. Excitation wavelength 514.5 nm, laser power 100 mW, entrance slit 500 microns, 30 exposures, 1.33 sec./exp.

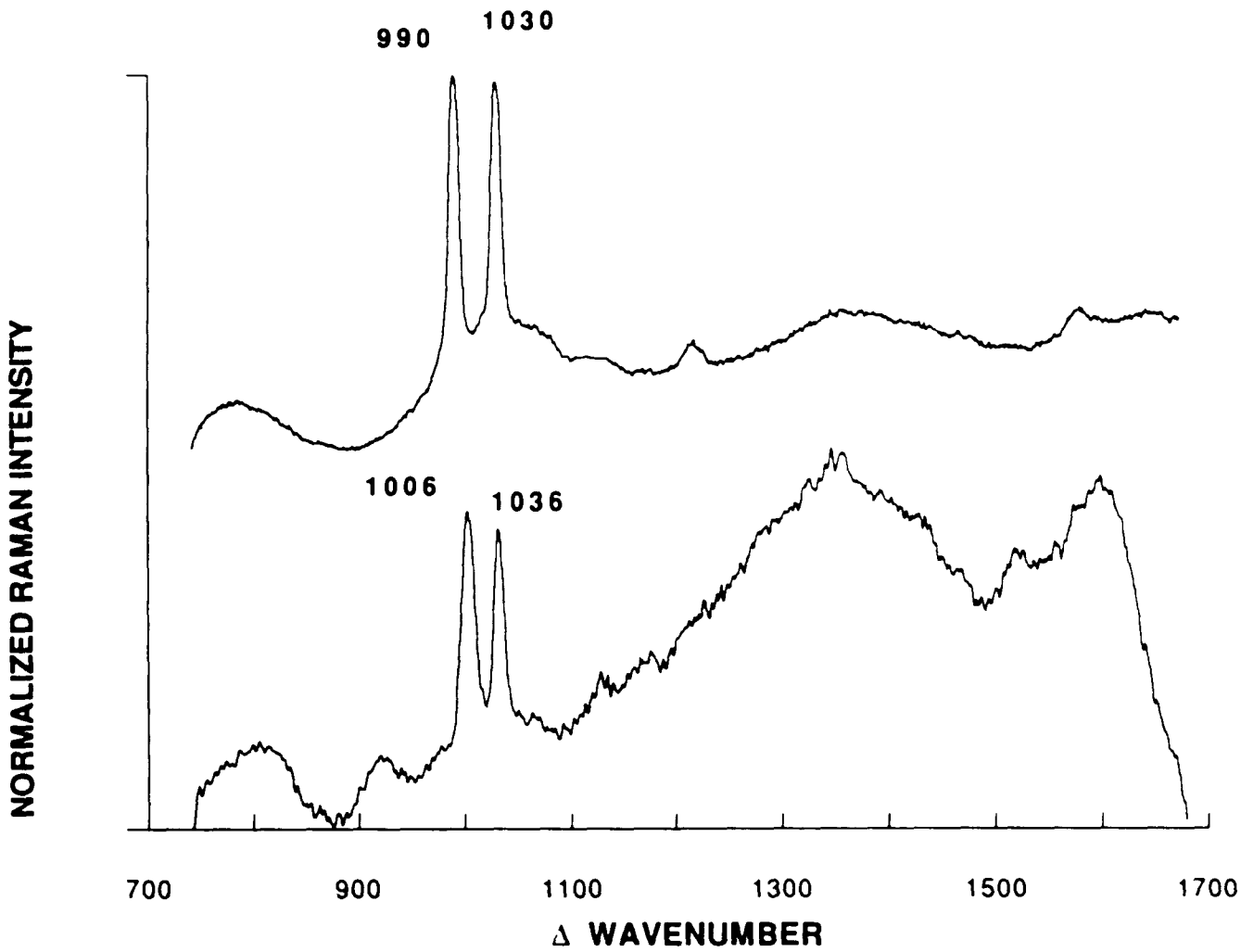
990
1030
1006
1036
NORMALIZED RAMAN INTENSITY
700
900
1100
1300
1500
1700
Δ WAVENUMBER

Figure 28 : Top. Raman spectrum of solid 2,2-dipyridylamine. Excitation wavelength 457.9 nm, laser power 100 mW, entrance slit 400 microns, 30 exposures, 1.33 sec./exp.
Bottom. SERS spectrum of 2,2'-dipyridylamine dissolved in in 50% ethanol (1.0×10^{-3} M), adsorbed on silver surface. Excitation wavelength 514.5 nm, laser power 100 mW, entrance slit 500 microns, 30 exposures, 1.33 sec./exp.

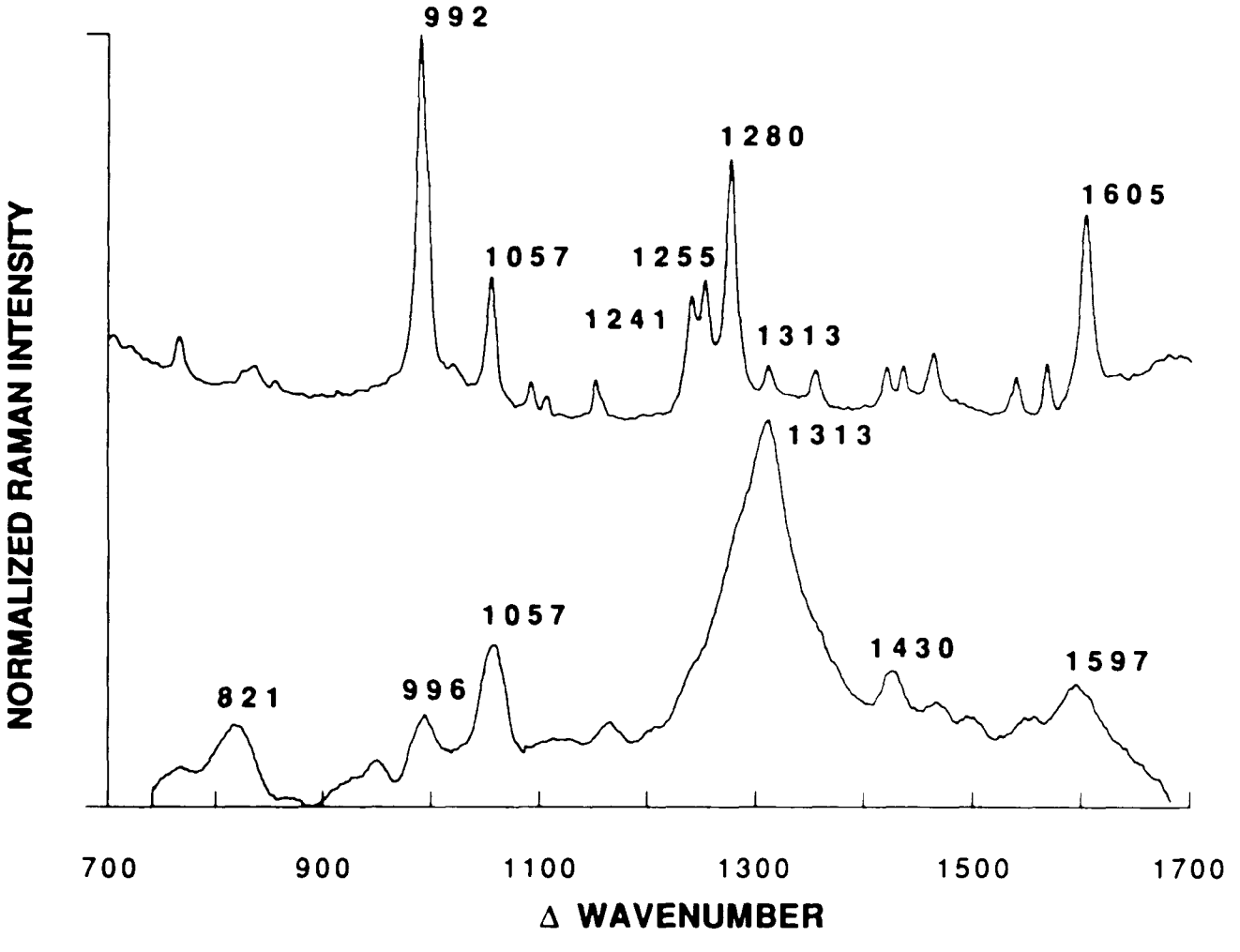
992
1280
1605
1057
1255
1241
1313
1313
1057
821
996
1430
1597
NORMALIZED RAMAN INTENSITY
700
900
1100
1300
1500
1700
Δ WAVENUMBER

DISCUSSION

CONCENTRATION DEPENDENCE OF SURFACE ENHANCEMENT

One of the questions addressed at an early stage of this investigation, was that of the importance of the adsorbate's concentration in the surface enhancement of its Raman spectrum. For this reason a series of dilution experiments was performed, using isomeric bipyridines. From stock solutions of these compounds a series of diluted solutions were prepared, and their SERS spectra were recorded under identical conditions. The relative Raman intensity of each of two selected peaks from each bipyridine, was plotted as a function of adsorbate concentration (concentration of compound when mixed with the silver sol). Figures 29 and 30 are two such graphs for 2,2' and 2,4'-bipyridine respectively. From these graphs it can be seen that, even though at small adsorbate concentrations, the SERS intensity increases almost exponentially with an increase in concentration. When the concentration becomes sufficiently high the intensity becomes almost independent of it. This can be seen from the leveling off of both graphs at about 1.0×10^{-3} M concentration of adsorbate. Similar results were obtained for the other bipyridines. These results tend to indicate that at sufficiently high concentrations of adsorbate the surface enhancement of its Raman spectrum is almost independent of its concentration.

Figure 29 : Plot of relative Raman intensity vs. adsorbate concentration for the 1305 and 1591 cm^{-1} peaks of 2,2-bipyridine adsorbed on silver sol.

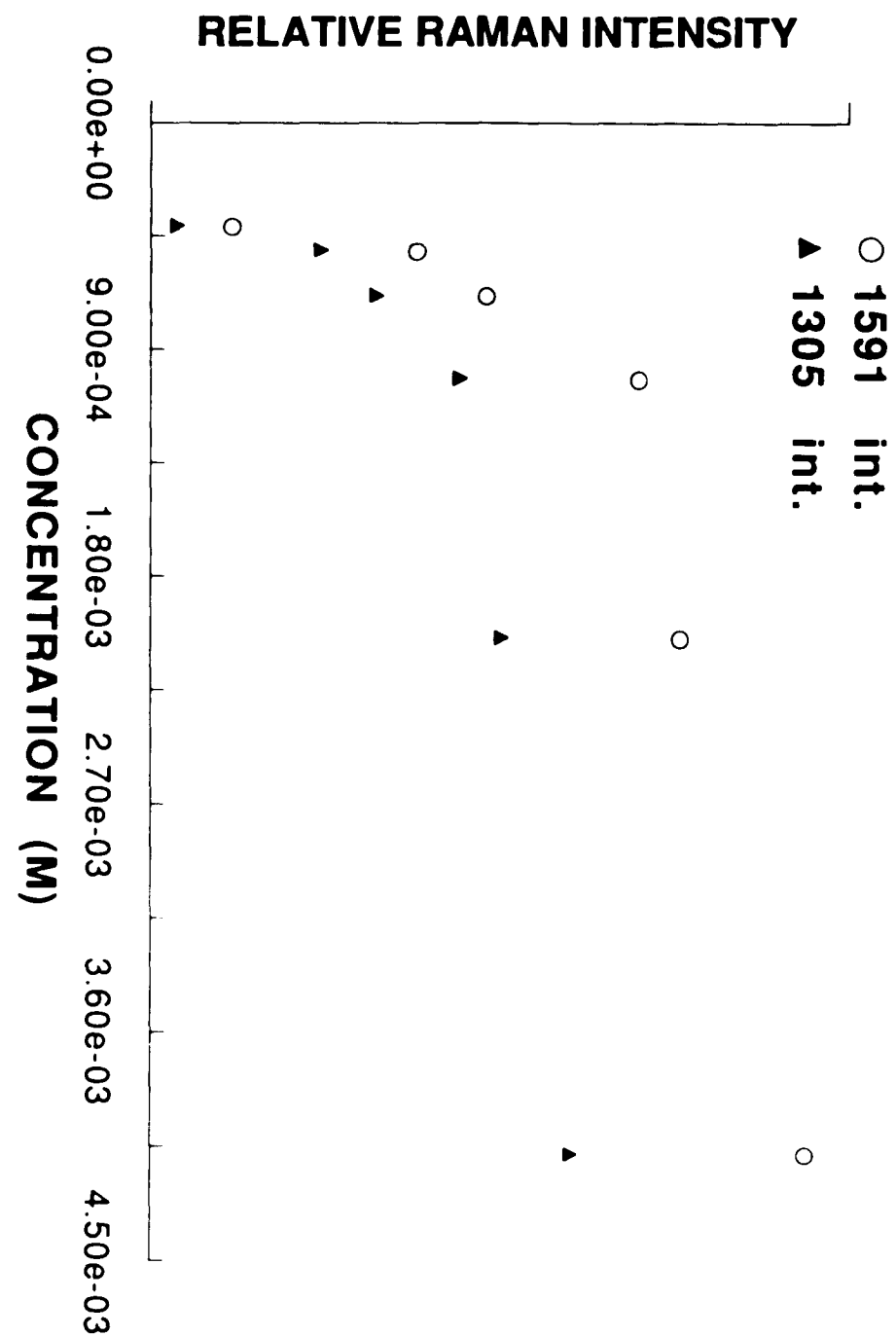
RELATIVE RAMAN INTENSITY
1591 int.
1305 int.
0.00e+00
9.00e-04
1.80e-03
2.70e-03
3.60e-03
4.50e-03
CONCENTRATION (M)

Figure 30 : Plot of relative Raman intensity vs. adsorbate concentration for the 1302 and 1610 cm^{-1} peaks of 2,4'-bipyridine adsorbed on silver sol.

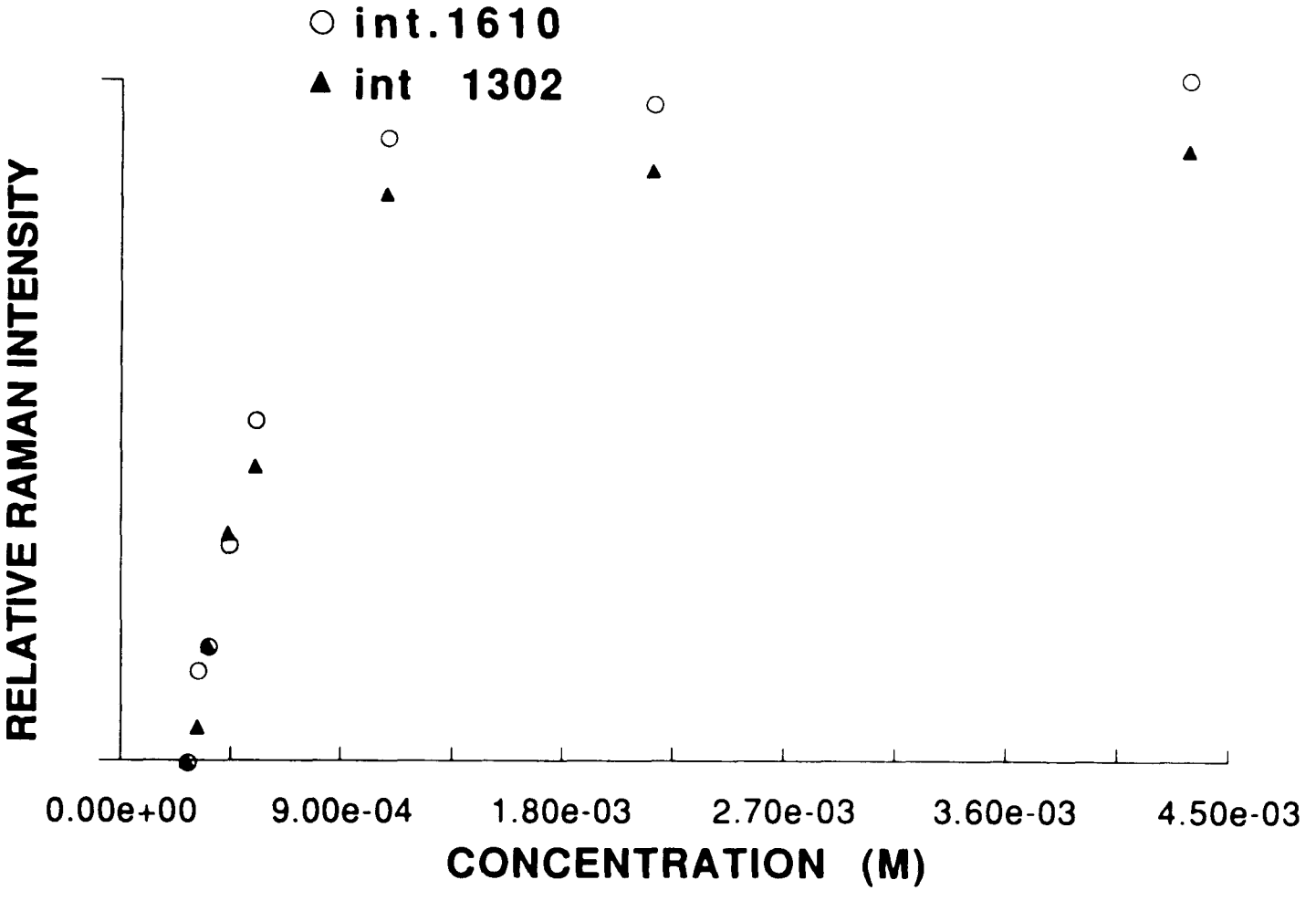
○ int.1610
▲ int 1302
RELATIVE RAMAN INTENSITY
0.00e+00
9.00e-04
1.80e-03
2.70e-03
3.60e-03
4.50e-03
CONCENTRATION (M)

In order to obtain an estimate of the amount of each bipyridine adsorbed on the silver surface, the amount of adsorbate remaining in solution was measured spectrophotometrically as follows.

Starting with stock solutions of equal concentrations, bipyridine and silver sol samples were mixed in the same fashion and under the same ratio as discussed earlier (5 parts sol to 1 part bipyridine). This gave an effective concentration of bipyridine in the sample of about 3.0×10^{-3} M. After preparing a fresh sample of each bipy by mixing it with the silver sol, it was centrifuged and the UV spectrum of the supernatant was recorded. This represents the unadsorbed bipyridine. The UV spectrum of a 5/1 water diluted solution of each bipyridine stock solution was also recorded. The difference in concentration between the supernatant and the 5/1 diluted solution is the amount of bipyridine that adsorbed on the surface. The results showed that the concentration of each bipyridine in the supernatant was very close to that of the equally water diluted solution ($3.3\text{-}3.5 \times 10^{-3}$ M),with no more than 1.0 or 2.0 % absorbance difference between the two solutions. This would indicate that only a very small amount of bipyridine adsorbs on the surface.

To further pinpoint the amount of adsorbate on the silver sol, each bipyridine was mixed with the sol in the same ratio

TABLE 1 : ESTIMATED SOLUTION CONCENTRATION OF BIPYRIDINES ADSORBED ON SILVER SOL

COMPOUND	CONCENTRATION (M)
2,2' bipyridine	2.26×10^{-5}
2,4' bipyridine	1.53×10^{-5}
3,3' bipyridine	1.49×10^{-5}
2,3' bipyridine	1.43×10^{-5}
4,4' bipyridine	1.36×10^{-5}

and then centrifuged until a clear supernatant was obtained. The supernatant was then removed carefully and replaced with water of exactly the same volume. The mixture was then shaken and centrifuged until clear. Assuming that all of the adsorbed bipyridine will go back into solution, the UV spectrum of each solution was recorded and the bipyridine concentration was calculated. These results are shown in table 1. Even though this method cannot be a highly accurate way of measuring the adsorbate concentration on the silver surface, it provides a range for the concentration of the adsorbed species, which is about 1.5×10^{-5} M, or about 200 times less than the original concentration of the compound in the sample (about 3.3×10^{-3} M).

From these results one would tend to assume that given sufficient concentration of an adsorbate, factors other than solution concentration must regulate the enhancement of its Raman spectrum, namely the mode of adsorption of the molecule with the surface.

ADSORPTION MODE OF COMPOUNDS ON AG SOL (SURFACE INTERACTION)

The interpretation of the SERS spectra of the compounds displayed in figures 10 through 28 entails the understanding of observed similarities or discrepancies in the surface enhanced spectra of members of the same class of compounds, as well an understanding of the different relative enhancement, or even the lack of it. Provided that concentration is not a factor in the enhancement mechanism, this enhancement must be dependent on the adsorption mode of these compounds on the surface which is regulated by molecular structure and geometry. In order to better understand the surface orientation of these compounds, their SERS spectra were recorded and studied in two spectral regions: 1) between 700-1700 cm^{-1}, and 2) between 2900-3200 cm^{-1}.

THE 700-1700 CM^{-1} SPECTRAL REGION

In this region the most prominent Raman active modes come from in plane vibrations from C-C and C-N bond stretching, with some contribution from in plane C-H bond wagging. In order to interpret the SERS spectra using surface selection rules, axes of molecular symmetry must be assigned to the compounds studied. For the sake of simplicity only planar

molecular structures will be assumed in assigning molecular symmetries. Figure 10 shows the molecular axes that will be referred to when components of the molecular polarizability are being discussed. According to the surface selection rules by Moskovits et al.(35-41), when a molecule adsorbs onto the metal surface one of these molecular axes would become the z axis (or normal) with respect to the metal surface. If a molecule adsorbs on the surface utilizing sigma electrons (i.e. from its nitrogens), this would mean that the aromatic rings are oriented perpendicular (normal) to the surface. This would imply that normal vibrational modes which involve in plane motion of C-C and/or C-N bonds,or C-H wagging that are perpendicular to the metal surface will give rise to the most intense SERS signals (35-43,89).

For an aromatic molecule that adsorbs perpendicular to the surface, the greatest SERS intensity would be expected from totally symmetric modes which derive their intensity from the a_{zz} component of the molecular polarizability (where z is the coordinate perpendicular to the metal surface). Vibrations that are out of the molecular plane, or are in plane but non-totally symmetric, will derive their intensity from the α_{xz} or α_{yz} components, respectively, and will show a lesser degree of surface enhancement. Vibrations that are out of plane are expected to be especially weak because most of them are

Raman inactive for the most symmetric compounds studied here. These modes also fall in a frequency region that is below 1000 cm^{-1}(90). If adsorption on the metal surface occurs through pi electrons, then the plane of the aromatic rings would lie parallel to the surface, so that totally symmetric in plane modes would be subjected to much less enhancement.

The solid and SERS spectra of the most symmetric compounds are considered first. 4,4'-bipyridine (Fig.11) is a molecule with D_{2h} symmetry, with xy defining the molecular plane (90), and 4-phenylpyridine (Fig.12) a C_{2v} symmetry molecule with yz defining the molecular plane (91). The solid spectrum of 4,4' bipyridine is nearly identical to that of solid biphenyl (fig.4 of ref.90), which is also a D_{2h} symmetry compound, except for small frequency differences. Thus the four strongest Raman bands in the spectrum of solid 4,4'-bipyridine at 1002,1300,1623 and 1609 cm^{-1}, can be correlated with those of solid biphenyl (table 2) at 1003(A_g), 1285(A_g), 1595(B_{1g}) and 1612(A_g) cm^{-1}. The same four bands are also most prominent in the spectrum of solid 4-phenyl pyridine at 1004, 1283, 1590 and 1602 cm^{-1}, even though this is a lower symmetry compound (C_{2v}) due to the single nitrogen at the 4 position.

In the SERS spectrum of the 4,4'-bipyridine (fig.11) the 1623 cm^{-1} band is no longer present. This is consistent with

its assignment as a vibration of B_{1g} symmetry. It is expected that totally symmetric modes (A_g) are expected to be subject to a greater surface enhancement. Modes that involve α_{xy} components (B_{1g}), where the molecular x is now normal to the surface assuming adsorption through the 4 nitrogen, would be less enhanced. The absence of the 1590 cm^{-1} band in the 4 phenyl pyridine SERS (fig.12) spectrum can also be explained in the same way. In the SERS spectrum of 4,4'-bipyridine the 1516 and 1220 cm^{-1} bands are relatively more enhanced and the 1002 cm^{-1} band in the solid spectrum has shifted upwards by 8 cm^{-1} in the SERS spectrum. For both of these compounds these observations are consistent with a model in which adsorption on the surface occurs through sigma donation by the nitrogen at the 4 position . Even though the symmetry of 4,4'-bipyridine could be lowered to C_{2v} upon adsorption, the similarity between the Raman and SERS spectra of 4-phenyl pyridine (being a C_{2v} molecule) indicates that this is expected to have little effect on the observed Raman spectral pattern. Previously reported SERS spectra of 4,4'-bipyridine (4) on a silver electrode are almost identical to the solution SERS spectrum reported here, which is consistent with sigma type adsorption through the 4 position nitrogen.

In the spectrum of solid 2,4'-bipyridine (fig.13) the major Raman bands are observed at 1000, 1302 and 1602 cm^{-1}, which can be correlated to the three most intense Raman active (A_{1g}) bands of biphenyl, even though 2,4'-bipyridine is of much lower symmetry (C_s). Additional bands of moderate intensity appear at 1071 and 1579 cm^{-1}. These bands may be compared to those of liquid 2-phenylpyridine (fig. 24), indicating that the nitrogen at the 2 position might be responsible for the new Raman bands.

On the silver surface, the SERS spectrum of 2,4'-bipyridine is more complex than its solid state spectrum (fig.13). This is an exception to the generally observed pattern where the SERS spectrum is either similar or simpler (containing fewer peaks) than the corresponding solid or liquid phase Raman spectrum. A set of two bands appears at 994, 1012 cm^{-1} and 1579, 1589 cm^{-1}. The 1600 cm^{-1} band is shifted upwards to 1611 cm^{-1}, and new bands of medium intensity appear at 1129 and 1378 cm^{-1}, along with several less intense peaks. These observations can be explained as follows: In the biphenyl Raman spectrum the in plane modes can be separated by symmetry into two sets of normal modes described as in phase and out of phase combinations of the same phenyl based mode (A_g and B_{3u}, B_{1g} and B_{2u} (table 2). In several cases the frequency differences of those pairs are small (i.e A_g, B_{3u} at 1612, 1597 and 1003, 965

TABLE 2 : IN AND OUT OF PHASE PAIRS OF THE IN PLANE MODES IN THE BIPHENYL RAMAN SPECTRUM (600-1700 cm^{-1})[a]

A_g	B_{3u}	B_{1g}	B_{2u}
1612	1597	1595	1570
1507	1482	1452	1432
1285	1176	1376	1383
1190	1040	1316	1283
1030	1008	1156	1156
1003	965	1090	1074
742	609	608	626

a. From reference 90. Symmetries refer to D_{2h} point group of biphenyl.

cm^{-1}). When two pyridyl groups, or a phenyl and a pyridyl group are joined and the symmetry is lowered (C_{2v} or lower) additional modes become totally symmetric and may appear as closely spaced bands in the Raman spectrum. The position of the nitrogens on the pyridyl rings can affect the frequency spacing, and it can be higher or lower than that of biphenyl. In the SERS spectrum the relative intensity of a pair of totally symmetric modes will depend on the degree to which the α_{zz} component (z being normal to the surface) contributes to the Raman intensity for each of them. Thus where a single band appears in the Raman spectrum, given the right surface orientation will appear as a doublet in the SERS spectrum. The reverse could likewise occur. For the SERS spectrum of 2,4'-bipyridine some of the modes that are derived from the B_{3u} or B_{2u} modes of biphenyl are almost as intense as those derived from A_g modes.

The relative spectral similarity of 2,4'-bipyridine with 4,4'-bipyridine and 4-phenylpyridine is one in which totally symmetric in plane C-C and C-N vibrations observed in the solid Raman spectra are primarily enhanced when these compounds adsorb on the silver surface. If this adsorption was occuring through a π type interaction, such vibrations would be less intense and out of planar modes might appear in the SERS spectrum. In the case of 2,4'-bipyridine adsorption seems

to occur through the 4' position nitrogen which is much less sterically hindered than the nitrogen on the 2 position. Such an orientation will result in enhancement of C-C and C-N vibrations that are perpendicular to the metal surface.

The SERS spectrum of N-methyl 4,4'-bipyridinium (fig.14) a species similar to 4,4'-bipyridine, but with a methyl group attached at the 4' nitrogen was found to be similar to that of 4,4'-bipyridine but with a major new band appearing at 1641 cm^{-1}. A similar band has been reported (91) upon protonation of coordinated 4,4'-bipyridine and it is most likely due to an upshifted out of phase component formerly around 1600 cm^{-1}.

The Raman spectrum of solid 3,3'-bipyridine (fig. 15) indicates a relatively high symmetry molecule (C_{2h} or C_{2v}). As for the 4 substituted molecules, three major bands appear at 1036,1307 and 1594 cm^{-1}. Another band of moderate intensity appears at 1051 cm^{-1}. All of these bands can again be correlated with a totally symmetric vibration of biphenyl. The liquid spectra of 2,3'-bipyridine (fig. 16) and 3-phenyl pyridine (fig. 17), both of which are low symmetry molecules (C_s at most), are expected to have all in plane modes totally symmetric and Raman active. For 2,3'-bipyridine a new band appears at 993 cm^{-1}. For 3-phenylpyridine two bands appear at 995 and 1006 cm^{-1} and a shoulder on the 1037 cm^{-1} band. Also a triplet of bands appears at 1588,1600 and 1611 cm^{-1}.

The bands in both spectra near 995 cm^{-1} may be related to a B_{1g} mode of biphenyl that is now totally symmetric. In the liquid spectrum of 3-phenylpyridine additional bands might be due to out of phase combinations, B_{2u} or B_{3u} modes which are now totally symmetric in the lower symmetry molecule. It is interesting to point out that the strong band at about 1300 cm^{-1} shows no additional nearby bands in the Raman spectrum of any of the compounds that were studied. From the biphenyl spectrum (90) it can be seen that the out of phase combination of this band (1285 cm^{-1} for biphenyl) lies at much lower frequency 1176 cm^{-1}.

The SERS spectra of 3,3'-bipyridine (fig. 15) and 2,3'-bipyridine (fig. 16) are almost identical to their Raman counterparts. This is consistent with sigma type adsorption through the 3 position nitrogen, which would maintain the symmetry of 2,3'-bipyridine but lower that of 3,3'-bipyridine, with no apparent effect to the spectral pattern.

The SERS spectrum of 3-phenylpyridine (fig. 17) is simplified as compared to its liquid counterpart, with only 3 major bands appearing at 1001, 1033 and 1601 cm^{-1}. Contrary to the case of 2,4'-bipyridine, here the intensity appears to be significantly lower for some out of phase combinations. Also in the SERS spectrum of 2,3' and 3,3'-bipyridine the relative intensity of the low frequency bands (at about 1030 cm^{-1}) is

higher than the 1300 and 1500 cm^{-1} area bands. These intensity differences as compared to SERS spectra of the 4 substituted series might be due to the relative orientation which series members assume upon surface adsorption. For the 4 substituted series, both rings would lie symmetrically along the surface normal, while for the 3 substituted series the center line of one pyridyl ring is skewed at an angle of about 60^0 from the surface normal (fig. 31). This would mean that the molecular axis system polarizability components involving the normal to the surface which contribute to a given mode, would vary significantly for otherwise similar normal modes of the two groups of compounds.

The Raman and infra-red spectra of 2,2'-bipyridine and coordinated 2,2'-bipyridine have been previously reported (91-96) and normal coordinate calculations performed (92,93,95,96). In the solid spectrum of 2,2'-bipyridine (fig. 18), bands which correspond to those appearing in Raman spectra of all compounds studied appear at 996,1303,1574 and 1591 cm^{-1}. Other bands also appear at 1046,1237,1448 and 1484 cm^{-1}. It is known that solid 2,2'-bipyridine has a trans conformation (C_{2h} symmetry). Biphenyl modes of both A_g and B_{1g} symmetry in D_{2h} are both now A_g, and as observed, give rise to significant Raman intensity. The SERS spectrum of 2,2' bipyridine (fig.18) has been reported by others(3,6,8,97) and it

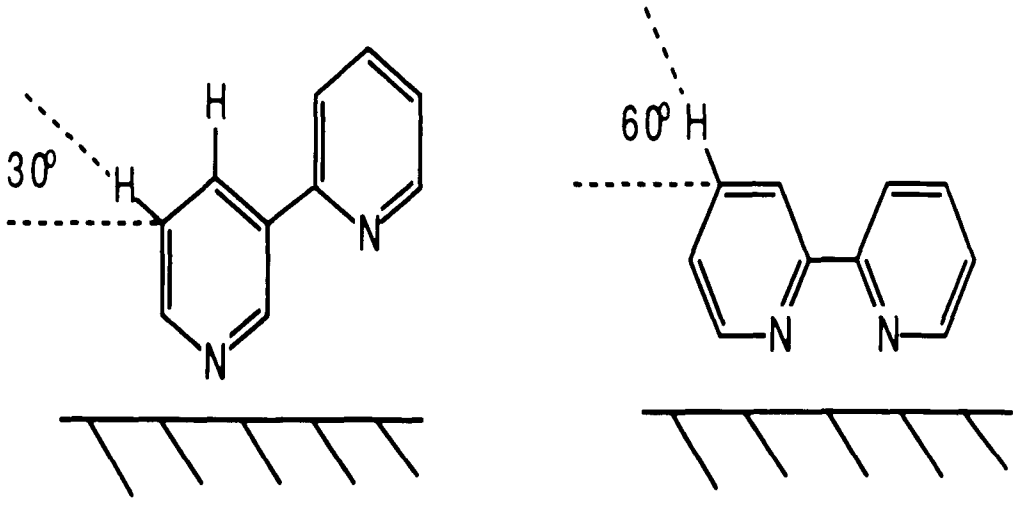

Figure 31 : Representation of expected type of interaction of pyridyl ring systems through sigma type donation to sol surface. Angles indicate the orientation of representative C-H stretching modes with the sol surface.

is different than its solid Raman spectrum. Most prominent is the absence of two major bands from the SERS spectrum at 1237 and 1448 cm^{-1}. This is indicative of a change of conformation of 2,2'-bipyridine upon adsorption on the silver surface from trans into cis (C_{2v} symmetry). There is strong evidence that this change of conformation takes place. As it can be seen from figure 19 the Raman spectrum of monoprotonated 2,2' bipyridine in 1.0 M Hcl is quite similar to that of its SERS spectrum. There is a small upward shift of some bands in the spectrum, but the spectral pattern is the same to that of 2,2'-bipyridine adsorbed on the silver sol. It is expected that the monoprotonated 2,2'-bipyridine molecule has a C_{2v} type symmetry also. This is possible through hydrogen bonding between the unprotonated nitrogen from one pyridyl ring and the protonated from the other. This type of interaction would result in a cis type conformation, similar to that of adsorbed 2,2'-bipyridine, and different than that of 2,2'-bipyridine dissolved in chloroform (trans). The broad band around 1616 cm^{-1} is most likely due to water in the sample. The remarkable similarity of the SERS spectrum of 2,2'-bipyridine to that of solid $Ag(2,2'bpy)_2^{+1}$ (fig.21) which is a planar Ag^{+1} coordination complex of 2,2'- bipyridine is also indicative of the conformational changes upon adsorption. The SERS spectrum of Ag^{+1} coordination complex is discussed in the following section. The SERS spectrum of 2,2'-bipyridine

reported here compares closely to reported SERS spectra of 2,2' bipyridine in 0.1 M Kcl on a silver electrode at a potential between +0.05 and -0.02 V (8). The results reported here are consistent with previous interpretations (3,8,97) that 2,2'-bipyridine interacts uniquely with the metal surface through sigma donation from both 2 position nitrogens in a chelating fashion.

Additional support for the chelating mode of interaction of 2,2'-bipyridine comes from the Raman and SERS spectra of 1,10-phenanthroline (fig.22) and 4,4'-dimethyl-2,2'-bipyridine (fig. 23). In 1,10-phenanthroline the similarity of the diimine chelation site, but inflexibility of the planar aromatic system precludes single nitrogen atom sigma donation upon adsorption. Interaction with the surface through the pi system seems unlikely based on the similarities between the Raman and SERS spectra. In 4,4'-dimethyl-2,2'-bipyridine a comparison between the Raman and SERS spectra indicates that a conformational change similar to that of 2,2'-bipyridine from a C_{2h} trans structure in the solid to a C_{2v} chelating structure on the silver surface. The Raman spectrum of the solid is comparable to that of solid 2,2'-bipyridine. The band pattern is similar but with shifts in frequencies and an additional band of moderate intensity at 1289 cm^{-1}. The shifts may be due to the redistribution of normal mode composition due to mixing of the carbon-methyl stretch with the pyridine ring modes.

The SERS spectrum of 4,4'-dimethyl-2,2'-bipyridine, like that of 2,2'-bipyridine, is simplified with the intensities of several bands now close to zero.(i.e 1237, 1289, 1427, 1448 cm^{-1}).

The Raman spectrum of liquid 2-phenylpyridine (fig. 24) has little resemblance to that of solid 2,2'-bipyridine and it is generally like those previously discussed. Three major bands at 1001, 1295 and 1603 cm^{-1} and a band of lesser intensity at 1584 cm^{-1} are the most prominent of the spectrum. Bands of even lesser intensity are also observed at 1042,1063,1241 and 1500 cm^{-1}. The SERS spectrum of 2-phenylpyridine shows the weakest enhancement of all studied for a stable adsorbate-colloid system. This is to be expected since adsorption through sigma donation from the 2 substituted nitrogen would be sterically hindered by the benzene ring at the 2 position to it. This steric hinderance prevents the pyridine ring from being normal to the surface, which results in weak enhancement of its SERS spectrum.

The SERS spectra of two more compounds 2,2'-dipyridyl-ketone and 2,2'-dipyridylamine were recorded. The SERS spectrum of 2,2'-dipyridylketone a compound where the two pyridine rings are held together by a carbonyl group (fig.25) showed no resemblance to its solid spectrum, or that of 2,2'-bipyridine on the silver surface. Only two bands at 1008 and 1050 cm^{-1} appear in the SERS spectrum, which correspond to the 1001 and 1050 cm^{-1} of the solid spectrum. The remaining bands of the solid spectrum at 1187, 1571,

1587 and 1682 cm^{-1} are absent in the SERS spectrum, which is an indication of conformational changes upon adsorption. Even though the conformation of 2,2'-dipyridylketone in the solid state is not known, it is interesting to point out that the SERS spectrum of 2,2'-dipyridylketone looks remarkably similar to that of pyridine adsorbed on the silver surface (fig.26). In the pyridine SERS spectrum which is well known since it was the first compound to be recorded using SERS (23), two major bands show at 1006 and 1036 cm^{-1} respectively. This SERS spectrum is very similar to its liquid Raman spectrum which shows again only two major peaks at 990 and 1030 cm^{-1} (fig. 27). It is well known that pyridine adsorbs through its single nitrogen in a fashion normal to the metal surface (23). The two bands of the 2,2' dipyridylketone spectrum at 1008 and 1050 cm^{-1} can be correlated with the 1006 and 1036 cm^{-1} band of pyridine adsorbed on the sol. Two more broad peaks at 1296 and 1595 cm^{-1} can also be correlated to two equally broad peaks around 1350 and 1597 cm^{-1} in the pyridine spectrum. It should also be pointed out that the band at 1682 cm^{-1} of the Raman spectrum of solid 2,2'-dipyridylketone, which is assigned to a symmetric carbonyl stretch, is absent from the SERS spectrum of the compound. This result would tend to indicate that the carbonyl group must have an almost parallel orientation on the metal surface, so that the contribution from the α_{zz} component of the molecular polarizability of this mode would be minimum,

resulting in the absence of this band in the SERS spectrum of the compound. Such an interpretation would indicate that 2,2' dipyridylketone adsorbs on the surface with one pyridine ring normal to the surface and the other lying flat on it, so that it will not contribute to the SERS spectrum significantly, thus making 2,2'-dipyridylketone essentially behaving as a single substituted pyridine molecule.

The spectrum of solid 2,2'-dipyridylamine (fig.28) a compound where the two pyridine rings are joined by an amine group, shows three major bands at 992, 1280 and 1605 cm^{-1} and three moderate ones at 1057, 1241 and 1255 cm^{-1}. Its SERS spectrum is similar to that of pyridine and 2,2'-dipyridylketone. The most prominent bands are those at 996 and 1057 cm^{-1} which can be correlated to the 1008 and 1050 cm^{-1} bands of 2,2'-dipyridylketone, and the 1006 and 1036 cm^{-1} bands of pyridine SERS spectra. The 2,2'-dipyridylamine SERS spectrum shows 2 broad peaks centered at 1313 and 1597 cm^{-1}, which also correlate to similar peaks at 1296 and 1595 cm^{-1} for 2,2'-dipyridylketone, and 1350 and 1597 cm^{-1} for pyridine. Such a spectral pattern would tend to indicate that this compound may adsorb on the surface in a pyridine fashion too. However, contrary to the expected type of adsorption of 2,2'-dipyridylketone, where only one pyridyl ring is normal to the surface, the 2,2'-bipyridine-amine,can adsorb with all three nitrogens (pyridyl rings and amino nitrogen).

This can be possible due to the sigma type donor capability of the amine group, and the smaller steric hinderance that it imposes to the pyridyl rings . This can be further substantiated from the C-H stretch portion of the SERS spectrum of the compounds which is discussed in the following section.

THE 2900-3200 CM^{-1} SPECTRAL REGION

In this region, the aromatic and aliphatic C-H stretching modes of the compounds studied can be observed. Because the C-H stretching modes do not mix to a great extent with other vibrations of the aromatic rings, their intensities in the surface enhanced spectra of the compounds provide the most specific evidence of the orientation of the adsorbed species with respect to the sol surface.(35-43,89). The SERS intensity associated with the symmetric stretching of a specific C-H bond or a group of equivalent bonds, will depend upon the angle at which the C-H bond lies in relation to the sol surface. Maximum intensity will be expected for the stretching of C-H bonds that are perpendicular (normal) to the surface. As the angle is reduced from normal (90^0) to parallel (0^0) to the surface, the SERS intensity is expected to be reduced accordingly. The SERS intensity of the C-H stretching modes will also be affected by the relative distance of the C-H bond from the metal surface. It has been shown that the enhancement of the SERS intensity decreases by a factor of ($1/r^3$) as the molecule moves away from the surface by distance (r) (32-34). For a pyridyl ring that is adsorbed through a nitrogen sigma donation on the sol surface, the C-H bond at the 4 position will be normal (90^0) to the surface, and should contribute significantly to the SERS intensity in the

C-H region. The other four C-H bonds lie at a 30^0 angle to the surface and their SERS contribution should be relatively minor.

For the isomeric bipyridines studied 3,3'-bipyridine (fig. 32) 2,3' and 2,4'-bipyridine (fig. 33) showed a single band in the C-H region between 3062 to 3067 cm^{-1}. This is the region where totally symmetric C-H stretch modes have been reported for biphenyl and 2,2'-bipyridine (90-95). 4,4'-bipyridine showed no detectable SERS C-H signal (fig.32), even though a SERS spectrum of the compound was obtained in the 700-1700 cm^{-1} region, and a strong C-H band is observed in the liquid Raman spectrum of the compound. 2,2'-bipyridine was the only one of the compounds studied that gave rise to two aromatic C-H stretch signals at 3066 and 3100 cm^{-1}(fig.34).

From the phenylpyridines studied, 3- and 4-phenylpyridine gave rise to a single C-H stretch band at 3061 and 3063 cm^{-1} respectively (fig. 35). The 2-phenylpyridine gave no observable C-H stretch signal even though a SERS spectrum was obtained in the 700-1700 cm^{-1} region, and a C-H stretch is observed in the liquid Raman spectrum of the compound.

In each of these cases the results are consistent with a sigma type adsorption on the surface through the least sterically hindered nitrogen, which will result in one or more C-H bonds being normal to the surface with the notable exception of 2-phenylpyridine.

Figure 32 : C-H stretch region SERS spectra of compounds adsorbed on silver sol. Top, 4,4'-bipyridine dissolved in water. Middle, 3,3'-bipyridine dissolved in water. Bottom, 2,2'-bipyridine dissolved in water. All parameters same as their 700-1700 cm^{-1} SERS counterparts.

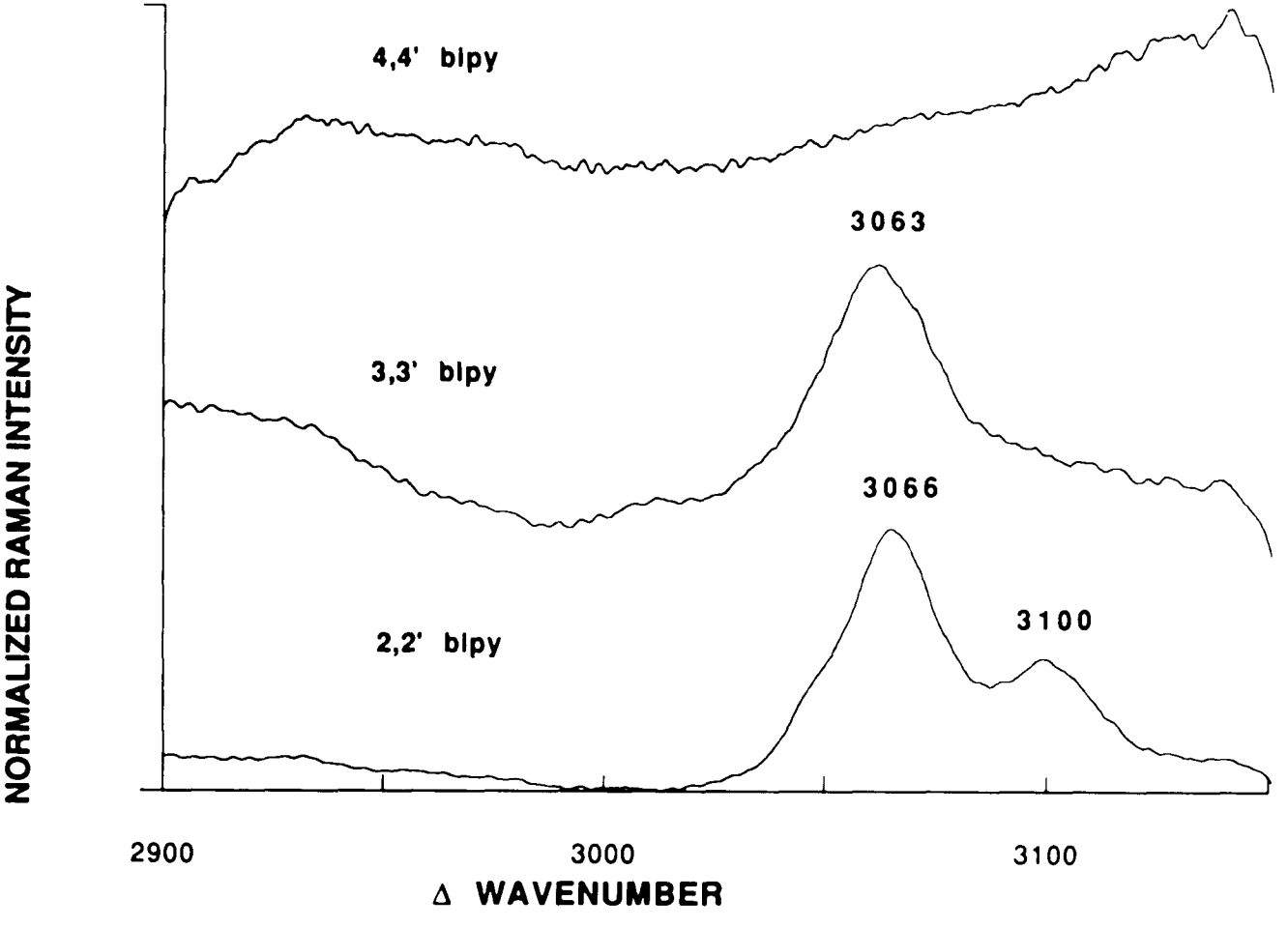
4,4' bipy
3063
3,3' bipy
3066
3100
2,2' bipy
NORMALIZED RAMAN INTENSITY
2900
3000
3100
Δ WAVENUMBER

Figure 33 : C-H stretch region SERS spectra of compounds adsorbed on silver sol. Top, 2,4'-bipyridine dissolved in water. Middle, 2,3'-bipyridine dissolved in water. Bottom, 2,2'-bipyridine dissolved in water. All parameters same as their 700-1700 cm^{-1} SERS counterparts.

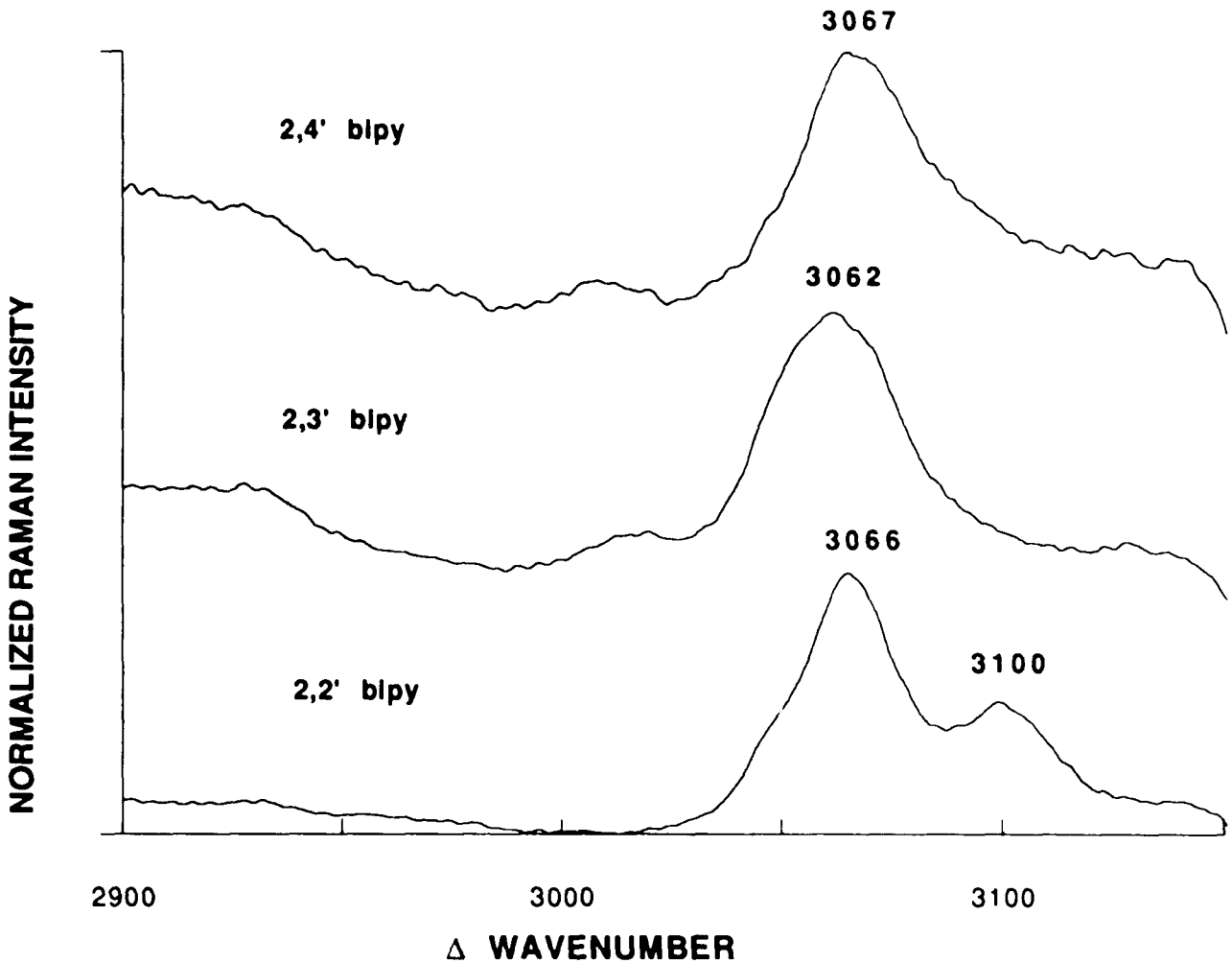
3067
2,4' bipy
3062
2,3' bipy
3066
3100
2,2' bipy
NORMALIZED RAMAN INTENSITY
2900
3000
3100
Δ WAVENUMBER

Figure 34 : C-H stretch region SERS spectra of compounds adsorbed on silver sol. Top, 1,10-phenanthroline dissolved in water. Middle, Ag(2,2' bipyridine)$_2$(+1) dissolved in water. Bottom, 2,2'-bipyridine dissolved in water. All parameters same as their 700-1700 cm^{-1} SERS counterparts.

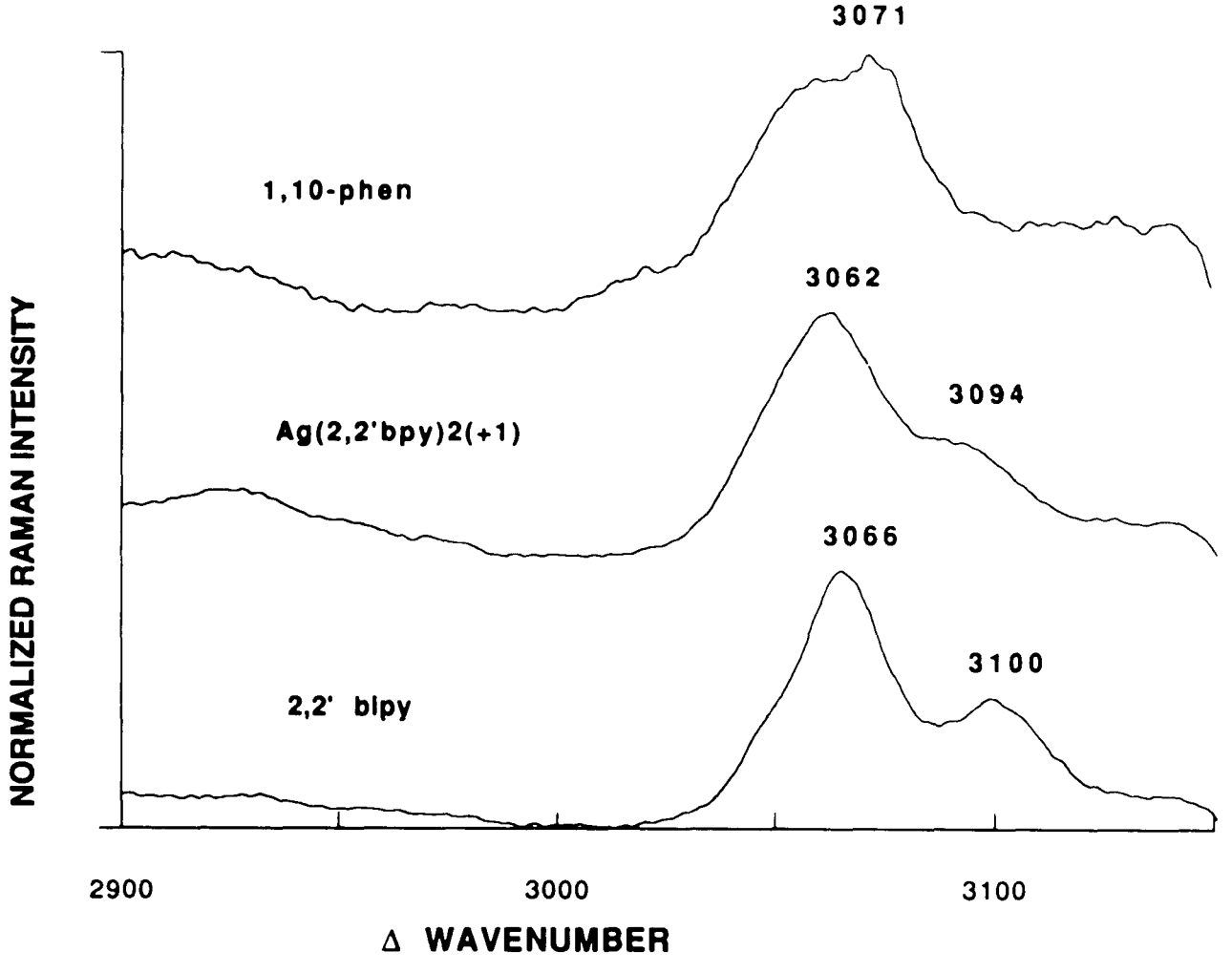
3071
1,10-phen
3062
3094
Ag(2,2'bpy)2(+1)
3066
3100
2,2' bipy
NORMALIZED RAMAN INTENSITY
2900
3000
3100
Δ WAVENUMBER

Figure 35 : C-H stretch region SERS spectra of compounds adsorbed on silver sol. Top. 4-phenylpyridine dissolved in 40% ethanol. Middle. 3-phenylpyridine dissolved in 40 % ethanol. Bottom. 2-phenylpyridine dissolved in 40 % ethanol. All parameters same as their 700-1700 cm^{-1} SERS counterparts.

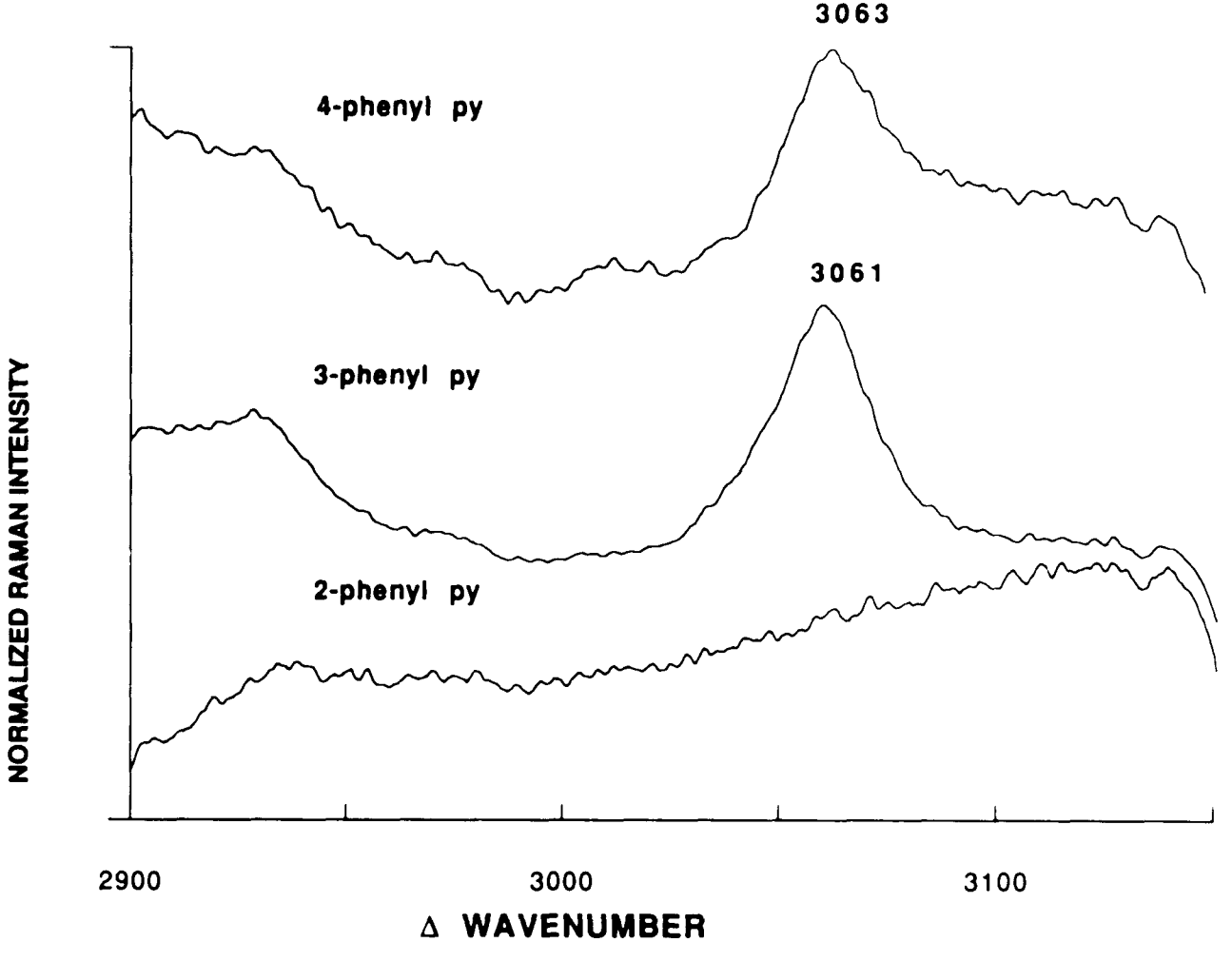
3063
4-phenyl py
3061
3-phenyl py
2-phenyl py
NORMALIZED RAMAN INTENSITY
2900
3000
3100
Δ WAVENUMBER

Figure 36 : C-H stretch region SERS spectra of compounds adsorbed on silver sol. Top. N-methyl-4,4'-bipyridine dissolved in water. Middle. 4,4'-dimethyl-2,2'-bipyridine dissolved in water. Bottom. 2,2'-bipyridine dissolved in water. All parameters same as their 700-1700 cm^{-1} SERS counterparts.

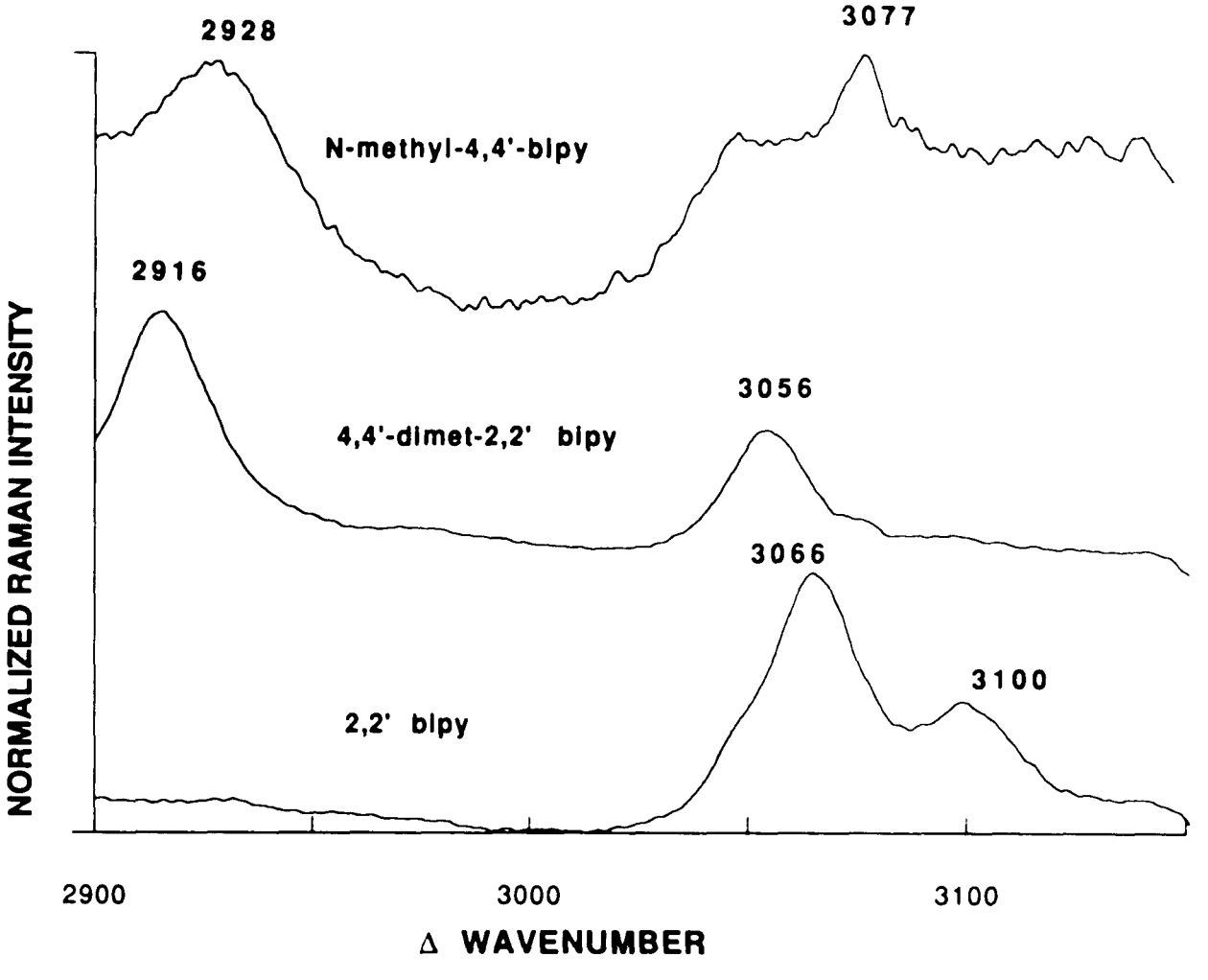
2928
3077
N-methyl-4,4'-bipy
2916
3056
4,4'-dimet-2,2' bipy
3066
3100
2,2' bipy
NORMALIZED RAMAN INTENSITY
2900
3000
3100
Δ WAVENUMBER

Figure 37 : C-H stretch region SERS spectra of compounds adsorbed on silver sol. Top, 2,2'-dipyridylamine dissolved in 50% ethanol. Middle, 2,2'-dipyridylketone dissolved in water. Bottom, pyridine dissolved in water. All parameters same as in their 700-1700 cm^{-1} SERS counterparts.

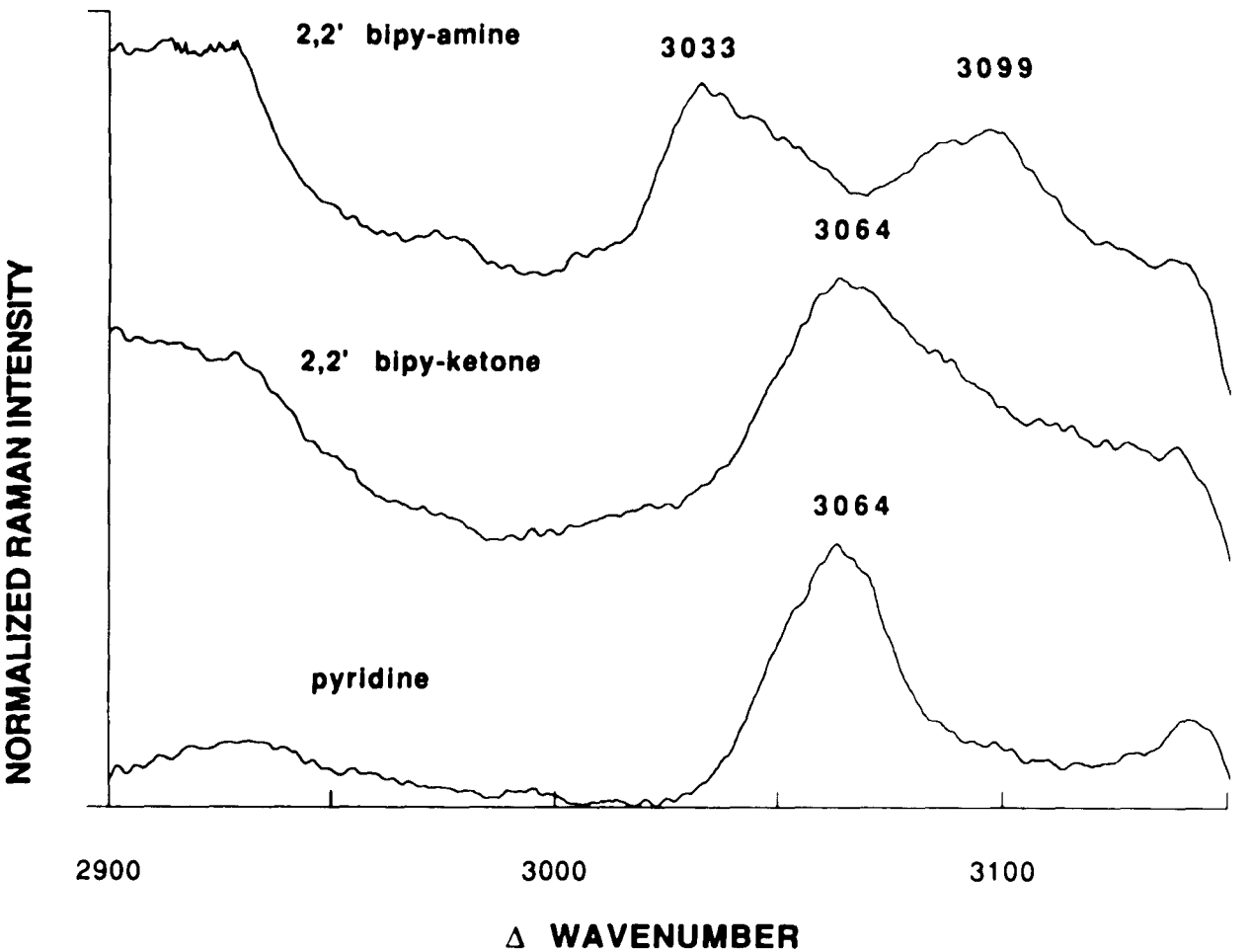
2,2' bipy-amine
3033
3099
3064
2,2' bipy-ketone
3064
pyridine
NORMALIZED RAMAN INTENSITY
2900
3000
3100
Δ WAVENUMBER

If 4,4'-bipyridine adsorbs on the surface through the 4 position nitrogen in a perpendicular fashion, this will result in an orientation where no C-H bonds will be normal to the surface. Instead all 8 C-H bonds are located at a 30^0 angle to the surface. Thus, these bonds are expected to contribute minimally to the SERS C-H spectrum. For this reason, no observable C-H stretch signal can be seen for 4,4'-bipyridine on the silver sol. On the other hand, when the remote 4' position is methylated in N-methyl-4,4'-bipyridinium a SERS signal is observed at 2928 cm^{-1} (fig. 36). This is assigned to an aliphatic methyl stretch now having a polarizability component normal to the surface, with an additional weaker signal at 3077 cm-1.

The lack of a C-H stretch signal in the SERS spectrum of 2-phenyl-pyridine makes the orientation of the compound on the sol surface difficult to describe. If one takes into account the steric hinderance to sigma donation through the single nitrogen because of the phenyl ring at the 2 position to it, it is possible that the compound adsorbs through a combination of sigma nitrogen donation, and pi type interaction with phenyl ring rotated approximately 90^0 about the C-C' interring bond. This would reduce the steric hinderance to the sigma donation and will also provide pi donation capability. Since the C-H bonds of the phenyl ring would lie parallel to the surface their contribution to the C-H SERS intensity is expected to be

minimal. The orientation of the C-H bonds of the pyridyl ring would be an irregular one with the C-H bonds off the surface normal, which would result in little or no contribution to the enhancement of the C-H stretch on the SERS spectrum.

The observation of two C-H stretch bands in the SERS spectrum of 2,2'-bipyridine provides additional support for the chelating orientation of the 2,2'-bipyridine on the sol surface. In this type of chelating adsorption (both nitrogens on the sol surface), six of the C-H bonds of the compound lie at a 60^0 angle to the surface, with the pair at the 6 and 6' positions just above the surface. Since this angle is much closer to the normal (90^0), the SERS intensity is increased. Similar results are observed from the SERS spectrum of $Ag(2,2'\text{-bpy})_2(+1)$ (fig 34) which shows a major band at 3062 cm^{-1} and a shoulder at 3094 cm^{-1}. It is expected that when this complex is dissolved in water it dissociates to form a single 2,2'-bipyridine molecule coordinated to silver (+1) atom.This is reinforced by the fact that upon adsorption, the silver sol destabilizes fast, which indicates the presence of charge (from the silver atom) on the surface. The possibility of simply having free 2,2-bipyridine in solution is excluded, since the UV spectrum of free water dissolved complex is different than that of free 2,2'-bipyridine in solution.

The SERS spectrum of 4,4'-dimethyl-2,2'-bipyridine (fig.36) shows a single aromatic C-H band at 3056 cm^{-1} and a strong methyl C-H stretch at 2916 cm^{-1}. This would imply that the intensity of the higher frequency band in the 2,2' bipyridine SERS spectrum is mostly due to the 4 and 4' position C-H bands, while the lower frequency band is due to the 6 and 6' position C-H bands with possible contribution from the 3 and 3' ones. The SERS spectrum of 1,10-phenanthroline shows a single C-H band at 3071 cm^{-1}(fig. 34).

An indication of the dependence of the C-H bond SERS intensity upon distance from the surface can be seen in Table 3. In this table the relative SERS intensity of the aromatic C-H stretch band is shown and compared to a band around 1300 cm^{-1} in the SERS spectrum of each of the compounds studied. For 2,4'-bipyridine and 4 phenylpyridine, which both are compounds expected to adsorb through the 4 position nitrogen, the C-H region intensity is significantly lower than the intensity of a prominent band which appears around 1300 cm^{-1} in the C-C and C-N stretching region in each spectrum. This ratio of intensities becomes equal to one in the case of 2,2'-bipyridine, which is expected to show a strong C-H stretch signal due to the chelating type of adsorption on the surface. This distance dependence is also clearly demonstrated from the methyl C-H stretch ratios between 4,4'-dimethyl-2,2'-bipyridine and N-methyl-4,4'-bipyridinium. The proximity of the methyl groups at the 4 and 4' position of

TABLE 3 : SERS INTENSITY OF C-H STRETCH RELATIVE TO 1300 CM^{-1} BAND

COMPOUND	RELATIVE SERS INTENSITY (C-H Stretch)
2,4'-BIPY	0.07
4-PP	0.10
N-METHYL 4,4'-BIPY	0.20
3,3'-BIPY	0.32
2,3'-BIPY	0.60
2,2'-BIPY	1.0
4,4'-DIMET. 2,2'-BIPY	0.82
4,4' DIMETHYL 2,2'-BIPY	1.4[b]
N-METHYL 4,4'-BIPY	0.55 [b]

a. Peak height ratioed to peak height of prominent band near 1300 cm^{-1} for each compound. All are aromatic C-H stretch, except last two entries.

b. Methyl C-H stretch.

4,4'-dimethyl-2,2'-bipy give rise to a strong C-H intensity ratio of 1.4 (methyl C-H band 1.4 times higher than 1300 cm^{-1} band), as compared to a 0.55 ratio for N-methyl-4,4'-bipyridinium where the methyl group is located in the remote 4' nitrogen position. All of the compounds studied showed similar relative Raman C-H stretch intensities in their liquid or solution Raman spectra as it can be seen from table 4. Thus, the change in enhancement must be due to the distance differences of these C-H bonds from the surface upon adsorption.

The relative enhancement of the C-H stretch signal upon adsorption of the compounds studied was calculated as the ratio of tneir SERS C-H stretch intensity to that of their liquid or solution Raman C-H stretch intensity and it is shown on table 5. 4,4'-bipyridine and 2-phenylpyridine were given a value of zero since no C-H stretch bands were observed in their SERS spectra. The highest relative C-H stretch enhancement was observed for 2,2'-bipyridine with a value of 3.8 (its SERS C-H stretch band was 3.8 times more enhanced than its liquid spectrum). The lowest observable enhancements were for 2,4'-bipyridine (0.4) and 4-phenylpyridine (0.5) which are in accordance with the expected type of adsorption of the compounds on the sol surface.

The SERS spectrum of 2,2'-dipyridylketone gave rise to a single C-H stretch band at 3063 cm^{-1}, which is exactly at the

TABLE 4 : RAMAN INTENSITY OF C-H STRETCH RELATIVE TO 1300 CM^{-1} BAND FOR LIQUIDS AND SOLUTIONS

COMPOUND	RELATIVE RAMAN INTENSITY CH-STRETCH
2,4'-BIPY ($CHCl_3$)	0.16
3,3'-BIPY ($CHCl_3$)	0.18
2,3'-BIPY (LIQUID)	0.24
2,2'-BIPY($CHCl_3$)	0.26
4,4'-BIPY ($CHCl_3$)	0.46
4,4'-DIMETHYL 2,2'-BIPY ($CHCl_3$)	0.31
4,4'-DIMETHYL 2,2'-BIPY ($CHCl_3$)	0.38[b]
2PP (LIQUID)	0.26
3PP (LIQUID)	0.26
4PP ($CHCl_3$)	0.20

Peak height rationed to peak height of prominent band near 1300 cm^{-1} for each compound. All aromatic C-H stretch
b. Methyl C-H stretch

TABLE 5: RELATIVE ENHANCEMENT OF C-H STRETCH SIGNAL UPON ADSORPTION ON SILVER SURFACE

COMPOUND	RELATIVE ENHANCEMENT C-H STRETCH
4,4'-BIPY	0.0
2,4'-BIPY	0.4
3,3'-BIPY	1.8
2,3'-BIPY	2.5
2,2'-BIPY	3.8
4,4'-DIMET. 2,2'-BIPY	2.6
4,4'-DIMET. 2,2'-BIPY	1.9[b]
2PP	0.0
3PP	2.6
4PP	0.5

Peak height rationed to peak height of prominent band near 1300 cm^{-1} for each compound. All aromatic C-H stretch.
b. Methyl C-H stretch.

same frequency as that of pyridine adsorbed on the silver sol (fig.37). This observation along with the spectral similarity of their SERS spectra in the 700-1700 cm^{-1} region reinforces the possibility of the 2,2'-dipyridylketone adsorbing on the sol surface with one pyridine ring perpendicular to the surface, and one parallel to it, which essentially would make the compound behave as a single substituted pyridine molecule on the silver surface. As it was mentioned before there was no C=O stretch observed in the SERS spectrum of the compound indicating a parallel orientation of the carbonyl group on the silver surface.

The SERS spectrum of 2,2' dipyridylamine gave rise to two broad C-H stretch bands at 3033 and 3099 cm^{-1}. No aromatic N-H stretch signal was observed in the SERS spectrum of the compound (area between 3200-3400 cm^{-1})(100-102). This is consistent with the proposed type of interaction of this compound with the sol, in which all three nitrogens are on the surface. Such a type of adsorption will have the hydrogen of the amino group almost parallel to the surface while keeping the two pyridyl rings almost normal to it, thus resulting in the observation of a C-H stretch signal but no N-H stretch in the SERS spectrum of the compound. The observation of a second C-H stretch signal as compared to one for pyridine and 2,2'-dipyridylketone or the solid Raman spectrum of the compound, might be due to the asymmetric orientation of its

two pyridyl rings upon adsorption on the silver surface which results into two C-H stretch signals.

Figures 38 through 40 are graphical representations of the expected type of interaction of the compounds studied with the silver sol surface based on their SERS spectra.

CONCLUSION

From the comparison of the surface enhanced and Raman spectra of the compounds studied, and in particular the information provided from the C-H stretch region of their SERS spectra, all results obtained indicate that given sufficient adsorbate concentration, surface enhancement is regulated by the molecular structure of the adsorbate. This study indicates that all the compounds investigated adsorb on the silver surface through sigma type interaction from their less sterically hindered nitrogen donor atom in a perpendicular fashion. The only exception to this pattern is 2-phenylpyridine which is prevented from using sigma type interaction only, with the sol surface due to steric hinderance imposed on its nitrogen by the phenyl ring adjacent to it.

Also, this study clearly demonstrated the importance of silver type sols, and in particular citrate sols as a substrate for obtaining and studying SERS spectra. The citrate sol used in this study has been relatively easy to prepare, gave excellent reproducible SERS spectra, and showed a long shelf life.

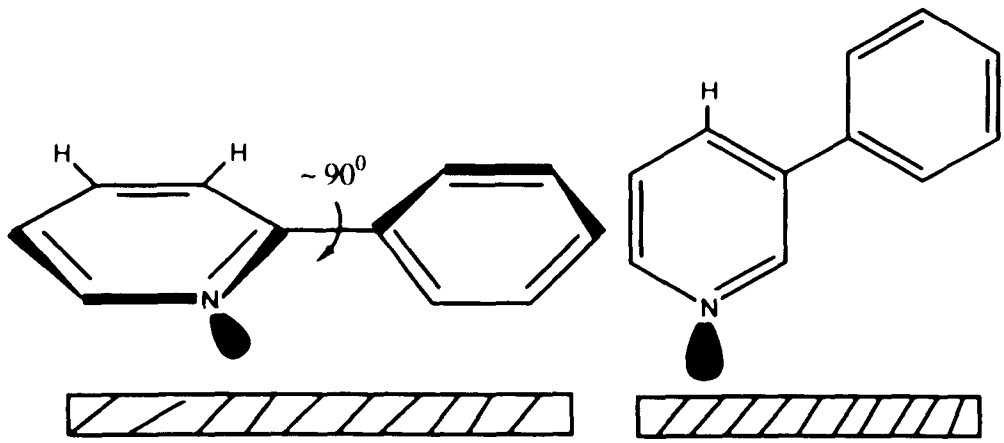

2-Phenyl-pyridine 3-Phenyl-pyridine

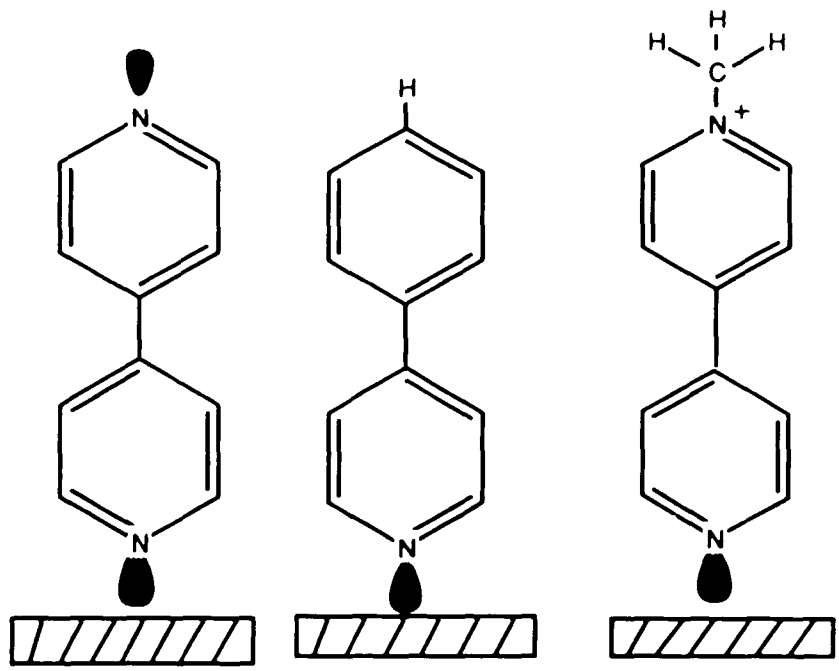

4,4'-Bipyridine 4-Phenyl-pyridine N-methyl-4,4'-bipyridinium

Figure 38 : Representation of the expected type of interaction of adsorbates with the silver sol surface.

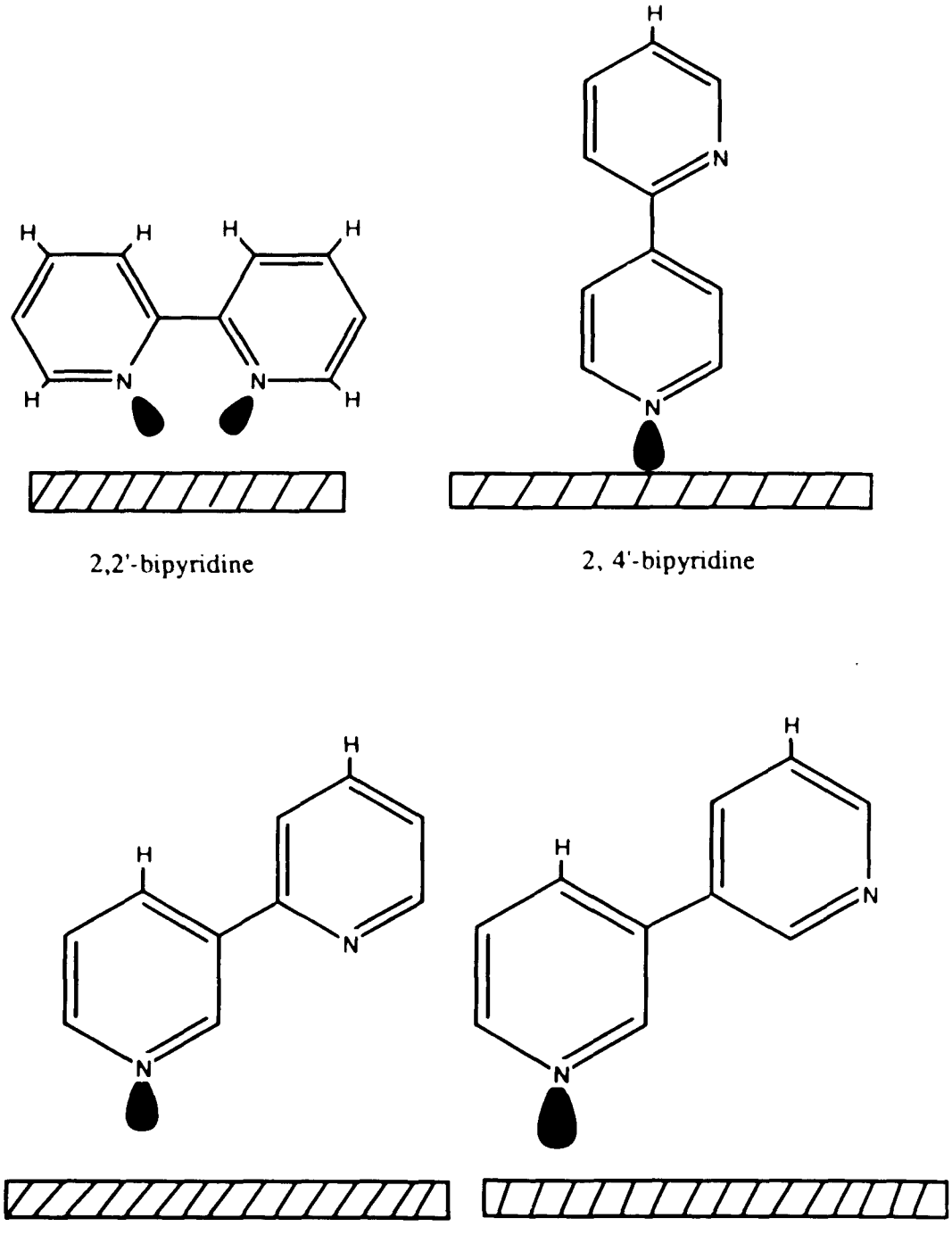

Figure 39 : Representation of the expected type of interaction of adsorbates with the silver sol surface.

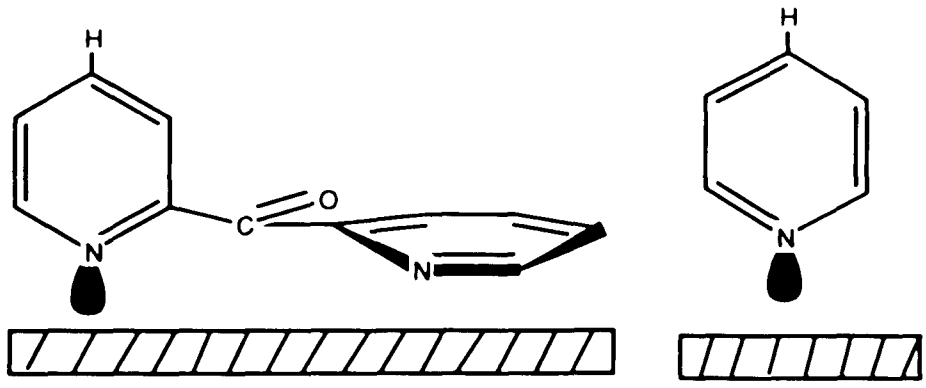

2,2'-Bipyridine-ketone

Pyridine

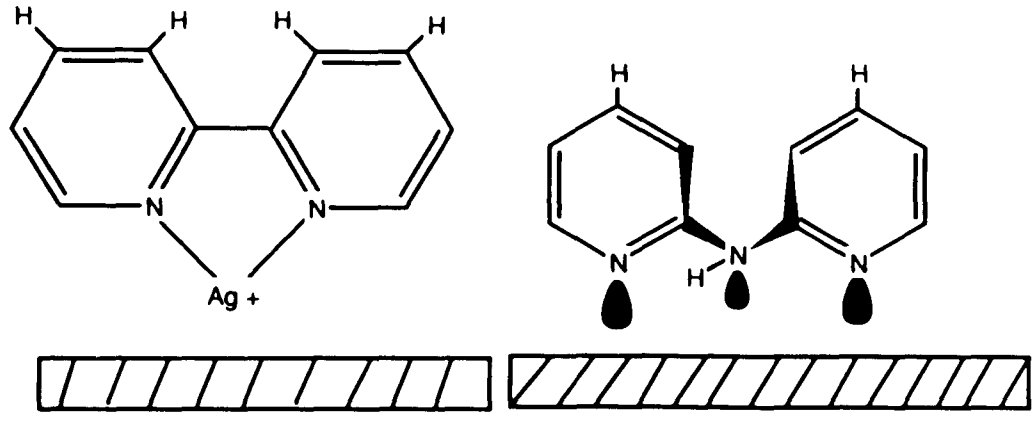

Ag-(2,2'-bpy)(+1)

2,2'-bipyridine-amine

Figure 40 : Representation of expected type of interaction of adsorbates with silver sol surface.

REFERENCES

1. Fleischmann , M. , Hendra , P.J. , McQuillan , A. , J. Chem. Phys. , 26 ,163 , 1974

2. Wetzel , H. , Gerischer , H. , Chem. Phys. Letters , 76 , 460 , 1980

3. Kim , M. , Itoh , K. , Chem. Letters , 357 , 1984

4. Cotton , T.M. , Kaddi , D. , Iorga , D. , J. Am. Chem. Soc. , 105 , No.25 , 7462 , 1983

5. Weaver , M.J. , Farquharson , S. , Magnuson , R.H. , J. Am. Chem. Soc. , 106 , 5123 , 1984

6. Cooney , R.P. , Mahoney , M.R. , Howard , M.W. , Spink , J. A. , Langmuir , 1, 273 , 1985

7. Weaver , M.J. , Gao , P. , J. Phys. Chem. , 89 , 5040 , 1985

8. Kim , M. , Itoh , K. , J. Electroanal. Chem. , 188 , 137 , 1985

9. Takahashi , M. , Niwa , M. , Ito , M. , J. Phys. Chem. , 91 , 11 , 1987

10. Fujita , M. , Ito , M. , Chem. Phys. Letters , 109 , 112 , 1984

11. Birke, R., Lombardi, J.S., J. Phys. Chem. , 92 , 5965, 1988

12. Van Duyne, R.P. , Maushaller, J.P., Janik-Czachor, M., Levinger, N., J. Phys. Chem. , 89, 4055, 1985

13. Jeanmarie, D.L., Van Duyne, R.P. , J. Electroanal. Chem. , 84 , 1 , 1977

14. Weitz, D.A., Garoff, S., Gersten, J., Nitzau, A., J. Chem. Phys. 78 , 5324 , 1983

15. Watanabe, T., Pettinger, B., Chem. Phys. Lett., 89 , 501 , 1982

16. Wokaun, A., Barker, A., Fluhr, W., Meier,M., J. Vac. Sci. Technol., 3, 1937, 1985

17. Graves, P.R., J. Chem. Soc., Chem. , Comm., 18, 1418 , 1986

18. Takahashi, M., Fujita, M., Ito, M., Surf. Sci., 158, 307 , 1985

19. Shin, G.S., Kim, J.J., Surf. Sci. , 158, 286, 1985

20. Weaver, M.J., Gao, P., Gostzola, D., Patterson, M.L., Tadayyiani, M.A., ACS Symp. Ser. , 307 , 135, 1986

21. Turkevich , J. , Stevenson , P.C. , Hillier , J., Disc. Faraday Soc. , 11 , 58, 1951

22. Frens , G.C. , Nature Physical Science , 241 , 20 , 1973

23. Greighton , J.A. , Blatchford , C.G. , Albrecht , M.G , J. Chem. Soc. Faraday II , 75 , 790 , 1979

24. Fabrikanos , A. , Athanasiou , S. , Lieser , K.H. , Z. Naturforsch , 18B , 612 , 1963

25. Lippitsch , M. , Chem. Phys. Letters , 74 , 125 , 1980

26. McQuillan , A.J. , Pope , C.G. , Chem. Phys. Letters , 71 , 349 , 1980

27. Wetzel , H. , Gerischer , H. , Pettinger , B. , Chem. Phys. Letters , 85 , 187 , 1982

28. Siiman , O., Bumm , L.A. , Callghan , R.A. , Blatchford , C.G. , Kerker , M. , J. Phys. Chem. , 87 , 1014 , 1983

29. Suh , J., DiLella , D.P. , Moskovits , M. , J. Phys. Chem. 87, 1540 , 1983

30. Creighton , J.A. , Blatchford , C.G. , Campbell , J.R. , Surf. Scie. 120, 435, 1982

31. Moskovits , M. , J. Chem. Phys. , 69 , 4159 , 1978

32. Wang , D.S. , Kerker , M. , Chew , H. , Appl. Opt. , 19 , 2256 , 1980

33. Kerker , M. , Wang , D.S. , Chew , H. , Appl. Opt. , 19 , 4159 , 1980

34. Kerker , M. , Siiman , O. , Bumm , L.A. , Wang , D.S. , Appl. Opt. , 19 , 3253 , 1980

35. Moskovits , M. , J. Chem. Phys. , 77 , 9 , 4408 , 1982

36. Moskovits , M. , Suh , J.S. , J. Phys. Chem. , 88 , 7 , 1293 , 1984

37. Moskovits , M. , Suh , J.S. , J. Phys. Chem. , 88 , 23 , 5526 , 1984

38. Moskovits , M. , Suh , J.S. , J. Am. Chem. Soc. , 107 , 6826 , 1985

39. Moskovits , M. , Suh , J.S. , J. Am. Chem. Soc. , 108 , 4711 , 1985

40. Moskovits , M. , Suh , J.S. , J. Phys. Chem. , 92 , 22 , 6327 , 1988

41. Moskovits , M. , DiLella , D.P. , Maynard , K.J. , Langmuir , 4 , 67 , 1988

42. Creighton , J.A. , Surface Science , 124 , 209 , 1983

43. Greenler , R.G. , Snider , D.R. , Witt , D. , Sorbello , R.S., Surf. Sci. , 118 415 , 1982

44. Campion , A. , Grizzle , V.M. , Mullins , D.R. , Brown , J.K. , J. Phys. , 44 , c10-341 , 1983

45. Hallmark , V.M. , Campion , A. , Chem. Phys. Lett. , 110 , 561 , 1984

46. Hallmark , V.M. , Campion , A. , Chem Phys. Lett. , 84 , 2933 , 1986

47. Hallmark , V.M. , Campion , A. , J. Chem. Phys. , 84 , 2942 , 1986

48. Hilderbrandt, P., Stockburger, M., J. Raman Spec., 16, 55, 1986

49. Gerischer, H., Faraday Discuss. Chem. Soc., 58, 219, 1974

50. Siiman, O., Lepp, A., J. Phys. Chem., 89, 3494, 1985

51. Hilderbrandt, P., Stockburger, M., J. Phys. Chem., 88, 5935, 1984

52. Cotton, T., Fan, N., J. Raman Spec., 19, 429, 1988

53. Siiman, O., Lepp, A., Kerker, M., J. Phys. Chem., 87, 5319, 1983

54. Bachackaschvilli, A., Katz, B., Priel, Z.E., Frima, S., J. Phys. Chem., 88, 6185, 1984

55. Pettinger, B., Gerolymatou, A., Ber. Bunsenes Phys. Chem., 88, 359, 1984

56. Garrell, R.L., Beer, K., Spectrochimica acta, 43B, 617, 1988

57. Ahern, A.M., Garell, R.L., Langmuir, 4, 1162, 1988

58. Suh, J.S., J. Raman Spec., 18, 409, 1987

59. Suh, J.S., Michaelian, K.H., J. Phys. Chem., 91, 598, 1987

60. Clavijo, R.E., Mutus, B., Aroca, R., Dimmock, J.R., Phillips,O.A., J. Raman Spec., 19, 541, 1988

61. Dinh. T.V., Hiromoto, M.K., Begun, G.M., Moody, R.L., Anal. Chem., 56, 1667, 1984

62. Moody, R.L., Fletcher, W.H., Dinh, T.V., Appl. Spect., 41, 966, 1987

63. Kwan, K., J. Raman Spec., 18, 57, 1987

64. Feilchenfeld, H., Siiman, O., J. Phys. Chem., 90, 2163, 1986

65. Von Raben, K.V., Chang, R.K., Laube, B.L., Barber, P.W., J. Phys. Chem., 88, 5290, 1984

66. Moskovits, M., Suh, J.S., J. Am. Chem. Soc., 108, 4711, 1986

67. Kim, M.S., Suh, S.W., Lee, H.I., J Raman Spec., 19, 491, 1988

68. Niki, K., Kawasaki, Y., Kimura, Y., Higuchi, Y., Yasuoka, N., Langmuir, 3, 982, 1987

69. Nabiev, I.R., Efremov, R.G., Chumanov, G.D., Biofizika, 31, 724, 1986

70. Sequaris, J.M.L., Koglin, E., Anal. Chem., 59, 527, 1987

71. Suh, S.W., Kim, M.S., J. Raman Spect., 18, 253, 1987

72. De Mul, F.F.M., Otto, C., Greeve, J., Proc. SPIE-Int. Soc. Opt. Eng. 492, 1985

73. Sequaris, J.M., Fritz, J., Lewinski, H., Koglin, E., J. Colloid Interface Sci., 105, 417, 1985

74. Spiro, T.G., Copeland, R.A., Fodor, P.A., J. Am. Chem. Soc., 106, 3872, 1984

75. Hester, R.E., DeGroot, J., J. Phys. Chem., 91, 1693, 1987

76. Itoh, K., Kim, M., Tsujino, T., Chem. Phys. Let., 125, 364, 1986

77. Aroca, R., Jennings, C., Kavac, G.J., Lautfy, R.O., Vincett, P.A., J. Phys. Chem., 89, 4051, 1985

78. Jennings, C., Aroca, R., Hor, A.M., Lautfy, R.O., Anal. Chem., 56, 2033, 1984

79. Koglin, E., Sequaris, J.M., Spectrosc. Biol. Mol., Eur. Conf., 1st., 221, 1985

80. Ivanara, T.M., Zh. Fiz. Khim., 60, 2641, 1986

81. Dinh, T.V., Alak, A.M., Anal. Chem., 59, 2149, 1987

82. Dinh, T.V., Alak, A.M., Moody, R.L., Spectrochimica acta, 43B, 605, 1988

83. Carrabba, M.M., Edmonds, R.B., Anal. Chem., 59, 2559, 1987

84. Dinh, T.V., Enlow, P.D., Proc.-APCA Annu. Meet., 78th, 85, 1985

85. Sequaris, J.M., Koglin, E., Z. Anal. Chem., 321, 758, 1985

86. Ishida, H., Fukuda, H., Katagiri, G., Ishitani, A., Appl. Spectroc. 40, 322, 1986

87. Krumholz, P., J. Am. Chem. Soc., 73, 3487, 1951

88. Meisel, D., Lee, P.C., J. Phys. Chem., 86, 3391, 1982

89. Allen, C.S., Van Duyne, R.P., Chem Phys. Lett., 63, 455, 1979

90. Zerbi, G., Sandroni, S., Spectrochim. Acta, 24A, 483 and 511, 1968

91. Caswell, D.S., Spiro, T.G., Inorg. Chem., 26, 18, 1987

92. Strukl, J.S., Walter, J.L., Spectrochim. Acta, 27A, 209, 1971

93. Strukl, J.S., Walter, J.L., Spectrochim. Acta, 27A, 223, 1971

94. Castellucci, E., Angeloni, L., Neto, N., Sbrana, G., Chem. Phys. Lett., 43, 365, 1979

95. Neto, N., Muniz-Miranda, M., Angeloni, L., Castellucci, E., Spectrochim. Acta, 39A, 97, 1983

96. Mallick, P.K., Danzer, G.D., Strommen, D.P., Kincaid, J.R., J. Phys. Chem., 92, 5628, 1988

97. Kim, M., Itoh, K., J. Phys. Chem., 91, 126, 1987

98. Long, D.A., "Raman Spectroscopy", Mc Graw Hill Inc., London, 1977, p.p. 1-73

99. Halpern, T., McKoskey, S.M., McMillan, J.A., J. Chem. Phys., 52, 3526, 1970

100. Steger, E., Garbe, S., Klosowski, J., J. Raman Spec., 14, 196, 1983

101. Shukla, A.R., Pathak, C.M., Dongre N.G., Shamir, J. J. Raman Spec., 17, 299, 1986

102. Vergoten, G., Fleury, G., Blain, M., Odiot, S., J. Raman Spec. 16, 143, 1985

A last thought

" ..... and so there ain't nothing more to write about, and I am rotten glad of it, because if I'd `a' knowed what a trouble it was to make a book I wouldn't `a' tackled it, and ain't a-going to no more."

Mark Twain, Huckleberry Finn